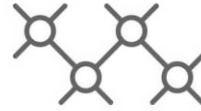




TECHNISCHE
UNIVERSITÄT
WIEN



Institut für
Computertechnik
Institute of
Computer Technology

A MASTER THESIS ON

Year-Round Household Energy Self-Sufficiency in Austria

IN PARTIAL FULFILLMENT OF THE REQUIREMENTS
FOR THE DEGREE OF

Diplom-Ingenieur

(Equivalent to Master of Science)

in

Energy Systems and Automation Technology (066 506)

by

Manuel Matzinger, BSc

01425437

Supervisor(s):

Ao.Univ.Prof. Dipl.-Ing. Dr.techn. Thilo Sauter

Projektass. Dipl.-Ing. Daniel Hauer, BSc

Univ.Ass. Dipl.-Ing. Stefan Wilker, B.Eng.

Vienna, Austria

December 2022



Die approbierte gedruckte Originalversion dieser Diplomarbeit ist an der TU Wien Bibliothek verfügbar
The approved original version of this thesis is available in print at TU Wien Bibliothek.

Abstract

Energy autarky for private households is a topic which has existed for a long time. People are living off grid to live a life of self-sufficiency or they take a recreational vehicle on vacation and want sufficient power. In many parts of the world the energy grid is simply non existent or very unstable. While the last point was a non issue in Austria for the longest time, the energy crisis is now more tangible than ever. To make energy self-sufficiency more feasible, a simulator was conceived and written in MATLAB which uses real world and modeled weather data. This data is then used to calculate the output of a Photovoltaic (PV) system of any given size, the output of a wind turbine and a load from a heat pump resulting from the heat demand depending on building parameters and the environment. In conjunction with a household load simulator, a energy storage model is created which stores or supplies depending on the energy situation of the household. While rough estimations for autarky in different regions exist, there can be significant differences in autarky within little spatial distance. This work shows that energy self-sufficiency depending on the setup and location is indeed possible and demonstrates the influence of geographical location on autarky throughout Austria. Furthermore it shows how scaling of PV and storage impacts autarky. While the effects of electrical heating on autarky was expected to be severe, this work puts in perspective just how much it impinges this ordeal. To achieve full autarky, components need to be scaled up excessively, there have to be ideal weather conditions at the location or the power consumption has to be reduced drastically in times where the energy yield from the generators is low.

Kurzfassung

Energieautarkie für Privathaushalte ist kein neues Thema. Menschen leben "off grid" um weitgehend zum Selbstversorger zu werden oder fahren mit einem Wohnmobil in den Urlaub und wollen weiterhin ausreichend Strom haben. In vielen Teilen der Welt ist das Stromnetz nicht existent oder instabil. Während der letzte Punkt für lange Zeit kein relevantes Problem in Österreich darstellte, hat ihn die Energiekrise wieder salonfähig gemacht. Um Energieautarkie greifbarer zu machen wurde ein Simulator in MATLAB geschrieben, welcher gemessene und modellierte Wetterdaten verwendet. Diese Daten werden verwendet um den Energiegewinn aus einer PV und einer Windturbine zu berechnen. Weiters erzeugt der Simulator aufgrund von gegebenen Gebäudeparameter einen Heizbedarf, welcher durch eine Wärmepumpe gedeckt wird die wiederum Strom benötigt. In Verbindung mit einem Haushaltlastprofilimulator und einem Energiespeichermodell können Erzeugung, Speicherung und Verbrauch komplett abgebildet werden. Während grobe Autarkieberechnungen für verschiedene Region existieren, können diese in geringer geographischen Distanz signifikant von einander abweichen. Diese Diplomarbeit zeigt, dass Energieautarkie möglich ist und demonstriert den Einfluss der verschiedenen Wetterbedingungen in Österreich auf die Autarkie. Es zeigt weiters wie die Skalierung von PV und Speichergröße auf die Autarkie einwirkt. Obwohl der Einfluss von elektrischem Heizen auf Energieautarkie als schwerwiegend angenommen wurde, zeigt die Arbeit wie stark dieser Effekt die Autarkie erschwert. Um vollkommen autark zu sein müssen die Komponenten massiv ausgelegt werden, ideale Bedingungen herrschen oder der Verbrauch in Zeiten wo wenig Energie erzeugt wird drastisch verringert werden.

Erklärung

Hiermit erkläre ich, dass die vorliegende Arbeit ohne unzulässige Hilfe Dritter und ohne Benutzung anderer als der angegebenen Hilfsmittel angefertigt wurde. Die aus anderen Quellen oder indirekt übernommenen Daten und Konzepte sind unter Angabe der Quelle gekennzeichnet.

Die Arbeit wurde bisher weder im In- noch im Ausland in gleicher oder in ähnlicher Form in anderen Prüfungsverfahren vorgelegt.

Copyright Statement

I, Manuel Matzinger, BSc, hereby declare that this thesis is my own original work and, to the best of my knowledge and belief, it does not:

- Breach copyright or other intellectual property rights of a third party.
- Contain material previously published or written by a third party, except where this is appropriately cited through full and accurate referencing.
- Contain material which to a substantial extent has been accepted for the qualification of any other degree or diploma of a university or other institution of higher learning.
- Contain substantial portions of third party copyright material, including but not limited to charts, diagrams, graphs, photographs or maps, or in instances where it does, I have obtained permission to use such material and allow it to be made accessible worldwide via the Internet.

Signature: _____

Vienna, Austria, December 2022

Manuel Matzinger, BSc

Dedication

This work is dedicated to my family who supported me and encouraged me along the way of my studies. It is also dedicated to all my study colleagues and friends with whom I traveled along this journey. Additional thanks go out to my supervisors Daniel Hauer and Stefan Wilker who helped me with a lot of valuable inputs. Special thanks go to my working colleague Franz Zeilinger, who allowed me to use his load simulator and also gave important insights. Finally it is dedicated to everyone who is interested in the topic of autarky and self-sufficiency. This mindset may seem unnecessary and restricting for some but independence in general is a virtue which is important to me.

Contents

Abstract	iii
Kurzfassung	iv
1 Introduction	1
1.1 Motivation	1
1.2 Research Questions	2
1.3 Structure of this Work	3
2 State of the Art	5
2.1 Types of Energy Generation	5
2.2 Types of Energy Storage	7
2.3 Current Available Simulators	9
3 The Amaterasu Autarky Simulator	17
3.1 General Tool Architecture	17
3.2 Acquiring & Verifying Data	18
3.3 Photovoltaic Model	24
3.4 Wind Turbine Model	36
3.5 Load Model (Residential Load Simulator)	39
3.6 Heat Model	42
3.7 Electrical Storage Model	48
3.8 Output of the AAS	50
4 Results	53
4.1 Validation and Accuracy of the Models	53
4.2 Location dependent Autarky Analysis of Different Sized Households	61
4.3 Autarky Depending on Photovoltaic and Battery Size	78

5 Conclusion and Outlook	85
Bibliography	87

List of Tables

3.1	Comparison of weather data at Innsbruck airport. GI is global irradiation and DI diffuse irradiation	19
3.2	Daily median of absolute global irradiation difference between ZAMG to PVGIS in Wh/m ² per month for 2019	22
3.3	Coefficients depending on ε [6] [58]	30
3.4	Updated coefficients depending on ε [55]	31
3.5	Albedo ρ for different surfaces	31
3.6	Coefficients to calculate angular losses [61]	32
3.7	Roughness length for different terrains [6]	33
3.8	Coefficients to calculate the temperature of rack mounted solar panels [64] [65]	33
3.9	Coefficients to calculate the temperature of roof mounted mono crystalline solar panels for different gap size [66]	34
3.10	Coefficients to calculate the temperature of roof mounted poly crystalline solar panels for different gap size [66]	34
3.11	Coefficients for calculation of solar power generation [55]	35
3.12	Load profile categories used in this work [78]	39
3.13	Amount of devices per household profile [77]	40
3.14	Load profile categories used in this work [78]	40
3.15	Thermal conductivity of commonly used building materials [6]	42
3.16	Coefficients for calculating soil temperature [84]	43
3.17	<i>airChange</i> in % of the room volume per hour according to [85]	45
3.18	Effective capacity depending on building material [87]	46
3.19	COP of different heat pumps depending on environmental temperature [91] [92] [93] . .	47
4.1	Comparison of the results of the RLS with average power consumption in Austria . . .	57
4.2	Classes of energy efficiency of buildings [95]	58

List of Figures

1.1	Example architecture for a energy autark household	2
2.1	PVGIS offgrid calculator [2]	9
2.2	PVGIS offgrid calculator load distribution [2]	10
2.3	Independence calculator from Volker Quaschnig [31]	11
2.4	Solar usage calculator from PVAustria - input fields [34]	13
2.5	Solar usage calculator from PVAustria - storage and results [34]	13
2.6	Autarky rate tool from STORE4HUC [36]	14
2.7	SUSI from Energieinstitut Vorarlberg [41]	15
3.1	Simplified architecture of the AAS	17
3.2	Temperature comparison Innsbruck 2016	20
3.3	Wind speed comparison Innsbruck 2016	20
3.4	Global irradiation comparison ZAMG to PVGIS in 2019	21
3.5	Solar energy generation with ZAMG and PVGIS data in 2019	22
3.6	Temperature comparison of ZAMG and INCA data in 2019	23
3.7	Wind speed comparison of ZAMG and INCA data in 2019	24
3.8	Illustration of the solar declination angle, taken from [54]	25
3.9	Sun path diagramm for Vienna	26
3.10	Sun path diagramm for Djibuti	27
3.11	Sun path diagramm for Sydney	28
3.12	Illustration of the AOI (taken from [6] with edited names)	29
3.13	Illustration of a wind turbine and its area of attack (taken from [6])	36
3.14	Power curve of Schachner SW5 [72], Antaris 5.5kW [73], Istabreeze Heli 4.0 [74]	38
3.15	Load per person depending on device groups for a working day in summer (top) and winter (bottom) (used with permission from [78])	41
3.16	Global irradiation on a house throughout the day	45

3.17	Course of heat pump demand and heat storage throughout a day	48
3.18	Output for one winter day from the AAS	51
3.19	Output for one summer day from the AAS	51
4.1	Comparison of monthly solar energy generation real vs. simulated	54
4.2	Comparison of daily solar energy generation real vs. simulated for June 2022	55
4.3	Comparison of daily solar energy generation real vs. simulated for October 2022	55
4.4	Detailed inquired information of small wind turbines in Austria, each value on the x-axis represents a different turbine (recreated from [10])	56
4.5	Simulated wind power generation with a 5kW turbine at 20m height in Austria with INCA data	57
4.6	Comparison of weekly averages between real and simulated data for the active power of a transformer in Köstendorf, Salzburg (used with permission from [78])	58
4.7	Soil temperature in 20cm depth at Innsbruck Airport 2020	60
4.8	Soil temperature in 20cm depth at Reichenau an der Rax 2020	60
4.9	Autarky in Austria for a small two person home depending on the year	63
4.10	Histogram of the time based autarky for a small two person home for the worst and best year	64
4.11	Load usage per month for a two person example household	64
4.12	Autarky in Austria for a large two person home depending on the year	66
4.13	Histogram of the time based autarky for a large two person home for the worst and best year	67
4.14	Autarky in Austria for a large four person home depending on the year	68
4.15	Histogram of the time based autarky for a large four person home for the worst and best year	69
4.16	Autarky in Austria for a large four person home depending on the year without electrical heating	70
4.17	Load Usage per month for a four person example household without electrical heating	71
4.18	Histogram of the time based autarky for a large four person home for the worst and best year without electrical heating	71
4.19	Autarky in Austria for a small two person home depending on the year with only solar generation	72
4.20	Histogram of the time based autarky for a small two person home for the worst and best year with only solar generation	73

4.21	Autarky in Austria for a small two person home depending on the year with only solar generation	74
4.22	Histogram of the time based autarky for a small two person home for the worst and best year with only wind generation	75
4.23	Solar power generation in Austria depending on the location in 2016	75
4.24	Wind power generation in Austria depending on the location in 2016	76
4.25	Heat demand for a small home in Austria depending on the location in 2017	77
4.26	Comparison of yearly mean PV generation and temperature	77
4.27	Load autarky depending on PV and usable storage size in Neusiedl am See in 2016 . . .	78
4.28	Load autarky depending on PV and usable storage size in Neusiedl am See in 2016 without electrical heating and 5459kWh power demand	79
4.29	Load autarky depending on PV and usable storage size in Rudmanns in 2016	80
4.30	Load autarky depending on PV and usable storage size in Tultschnig in 2016	81
4.31	Load autarky depending on PV and usable storage size in Liezen in 2016	82
4.32	Load autarky depending on PV and usable storage size in Imst in 2016	82
4.33	Time based autarky in 2016 for different Locations with the base- and 30/30 System . .	83
5.1	Load autarky for a four person household without electrical heating in 2016	86

Acronyms

AAS "Amaterasu Autarky Simulator". ix, xiii, xiv, 1, 17, 18, 39, 47, 50, 51, 53, 61, 85, 86

AC Alternating Current. 6, 7, 35, 49

ADRES "Autonome Dezentrale Regenerative EnergieSysteme". 39

aDSM "Aktives Demand-Side-Management durch Einspeiseprognose". 39

AM Air Mass. 30

AOI Angle Of Incidence. xiii, 26, 27, 29

API Application Programming Interface. 18, 19

BMS Battery Management System. 8

COP Coefficient of Performance. xi, 47, 65

DC Direct Current. 5, 7, 35, 38, 49

DOD Depth of Discharge. 7, 8

HWB_{Ref,SK} Heizwärmebedarf Referenz-Lüftungsleitwert Standort Klima. 58, 59

INCA "Integrated Nowcasting through Comprehensive Analysis". xiii, xiv, 18, 19, 20, 23, 24, 56, 57, 59

PV Photovoltaic. iii, iv, xv, 1, 5, 6, 10, 11, 12, 14, 15, 17, 18, 19, 22, 24, 33, 34, 53, 61, 67, 73, 76, 77, 78, 79, 80, 81, 82, 85, 87

PVGIS "Photovoltaic Geographical Information System". xi, xiii, 2, 9, 10, 12, 16, 19, 20, 21, 22, 28, 29, 36, 53, 59

RLS Residential Load Simulator. xi, 2, 17, 18, 39, 40, 42, 56, 57

SIA Solar Irradiation Absorption. 44, 59, 61

SOC State of Charge. 50, 59, 61

SUSI "Strom Unabhängigkeits Simulation". xiii, 15, 16

TAWES "Teilautomatisches-Wetter-Erfassungs-System". 21

TMY "Typical Meteorological Year". 19, 28, 36

ZAMG "Zentralanstalt für Meteorologie und Geodynamik". xi, xiii, 18, 19, 21, 22, 23, 24, 36, 53

Chapter 1

Introduction

1.1 Motivation

At the time of writing (Fall 2022), energy prices all across Europe are rising towards an all time high in the history of the European energy market. Difficulties with the gas supply create discussions about power rationing and the possibilities of country wide blackouts. Not only blackouts or controlled grid shut downs are the reason for this work. Many people have the desire to be energy self-sufficient and live independent of the power grid. Additionally, when taking on a broader perspective, many parts of the world do not have access to a power grid at all or it is unstable. For these people, it is not a matter of convenience or ideals but a matter of living a better life through the possibilities which electrical power provides. For these reasons, the drive for self-sustained energy systems is on the rise. While grid connectivity is still required by most local authorities, a hybrid inverter with a smart meter allows to cut oneself off from the grid and avoid a blackout on the personal premises. Energy autarky is important when factoring in how much of our living standard is dependent on electrical power.

Demand for renewable energy systems is at an all time high, components for Photovoltaics (PVs), i.e. panels and especially inverters have delivery times up to a year. This master thesis's goal is the design and implementation of the "Amaterasu Autarky Simulator" (AAS), a tool which aims to allow a better understanding of energy autarky for private households in Austria. Amaterasu is the goddess of the sun in Japanese mythology. Considering that PV is a big part of this tool and the name Amaterasu has nice ring to it in conjunction with autarky, it seemed a fitting name for this work. Even though Austria as a country is not very large, it has a diverse climate [1]. The AAS considers geographical climate differences and calculates an autarky factor accordingly. That leads to distinct generation differences and heat demands depending on the location. This allows for an adequate autarky analysis everywhere in Austria to verify how and if the need for self-sustained energy is possible. Besides that, information

about the simulation can be accessed at every point of the simulated year. The weather and irradiation data is taken from the EU Project "Photovoltaic Geographical Information System" (PVGIS) [2]. For the load profiles of the household the high resolution model Residential Load Simulator (RLS) [3] is used.

To further clarify the system architecture, Figure 1.1 shows how a simplified setup could look like in real life.

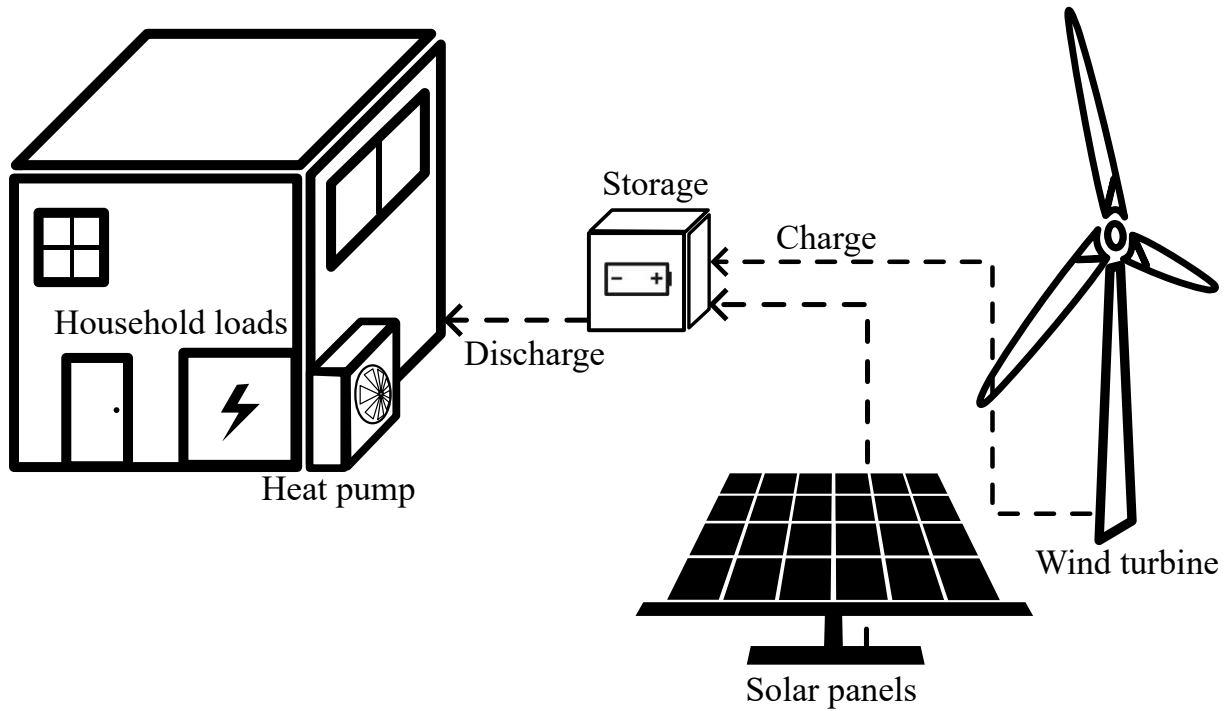


Figure 1.1: Example architecture for an energy autark household

1.2 Research Questions

This work aims to create an accurate enough model to answer these following questions:

- Is year round energy autarky for private households in Austria possible?
- Which influence do geographical conditions in Austria have on autarky?
- Which technologies are needed/sensible for different locations?
- How does scaling of the components influence autarky?

All these examinations aim to satisfy the energy consumption of a typical household. At the end of this thesis, these questions will be revisited and answered.

1.3 Structure of this Work

In this master thesis, chapter 2 is about the basics of commercial available energy generation and the different types of energy storages available. Additionally, an overview of available autarky simulators is given. Chapter 3 describes the data acquisition, the used programming language and the different classes of the model and calculation methods in detail. After that, chapter 4 is about the results and insights gained from the simulation and the answer to the previously asked research questions. At last conclusions about the whole work are drawn.

Chapter 2

State of the Art

This chapter gives an overview about the basic types of renewable energy generation which are commonly available. After that some of the readily available energy storage systems are covered. Furthermore, a few representative autarky simulators are analyzed.

2.1 Types of Energy Generation

In this section some of the most readily accessible energy producers are reviewed. Their up- and down-sides are discussed and their availability in Austria is determined.

2.1.1 Solar Power

The amount of PV systems installed in Austria steadily rises and shows currently no signs of stopping [4]. The reason for this besides the rising energy costs is that solar panels are currently the cheapest form of power generation. Depending on the size of the installed system, the costs ranged from 1300-1800€ per installed kilowatt (kW) system power [5]. The current situation while writing this (fall 2022), is that an extreme demand for the components and impacts on the supply chain have led to increased costs for the first time in years. Solar cells use the internal photoelectric effect in conjunction with the properties of semiconductors to produce power. The theoretically maximum efficiency of crystal silicon is 29% [6]. Efficiency in this case means, that only 29% of the incident irradiation can be converted to electrical energy. Currently commercial available modules achieve an efficiency of about 22% [7].

The biggest advantage of solar modules is that they come in various sizes and can be mounted in different ways. Additionally, installation on roofs allow them to take up space which would be most likely unused anyway. Manufacturers promise a power output of 92% after 25 years [7], making them a long lasting energy generator which does not require maintenance. Since the PV modules generate Direct Current (DC) power, it can directly charge an energy storage with a charge controller, or be

converted to usable Alternating Current (AC) power with the help of an inverter. The only downside of them is that their energy production throughout the day is seldomly used by most people. Because most people are at work during the day and use the majority of energy in the evening, a large portion of the energy from the PV system is unused.

All the reasons mentioned above make solar panels the most common type of renewable energy for private households. Affordable costs and easy installation allow power production everywhere the sun reaches.

2.1.2 Wind Power

Large wind turbines are often seen when traveling rural areas in most countries. As demand for renewable energy rises, the interest in wind turbines is increasing. The biggest wind turbine existing is the Siemens "SG 14-222 DD", an offshore type with a rotor diameter of 222m and a rated power of 14MW. In the wind park Andau in Austria, wind turbines of the type "Enercon 101" [8] with a rotor diameter of 101m and a rated power of 3MW are installed. The main advantage of wind power is also its biggest disadvantage. Depending on the location, sufficient wind can occur all the time, only on some days or not at all. For this reason, other than solar power, wind power is heavily dependent on the locality. Wind turbines for households however, are not a common sight. Legal requirements vary on the state and municipality [9] and many locations do not have sufficient wind to justify a wind generator. Additionally, wind turbines do require a lot more installation work (foundation, tower) compared to solar panels which can just be placed on roofs. Furthermore, the overall cost of setting up a wind turbine range from 3000-8000€ per kW [10], making them a lot more expensive than PV systems. Because moving parts are involved, regular maintenance is also needed. Smaller wind turbines generate AC power with a permanent magnet synchronous, motor so a rectification circuit is needed before charging a energy storage or using a inverter to transform it. The aforementioned reasons make wind generators seem like a much worse choice compared to PV systems. But considering autarky and self-sustainment of energy, a power generator which acts independent of sun, especially for the winter months, is sorely needed.

2.1.3 Hydro Power

Hydroelectric power is the most location specific kind of power generation. Big hydroelectric power plants use dams to create a height difference for the water to gain sufficient potential energy to drive a turbine. For small scale so called "micro hydro" generators, a water intake combined with a penstock over a large height difference is used to create appropriate pressure for driving the turbine. Again, moving parts, pipes, valves, water intake and the amount of forces involved make this type of energy

generation one which also needs regular maintenance. The price for a 1200-4000W generator alone with a turbine and water box is around 1000€ [11]. Construction of the intake, penstock and generator house however, increase this price significantly. Like the wind generator it produces AC power which needs to be rectified to DC.

The main advantage of hydro power is, even though output mostly changes throughout the year depending on precipitation and season, its consistency. Compared to solar and wind, hydro power does not fluctuate erratically.

The deal breaker and the reason this type of energy production was not modeled in this work, is because very little properties have the requirements to install such a system. Furthermore, the legal requirements for usage of water sources in Austria [12] are very strict and further decrease the availability of this power source for private use.

2.2 Types of Energy Storage

In this section, a few energy storage systems are discussed. Each of them has its own properties and is used depending on the requirements. They are used to bridge periods of time when no or less energy is produced (i.e. night time for solar panels, days with bad weather). Long term storage (energy stored for months and longer) is quite expensive most of the time. To offset this, conventional batteries with larger capacities are used to account for longer periods of time where power generation is impaired or not available.

2.2.1 Lead-Acid Batteries

Lead-acid based batteries are the most used accumulator worldwide [6]. For example, the combustion engine car industry uses one for the starter battery. By having thicker battery plates, separators and denser active materials a so called "deep cycle" battery is made. These types of batteries allow for more charge/discharge cycles (about 800-3000 at 50% Depth of Discharge (DOD) [13] [14]) with less degradation.

Lead-acid batteries like other suffer from self-discharge depending on temperature. For lead based batteries this value ranges from 3-10% [6] [15] [16] of the maximum capacity at 25°C. Lead-acid batteries have an energy efficiency of around 70% [6] [17]. For example, when the the battery is charged by 100Wh, around 142Wh of energy is needed to achieve this. When more current is drawn, their efficiency and usable capacity is lowered. Additionally, to achieve a longer lifespan of these batteries, they should not be discharged to less than 50% of their rated capacity. This is why most usable capacities of lead-acid type batteries are only half of their maximum capacity. Charging of these accumulators is quite

simple, since the state of charge can be monitored by their voltage. Costs of these batteries are low compared to other types of energy storages. The cost for lead-acid batteries for example [18] [19] are about 400-750€ per usable kilowatt hours (kWh) of storage. One big advantage of these batteries is that they are almost fully recyclable [20].

Overall, deep cycle lead acid batteries have quite a lot of downsides considering efficiency and lifespan, but on the contrary are quite cheap, easy to charge and have a low ecological footprint as its components can be easily recycled.

2.2.2 Lithium Based Batteries

Lithium based batteries (lithium-iron-oxid, lithium-cobalt-oxid etc..) have a high energy density, a large amount of charge/discharge cycles (4500 cycles at 80% DOD [21]) and a high efficiency factor ($\geq 96\%$ [22]). Furthermore, their self-discharge is also quite small and ranges from 2-3% of their usable capacity per month. Because of these advantages compared to lead-acid batteries, lithium based accumulators become more and more popular. Depending on manufacturer and size, they are a bit more expensive than lead-acid batteries ranging from 670-950€ [23] [24] per kWh usable storage. The biggest disadvantage of these types of accumulators is that they are very sensible to critical conditions like deep discharge or overcharging, which can lead to fire or explosions [6]. For this reason, a Battery Management System (BMS) is needed for these types of batteries. Another disadvantage is that currently only a small amount of lithium based batteries is recycled [25]. This is because lithium batteries have a complex design and disassembly is much more complicated compared to lead-acid.

Overall, lithium based batteries perform better than lead-acid in every aspect except price and the possibility for recycling. While the price will get lower with time, it will take a lot longer to match the 99% recycling rate of lead based energy storage.

2.2.3 Hydrogen Based Storage

Hydrogen based electricity with a fuel cell already exists for a long time. It is brought up again and again as an option for electric vehicles. A company based in Berlin, Germany called Home Power Solution [26], now uses this concept as an energy storage for households. Their system consists of a (assumed to be lithium based) 20kWh so called "short term" storage and a hydrogen tank system which can store up to 300kWh of electrical energy [27]. It claims an efficiency of 70% for the creation of hydrogen and a 50-60% efficiency for the fuel cell to turn hydrogen back to electricity [28]. The round trip efficiency in the worst case would add up to 35%. Warmth created by the process can apparently also be used to heat up water, increasing the overall efficiency. Two great advantages are no storage losses from the hydrogen storage and a very large usable electrical capacity. The company claims their

price ranges from 85000-125000€ which is quite a lot. Considering the overall usable capacity (battery + hydrogen tank) of 320kWh, this results in about 390€ per kWh stored which even rivals the price of lead-acid batteries.

2.2.4 Energy Storage - Conclusion

Even though the reviewed energy storage systems differ from each other significantly, they all have a set efficiency for charging/discharging, maximum power in- and outputs and some or none self-discharge. For this reason the model in this work is kept rather simple to allow the simulation of different storage types by setting up the parameters of the storage individually.

2.3 Current Available Simulators

Tools to calculate energy self-sufficiency are commonly available in the internet. A representative few of them are described and their characteristics highlighted.

2.3.1 PVGIS

Besides being the main data supplier for irradiation (more on that in chapter 3), PVGIS also has an option to simulate performance for off grid systems [2] which can be seen in Figure 2.1. A very important factor

The screenshot displays the PVGIS off-grid calculator interface. At the top, it shows the cursor location (48.041, 16.986) and the selected location (47.967, 16.940) with an elevation of 166m. The PVGIS version is 5.2. The 'Use terrain shadows' section is active, with 'Calculated horizon' checked. Below this, there are buttons for 'csv' and 'json' exports, and a 'Datei auswählen' button. The main section is titled 'PERFORMANCE OF OFF-GRID PV SYSTEMS'. It features a sidebar on the left with options: GRID CONNECTED, TRACKING PV, OFF-GRID (selected), MONTHLY DATA, DAILY DATA, HOURLY DATA, and TMY. The main area contains several input fields: Solar radiation database* (PVGIS-SARAH2), Installed peak PV power [Wp]* (1000), Battery capacity [Wh]* (1100), Discharge cutoff limit [%]* (0.00), Consumption per day [Wh]* (1000), and checkboxes for 'Upload horizon file' and 'Upload consumption data'. There are also input fields for Slope [°]* (35) and Azimuth [°]*. At the bottom, there are buttons for 'Visualize results', 'csv', and 'json'.

Figure 2.1: PVGIS offgrid calculator [2]

for this model is that the irradiation data is probably the most dynamic compared to the other models shown here, since it uses satellite data which are covering almost the whole planet. The discharge cutoff limit describes how "deep" the battery is allowed to discharge itself. In the example, 0.001 means that with a 10kWh battery, 9.99kWh can actually be used. A simple consumption data file can be uploaded, which contains a factor for each hour of the day which is multiplied with the "consumption per day parameter" (Figure 2.1). The default one (one factor per hour of day, the sum of them is 1) supplied by the website is a single row csv-file which can be seen plotted in Figure 2.2. It is used for every day of the year.

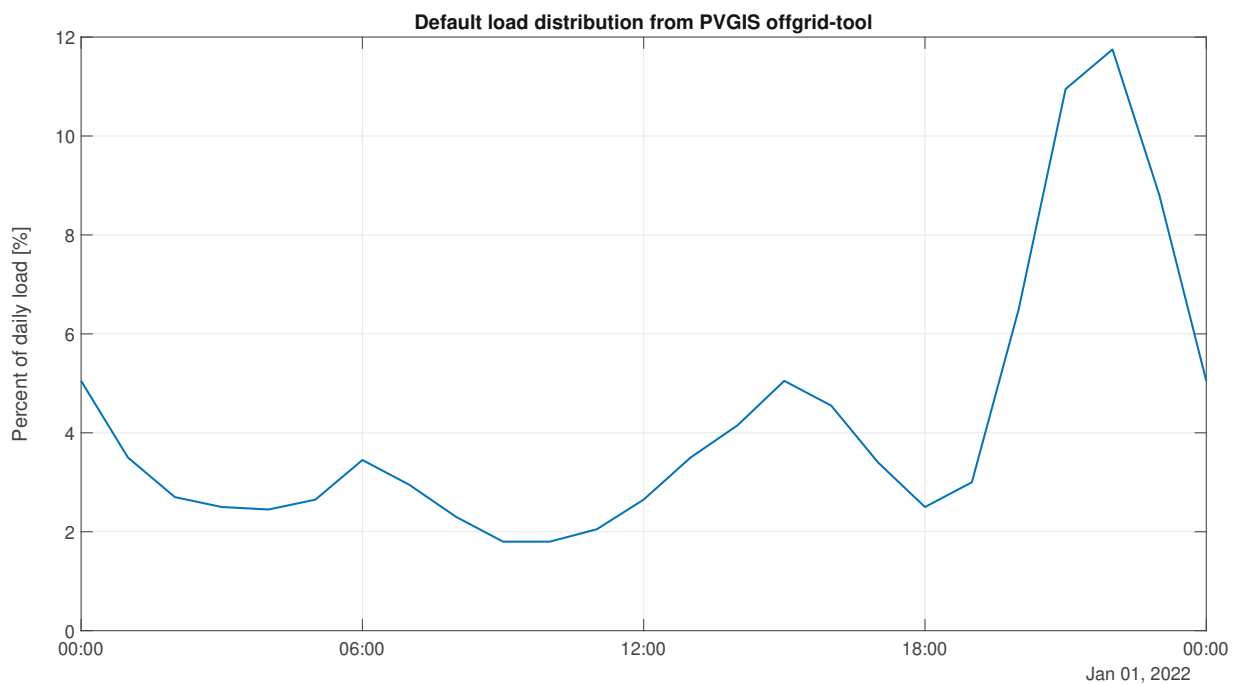


Figure 2.2: PVGIS offgrid calculator load distribution [2]

It is a rather conservative tool, as it uses an overall efficiency ratio of 67% for the whole model [29]. This is intended to cover battery and inverter losses as well as efficiency degradation from the components.

Its outputs consist of the average daily energy generation per month, the average daily energy overproduction, the amount of days the battery is full/empty per month and the statistical information of the average battery charge state per month.

Overall, it can be used to get a very rough and conservative estimation about autarky considering that not many parameters are available. A downside is that it only supports PV and no other electrical generators.

2.3.2 Independence Calculator

Prof. Dr.-Ing habil. Volker Quaschnig is a scientist and author. His book "Regenerative Energiesysteme" [6] was one of the cornerstones and inspirations for this work. On his personal website [30], an autarky calculator is also supplied [31]. The site claims that the computed values can differ up to 10% compared to real systems depending on location and consumption behavior. The user interface of the Independence Calculator is shown in Figure 2.3. The solar power generated is calculated by using one

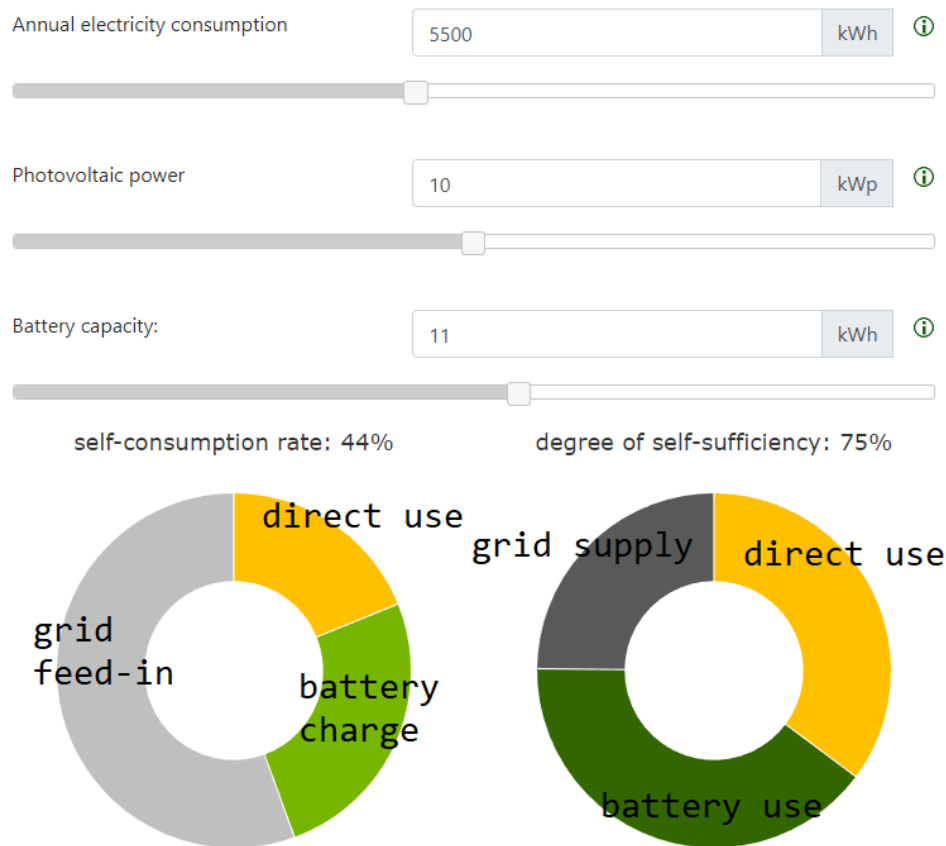


Figure 2.3: Independence calculator from Volker Quaschnig [31]

minute average data from 2002-2006 from the meteorological observatory in Lindenberg, Germany [32]. The solar panels are fixed at a 35° tilt angle and are oriented south. For the PV, an overall performance factor of 83% is used.

The battery has a mean watt hour efficiency of 95%. It is very important to note, that the battery only discharges to 20% and charges to 80% effectively using only 60% of the capacity which is considered as the usable battery capacity parameter. This means that an 11kWh battery in this calculator has a "real" nominal capacity of ≈ 18.34 kWh.

The load distribution of the annual power consumption uses the VDI 4655 (reference load profiles of single family and multi family houses for the use of combined heat and power (CHP) systems).

Additional to Figure 2.3, the simulator shows graphs of self-consumption and self-sufficiency depending on the yearly load, battery and PV size.

Overall, it is an adequate rough estimation and visualization for a given system but sadly, it has even less possibilities for configuration than the PVGIS tool. The fixed PV location and tilt/azimuth further limits its capabilities.

2.3.3 PVAustria

The "Sonnenklar" calculator from PVAustria [33] is also a tool which calculates self-sufficiency (Figure 2.4, 2.5). Details about the calculation methods are not given at all, for questions, a reference to the contact form of PVAustria is given.

While every input parameter has an imposed limit, this tool allows to configure the yearly load and its usage distribution with "how many people are at home during the day on working days". This can be "none", "less than half", "about half", "more than half" or "all". An assumption can be made that because almost only the amount of direct energy usage from the PV increases, the more people are at home, the more the given load distribution centers towards the middle of the day.

The PV tilt can be set in 10° steps from 0-70 and the orientation can be set in 45° steps. The location for irradiation data is given as "Vienna and surrounding area" and is fixed at this "location".

To increase the self-consumption, the option of an electrical load management system is given which seems to further shift the load towards the middle of the day, the effect of the shown test case is 200kWh additional self-usage. Furthermore, there is the possibility of a storage system, either lithium or lead based. Again this simulator uses "usable capacity" which for a lead based storage translates to 50% of nominal capacity with an 80% efficiency and with lithium 90% of nominal capacity and an overall efficiency of 90%. It also allows an option for electrical heating of warm water which does not affect the autarky at all. It is modeled like a dump load which uses excess power generation instead of feeding it to the grid. This exists to allow to use an abundance of energy and is only shown as a performance indicator.

Even though the details of the underlying model are unknown the tool also seems to give a rough estimation for the installation of a PV system and storage. Again, the location of the system is fixed and the parameters are only changeable to some degree. The autarky factor is not given and can not be calculated easily since the output "self-usage with the storage" includes unknown losses so the sum of "self-use direct", "self-use with storage" and "power from grid" sums up to more than the given yearly load.

Figure 2.4: Solar usage calculator from PVAustria - input fields [34]

Kategorie	Wert (kWh)
Erwarteter PV-Ertrag	10.864 kWh
Eigenverbrauch direkt	2.161 kWh
Eigenverbrauch mittels Akku	2.258 kWh
Eigenverbrauch Warmwasserbereitung	0 kWh
Summe Eigenverbrauch im Haushalt	4.419 kWh
Einspeisung ins Stromnetz	6.445 kWh
Strombezug aus dem Netz	1.194 kWh

Kategorie	Wert (kWh)
Eigenverbrauch direkt	2.161
Eigenverbrauch mittels Akku	2.258
Eigenverbrauch Warmwasserbereitung	0
Einspeisung ins Stromnetz	6.445
Strombezug aus dem Netz	1.194

Figure 2.5: Solar usage calculator from PVAustria - storage and results [34]

2.3.4 Autarky Rate Tool

The autarky rate tool is developed by the STORE4HUC [35] project. It aims to supply an evaluation of technical, economical, ecological effects and the autarky rate of the given system. The graphical interface of this tool is shown in Figure 2.6. Something which distinguishes it from the rest is that it

The screenshot displays the graphical user interface of the Autarky Rate Tool, organized into four main sections:

- TYPE OF POWER GENERATION:** Includes fields for TYPE (Photovoltaics), PEAK POWER (10 kWp), ORIENTATION (South), and INCLINATION (40°).
- STORAGE PARAMETER:** Includes fields for USEFUL CAPACITY OF STORAGE (10 kWh) and CHARGING CAPACITY (10 kW).
- CONSUMER CHARACTERISTICS:** Includes fields for CONSUMPTION (5500 kWh/period), CONSUMER TYPE (Family household (2 adults, 3 children)), and COUNTRY (Austria).
- EVALUATION PERIOD:** Includes a date range from 01.01.2022 to 31.12.2022.

Figure 2.6: Autarky rate tool from STORE4HUC [36]

has the option to calculate autarky with not only a PV system but with a wind turbine and a small scale hydropower station as well [37]. The PV power is calculated by using global irradiation data in Neulengbach in Austria from 2016 with an efficiency factor of a solar panel and the overall peak power of the system. The wind power on the other hand is calculated by using a yearly power measurement from Neusiedl am See in 2018 and scaled up according to the user input. The small hydropower station was only measured for one week at an undisclosed location in Austria in 2018. The description claims it did not change a lot over the year so the weekly profile is repeated. Once more, it is scaled up according to the peak power input of the user. A few load profiles are supplied by the LoadProfileGenerator [38] which is another tool to generate load profiles for a year [39]. Again, this allocates the yearly consumption accordingly. Ecological and economical data of the setup are also available. The overall resulting autarky rate is defined by how much of the given household load the system is able to supply. Additionally, it shows how many hours of the year the setup supplies the household with energy.

The performance of the storage system is influenced heavily by the charging capacity. When a storage with 10kWh hours capacity and 10kW charging power is chosen, the system performs worse than when the charging power is 5kW since the so called storage efficiency gets worse with a higher charging power (62.4% with 5kW and 48.4% with 10kW). A higher charging/discharging power leads to an so called increased "own consumption via storage", less feed in to the grid and less hours of

self-supply and more power purchased from the grid thus less autarky. The effect from the "charging capacity" parameter is in general very confusing.

In conclusion, the tool has a highly sophisticated load profile model behind it but lacks different locations for its generation data like the other models mentioned. Compared to other simulators, the storage seems to be modeled very differently.

2.3.5 Benefit Tool/SUSI

Both the Benefit Tool for renewable energy communities [40] as well as the "Strom Unabhängigkeits Simulation" (SUSI) [41] are developed by "Energieinstitut Vorarlberg" [42]. For these tools, the origin of

Strombedarf Gebäude		PV-Anlage	
Strombedarf Haushalt	3000 kWh/Jahr	PV-Größe	10.0 kWp
Heizsystem	<input type="radio"/> nicht elektrisch <input type="radio"/> Infrarot <input checked="" type="radio"/> Wärmepumpe	Ausrichtung	<input checked="" type="radio"/> Eine Richtung <input type="radio"/> 50% Ost/West
Wärmepumpe Effizienz	3.5 JAZ (Jahresarbeitszahl)	Anstellwinkel Abweichung von Horizontale	40 °
Gebäude Heizwärmebedarf	30 kWh/m ² a	Ausrichtungswinkel Abweichung von Süd	0 °
Bruttogeschoßfläche	150 m ²	PV-Ertrag	9147 kWh / Jahr
Personen im Haushalt	4 Personen	davon direkt nutzbar	1771 kWh / Jahr
Bedarf Haustechnik	2477 kWh / Jahr	Batteriespeicher	
Strombedarf gesamt	5477 kWh / Jahr	Batterie vorhanden?	<input checked="" type="radio"/> ja <input type="radio"/> nein
		Batteriegröße	10.0 kWh
		zusätzl. nutzbar	359 kWh / Jahr

Figure 2.7: SUSI from Energieinstitut Vorarlberg [41]

the used data and the used load profiles are unknown. The SUSI seems to be the overall more elaborate one of the two. SUSI is the first simulation where a rough estimation of the load depending on the heat demand of the household can be calculated. Additionally, it allows the PV system to be split into an east/west configuration. A battery system can be implemented as well, giving further options to improve the self-sufficiency.

Both tools put out a self-usage percentage and an autarky factor. The autarky factor of SUSI is claimed to be averaged over 25 years including aging effects of the battery and solar panels. What is interesting to mention is the fact that with a similar inputs, the autarky factor of the benefit tool

and SUSI vary greatly from each other (15-20%). Plots considering the CO_2 output and economic parameters are also available. In short, this is once more a simulation model which does not take geographical information into account. The load profiles are not directly changeable or known. An upside is the additional load demand depending on the heating system which is a nice addition and seems to influence the load distribution.

2.3.6 Existing Models - Conclusion

Overall, the models only give a rough estimation of the viability and quality of the given inputs. Except for the one from PVGIS, all other simulators use fixed irradiation profiles. Another aspect are the load profiles. Depending on the model, they severely vary in complexity and depth. Some simulations handle the storage system in a reasonable way, while others produce results which are not quite plausible. All those aspects call for an autarky simulator which can produce reliable results for different locations and their respective environmental characteristics.

Chapter 3

The Amaterasu Autarky Simulator

In this chapter, the different parts of the autarky model which was created to analyze energy self sufficiency in Austria are shown. At first, the architecture of the tool is presented and a short overview of the used programming language is given. The weather data sources are described and discussed on their validity. The main content of this chapter is the exemplification of the different classes used in the MATLAB program which represents the Amaterasu Autarky Simulator (AAS).

3.1 General Tool Architecture

Figure 3.1 shows the general architecture of the AAS. The input consists of weather data, load profiles and system parameters (PV, wind turbine, storage, heating components, building, etc.). This input is used with the respective modules to generate data of a household for a whole year. Additionally, selected key performance factors are derived from the simulation. As already mentioned, the load

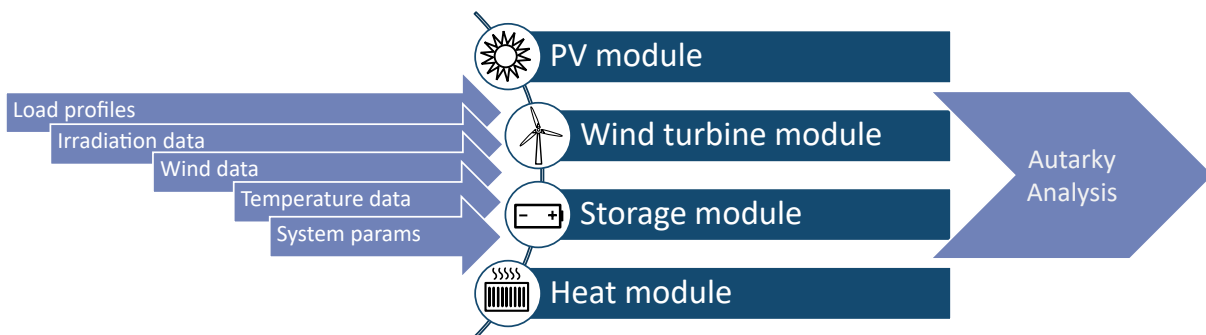


Figure 3.1: Simplified architecture of the AAS

profiles come from the RLS (a separate program) which is described in Section 3.5. The four main models are described in Section 3.3, 3.4, 3.6 and 3.7.

The main requirement for the programming language was the ability to be able to handle large

amounts of data. Additionally, it ideally should be able to calculate large vectors for improved computation time and plot data cleanly. These requirements point to either Python [43] with the Numpy [44] library or Matlab [45]. Since the "Residential Load Simulator" RLS was also written in Matlab and saves its data in .mat files, Matlab was chosen for this work. Additionally, it also allows for uniform and clean data visualization without the need for external libraries. The version used in the AAS is R2021b.

3.2 Acquiring & Verifying Data

The most important input for the proper function of the AAS is proper weather and irradiation data. To satisfy the minimal data needs of the subclasses following inputs are required:

- Global irradiance on a horizontal plane $\left[\frac{W}{m^2}\right]$
- Diffuse irradiance on a horizontal plane $\left[\frac{W}{m^2}\right]$
- Air temperature $[^{\circ}C]$
- Wind speed $\left[\frac{m}{s}\right]$

With these inputs and accompanying parameters, the model is able to calculate PV and wind power generation. Additionally, it allows for a heat model to be created.

3.2.1 ZAMG Data Hub

The "Zentralanstalt für Meteorologie und Geodynamik" (ZAMG) [46] is Austria's largest source of all types of weather data. They also provide their weather data free of charge under the creative common license [47]. Their data can be accessed at their own data hub [48]. There, different measurements can be either gotten via an Application Programming Interface (API) or direct download.

ZAMG Weather Stations with 10min/1h Resolution

The weather station 10min/1h [49] [50] data is a weather dataset with 261 stations in Austria with a great amount of different data i.e. air pressure, humidity and soil temperature in different depths. Out of 261 stations 249 measure global irradiance. Sadly, only a selected few out of those 249 have measurements for diffuse irradiation, making this data source except for those few locations not very viable.

ZAMG INCA_L hourly

The "Integrated Nowcasting through Comprehensive Analysis" (INCA) [51] is an hourly 1km x 1km grid dataset for Austria. This would be nearly ideal, since location specific weather data can be downloaded

Table 3.1: Comparison of weather data at Innsbruck airport. GI is global irradiation and DI diffuse irradiation

Data	Temperature [°C]	Wind speed [m/s]	avg. GI [W/m ²]	avg. DI [W/m ²]
ZAMG 2020	9.8	2.27	154.79	61.51
INCA 2020	9.91	1.84	154.61	-
PVGIS_v2 2020	4.90	0.88	152.29	63.46
PVGIS_v1 TMY	13.20	1.45	142.38	67.54

via API call by giving a time range and the coordinates. Again, only global irradiation is available, thus making this dataset on its own not viable.

3.2.2 PVGIS

The PVGIS [2] uses satellite data and Climate Reanalysis Data [52] to calculate irradiation data for almost every location on the planet. The grid resolution ranges depending on the location from 5.55km to 30km with the smallest time resolution being one hour. Additionally, it uses terrain elevation information with a resolution of about 90m. This allows it to consider shadowing effects from hills and mountains. It has to be mentioned that shadowing from buildings or trees is not considered.

Its original purpose is to give an accurate estimation of PV systems around the planet. It provides all the required data from 2005-2016/2020 (depending on the database/version) and additionally a "Typical Meteorological Year" (TMY) which combines different months to simulate an average year. The data can also be requested with an API call making this data very viable for the given purpose. The only downside with this data is the accuracy of the temperature and wind data. With the newer version of the dataset, temperature and wind values seem to be too low in west Austria. This most likely results from the fact that the data is somewhat interpolated and in mountainous regions this effect is most prominent because of large changes within comparatively small distances. The airport in Innsbruck for example has a ZAMG weather station which can be used to compare the different data.

For the PVGISv1 version the TMY data is taken because its data ranges from 2005-2016 and in 2016 the weather station at the Innsbruck airport did not have data for diffuse irradiation. The overview in Table 3.1 shows that the yearly average of the irradiances are quite similar which at first glance seems accurate enough. Problems arise on the temperature and wind speed (Figure 3.2,3.3) values. A low temperature value leads to an unrealistic heat demand while an inaccurate wind speed could produce too much or too little energy. Both affect the accuracy of the autarky analysis. When using a specific yearly data set, the best case is using the irradiance data from PVGIS and temperature and wind data from INCA. Although the temperature and wind speed from INCA is also not always the same compared to the measured station data, it is the most accurate location flexible weather data available. The only

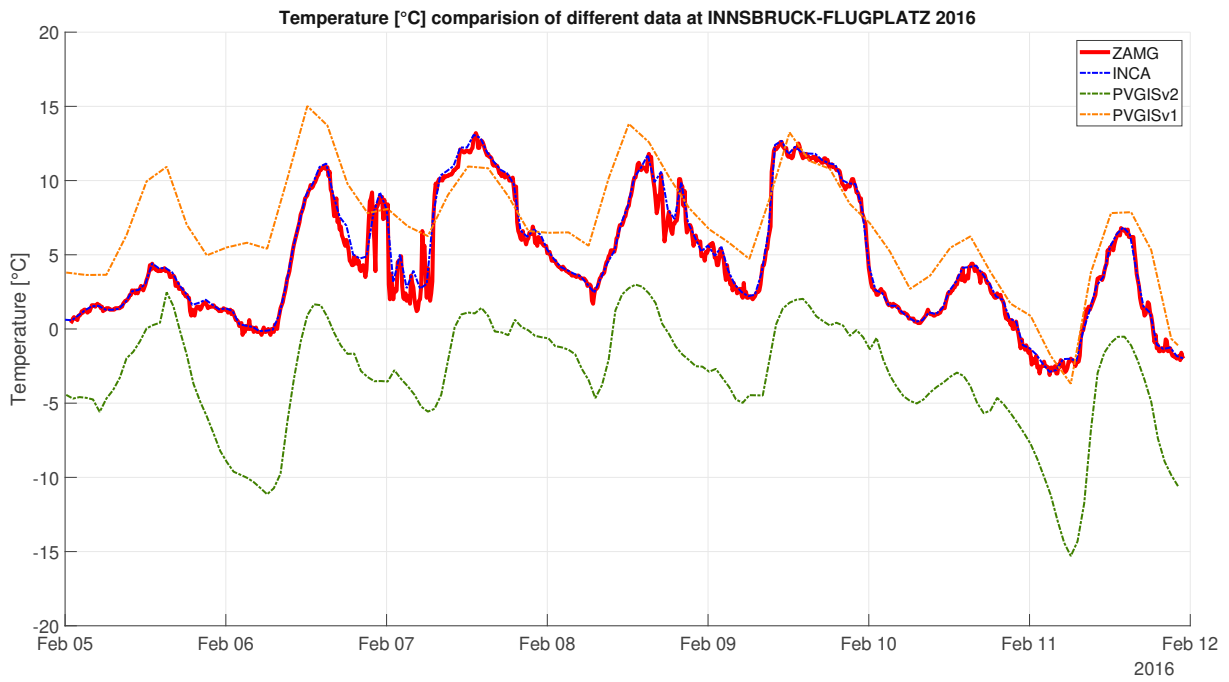


Figure 3.2: Temperature comparison Innsbruck 2016

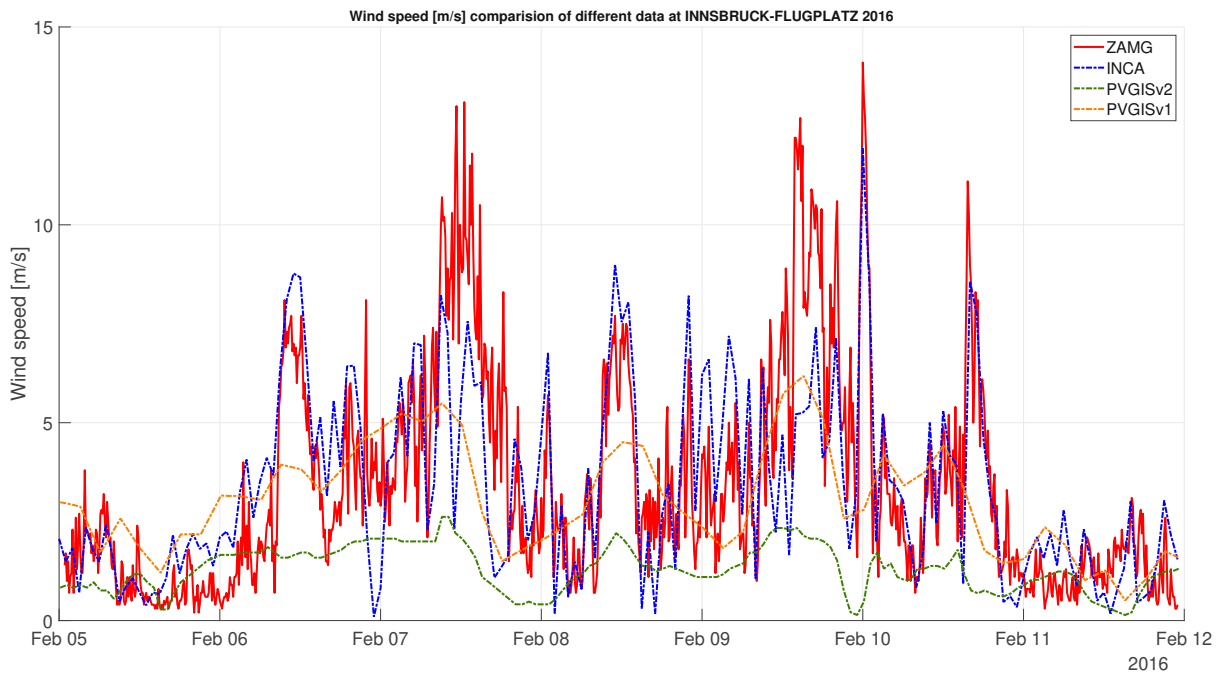


Figure 3.3: Wind speed comparison Innsbruck 2016

downside is that INCA is only available since 2011 and PVGIS is given from 2005-2020.

3.2.3 Verifying Data

Irradiation Data

The irradiation data used in this work is taken from PVGIS which is based on satellite data and a model. A comparison with real measured data from the ZAMG weather stations to verify the data is accurate. The only downside is that not all weather stations provide global irradiation and even less of them diffuse irradiation. Of 261 weather stations which provide global irradiation data, only five of them in all of Austria provide measurements for diffuse irradiation:

- Wien-Hohe Warte
- Innsbruck Flugplatz
- Graz Universität
- Klagenfurt Flughafen
- Sonnblick ("Teilautomatisches-Wetter-Erfassungs-System" (TAWES))

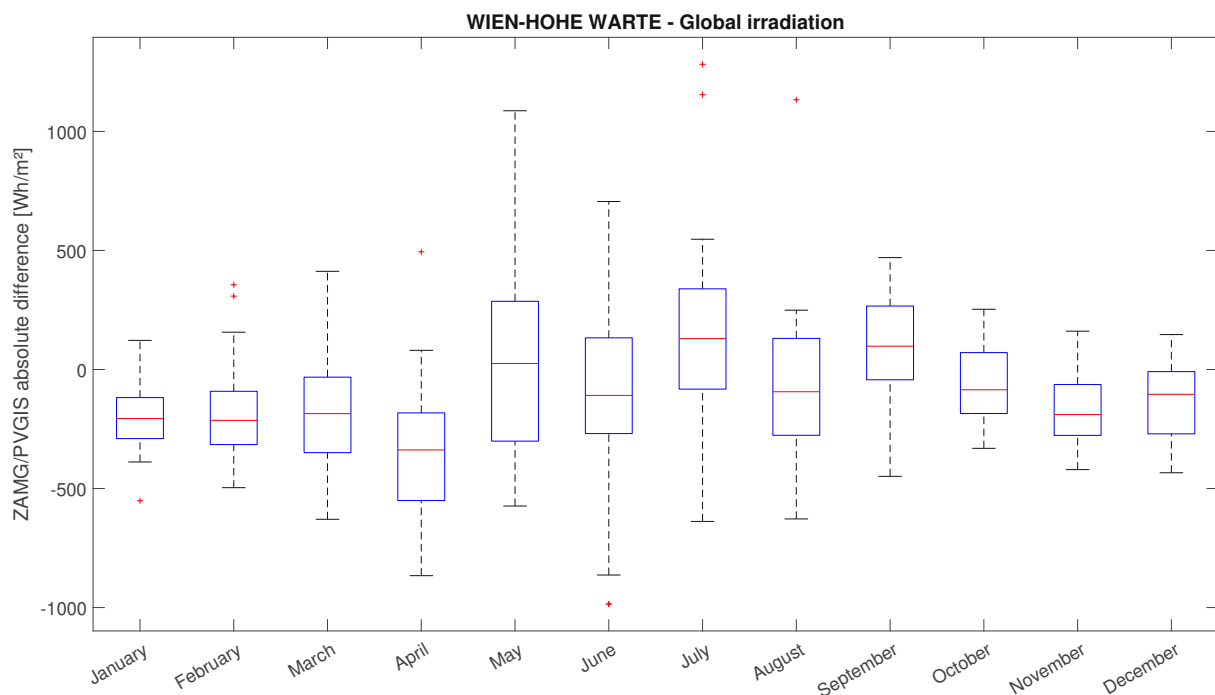


Figure 3.4: Global irradiation comparison ZAMG to PVGIS in 2019

Table 3.2 shows the median difference between the amount of global irradiation which hits the ground daily per month. This means on average, in Vienna January 2019, ZAMG measured 204.62 Wh/m^2 less global irradiation throughout the day compared to PVGIS. Depending on the location, the differences in fall and winter differ a lot without any detectable pattern. The large difference at Sonnblick could stem from the fact that the PVGIS model takes cloud cover into account but since Sonnblick is at 3109m sea

Table 3.2: Daily median of absolute global irradiation difference between ZAMG to PVGIS in Wh/m² per month for 2019

Station	Jan	Feb	Mar	Apr	May	June	July	Aug	Sep	Oct	Nov	Dec
Wien	-204.62	-213.54	-185.8	-337.54	23.99	-108.53	127.93	-99.03	90.82	-91.01	-193.50	-113.00
Klagenfurt	-9.00	-4.73	-121.07	-103.53	242.00	-92.52	-112.83	-23.03	-14.62	-81.00	-163.50	-125.89
Graz	-108.31	-127.46	-170.07	-252.06	-144.00	-285.24	31.00	62.31	-26.03	-18.07	-181.99	-151.91
Innsbruck	273.99	-49.09	-26.03	150.91	549.00	-10.54	318.69	121	-12.70	-35.00	104.99	-10.00
Sonnblick	1040	2828	2912	1642	1770	122.47	392.00	52.00	856.93	625.75	756.21	666.00

level there seem to be far less clouds than at lower altitudes. The resulting solar power generations at Hohe-Warte in Vienna can be seen in Figure 3.5. The difference in power generated for a 10kW PV system (oriented south and tilted 38°, installed at a free standing rack) over the year 2019 is 666kWh (or 5.12%) more for the PVGIS data. In the critical months of November, December, January and February, where there is less solar power in general, the difference in energy production ranges from 120-180kWh per month. Since for most of Austria, measured diffuse irradiation data is not available, when using the PVGIS data as a substitute, the aforementioned effects should be taken into account when analyzing autarky data.

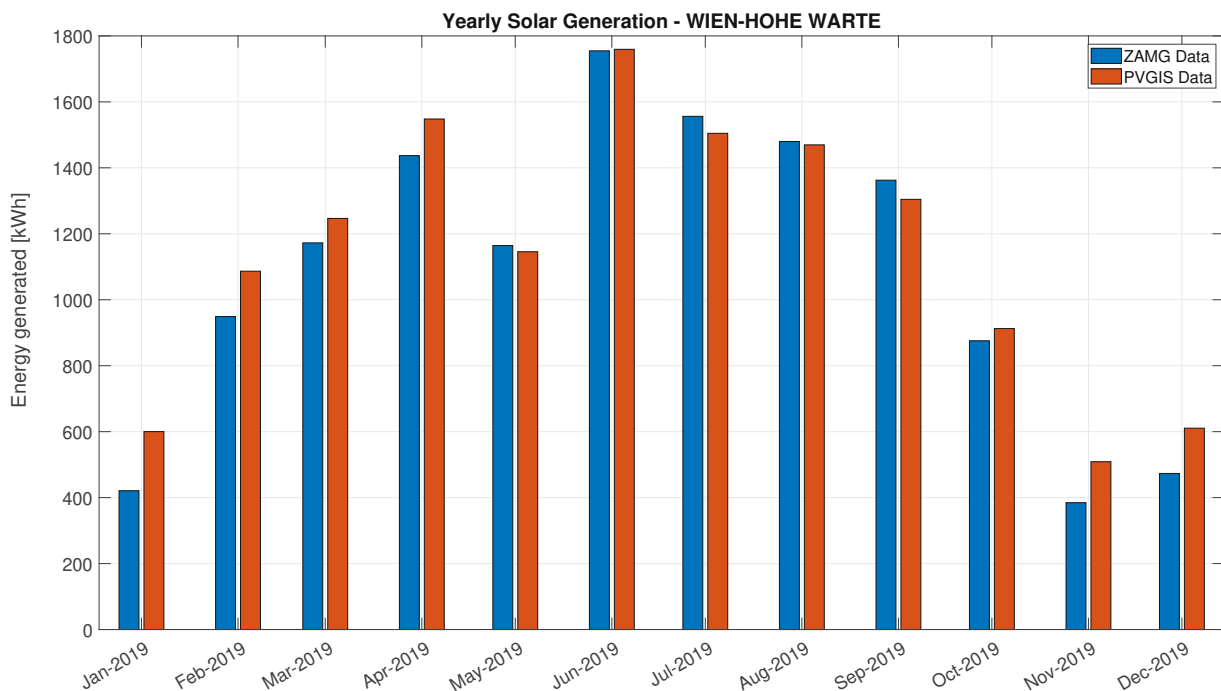


Figure 3.5: Solar energy generation with ZAMG and PVGIS data in 2019

Temperature and Wind Data

As mentioned before, the temperature and wind data is taken from the INCA dataset. Figure 3.6 shows the absolute hourly temperature difference and Figure 3.7 shows the absolute hourly wind speed difference. In both figures, the measured data from ZAMG weather stations are compared to the modeled ones from INCA. In general, temperature and wind speed data is much more accurate compared to the irradiation data. For this reason, a detailed table comparing different locations monthwise is not given here. It has to be mentioned, that at very high altitudes and rough terrain like the station at Sonnblick, the temperature in reality is lower and the value of the wind speed is higher compared to the INCA data. This seems to result from the 1km grid interpolation because there is a large altitude difference within a relatively small distance (i.e., 800m altitude difference in 1km horizontal distance for Sonnblick). Overall, the temperature and wind speed are accurate enough for the model.

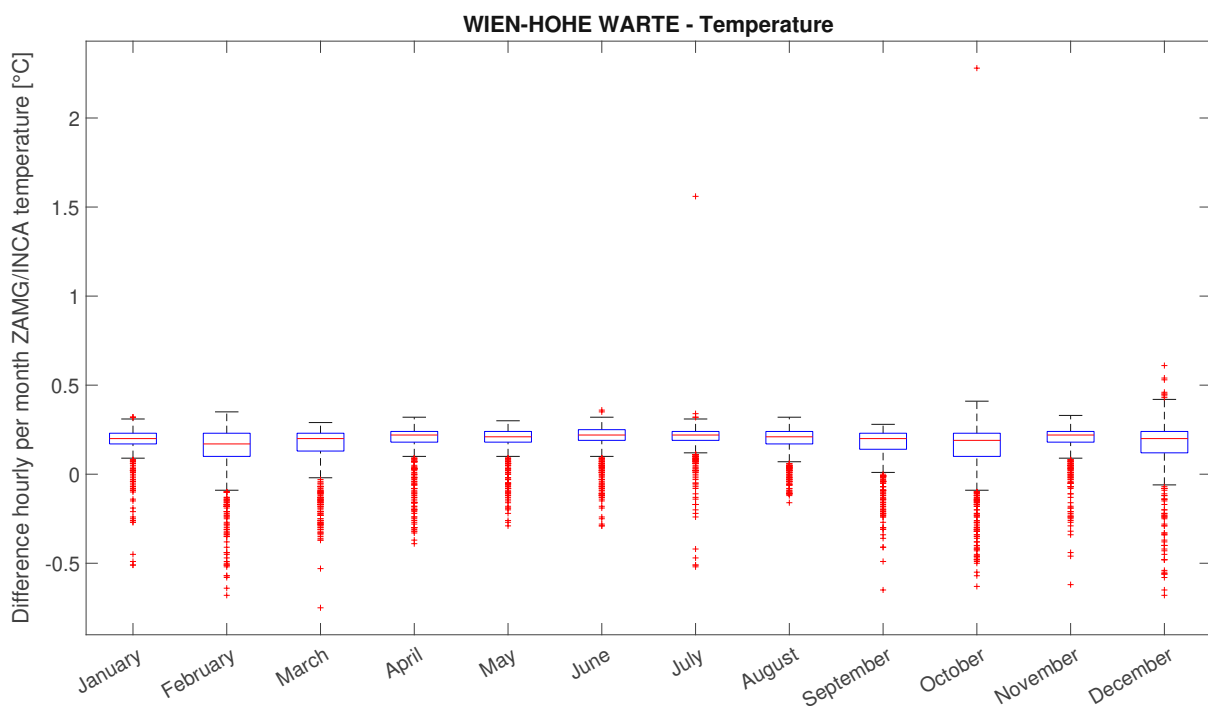


Figure 3.6: Temperature comparison of ZAMG and INCA data in 2019

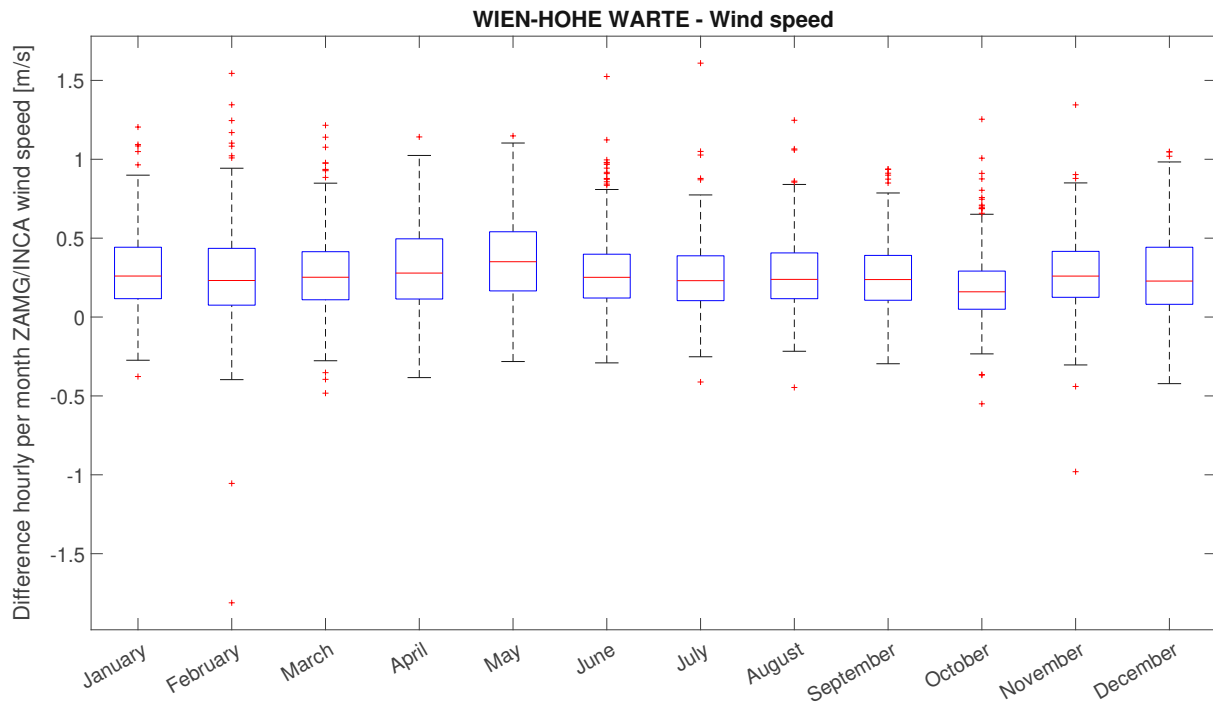


Figure 3.7: Wind speed comparison of ZAMG and INCA data in 2019

3.3 Photovoltaic Model

The PV model is the most important one when considering autarky. Except for shadowing and extreme weather conditions, solar panels provide power throughout the year without long periods of absolutely no energy generation.

3.3.1 Calculation of Sun Angles

To calculate the energy generation, the sun's position throughout the day depending on the location needs to be understood [6] [53]. With the parameter

$$J' = 360^\circ \cdot \frac{\text{DayOfYear}}{\text{DaysInYear}} \quad (3.1)$$

the sun declination $\delta(J')$ can be calculated:

$$\delta(J') = [0.3948 - 23.2559 \cdot \cos(J' + 9.1^\circ) - 0.3915 \cdot \cos(2 \cdot J' + 5.4^\circ) - 0.1764 \cdot \cos(3 \cdot J' + 26^\circ)]^\circ \quad (3.2)$$

Figure 3.8 shows the solar declination angle, it ranges between $+23.45^\circ$ and -23.45° during the year, a

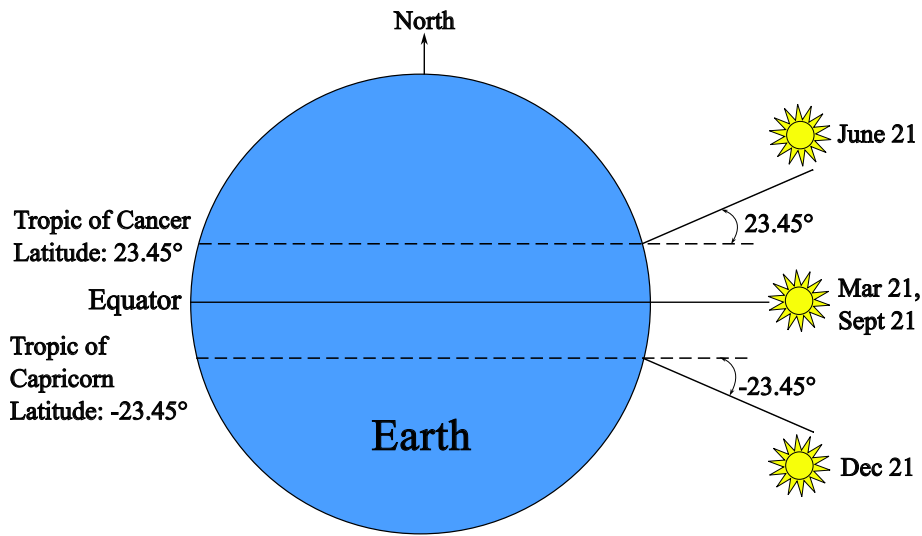


Figure 3.8: Illustration of the solar declination angle, taken from [54]

time Equation $T_{eq}(J')$ which corrects for the eccentricity of the Earth's orbit and its axial tilt is needed

$$T_{eq}(J') = [0.0066 + 7.3525 \cdot \cos(J' + 85.9^\circ) + 9.9359 \cdot \cos(2 \cdot J' + 108.9^\circ) + 0.3387 \cdot \cos(3 \cdot J' + 105.2^\circ)]min \quad (3.3)$$

With the local time LT in minutes, the timezone TZ in hours (i.e. CET $TZ = +1h$, CEST $TZ = +2h$) and the longitude of the location λ , the mean location time MLT is calculated.

$$MLT = [LT - TZ \cdot 60 + 4 \cdot \lambda \cdot min/^\circ] \quad (3.4)$$

It is very important to note that Equation 3.4 will calculate the sun height according to the local timezone. In this model, all the received irradiation data has timestamps in UTC. To calculate the sun height accordingly, TZ needs to be 0. The factor 4 is because the earth rotates 1° every minute. The last two equations 3.3 and 3.4 lead to the true location time TLL .

$$TLL = [MLT + T_{eq}(J')]min \quad (3.5)$$

To calculate the hour angle ω , TLL needs to be converted to hours ($TLL_h = TLL/60$)

$$\omega = [12 - TLL_h] \cdot 15^\circ/h \quad (3.6)$$

with the latitude of the location φ and the sun height γ_s , the required sun azimuth α_s can be calculated.

$$\gamma_s = -\arcsin(\cos(\omega) \cdot \cos(\varphi) \cdot \cos(\delta(J')) + \sin(\varphi) \cdot \sin(\delta(J'))) \quad (3.7)$$

$$\alpha_s = \begin{cases} 180 - \arccos\left(\frac{\sin(\gamma_s) \cdot \sin(\varphi) - \sin(\delta)}{\cos(\gamma_s) \cdot \cos(\varphi)}\right) & TLT_h \leq 12h \\ 180 + \arccos\left(\frac{\sin(\gamma_s) \cdot \sin(\varphi) - \sin(\delta)}{\cos(\gamma_s) \cdot \cos(\varphi)}\right) & TLT_h \geq 12h \end{cases} \quad (3.8)$$

It is important to note that when calculating Equation 3.8, the geographical north is equal to 0° and south is 180° . By subtracting 180° from α_s 0° will be south and $\pm 180^\circ$ north which is the reference system used in this work.

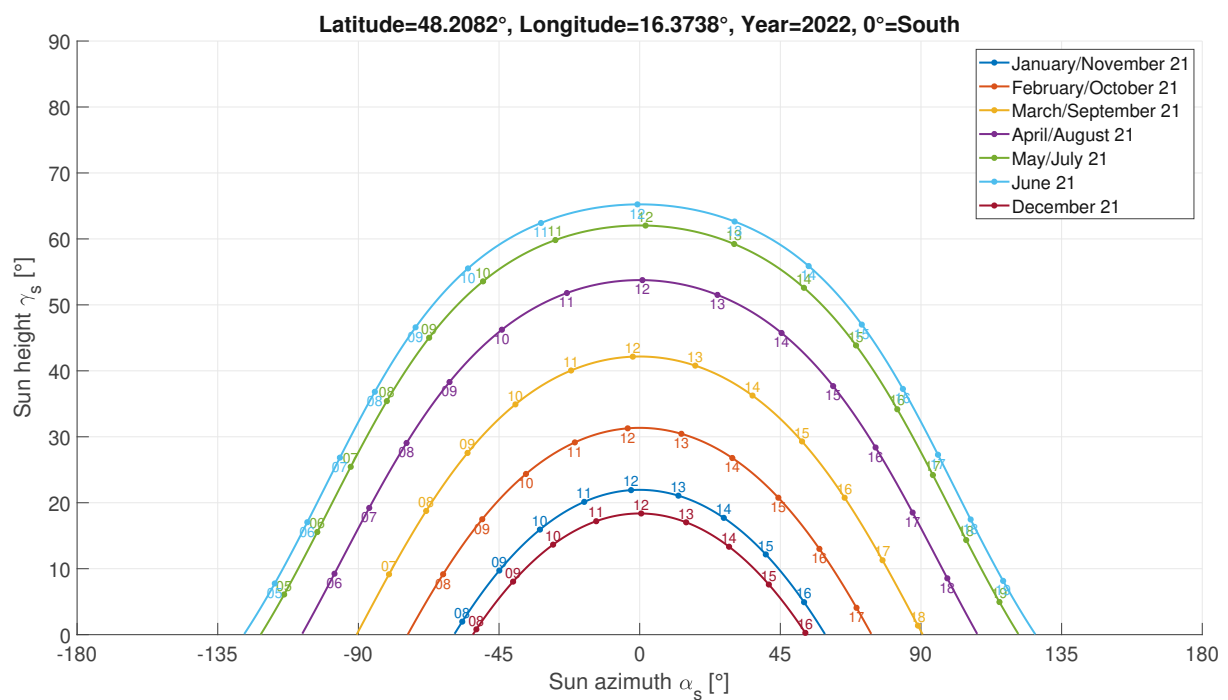


Figure 3.9: Sun path diagram for Vienna

Figures 3.9, 3.10 and 3.11 show the course of the sun throughout the year at different times. When the longitude of the location is between the values of the solar declination angle ($\pm 23.45^\circ$, Figure 3.8), the general notion that the sun has its highest point always in the same direction is not applicable (Figure 3.10).

The sun angle on a horizontal plane also labeled the zenith angle Θ_z can be easily derived with:

$$\Theta_z = 90^\circ - \gamma_s \quad (3.9)$$

Since most solar panels are placed horizontal to the ground, the so called Angle Of Incidence (AOI)

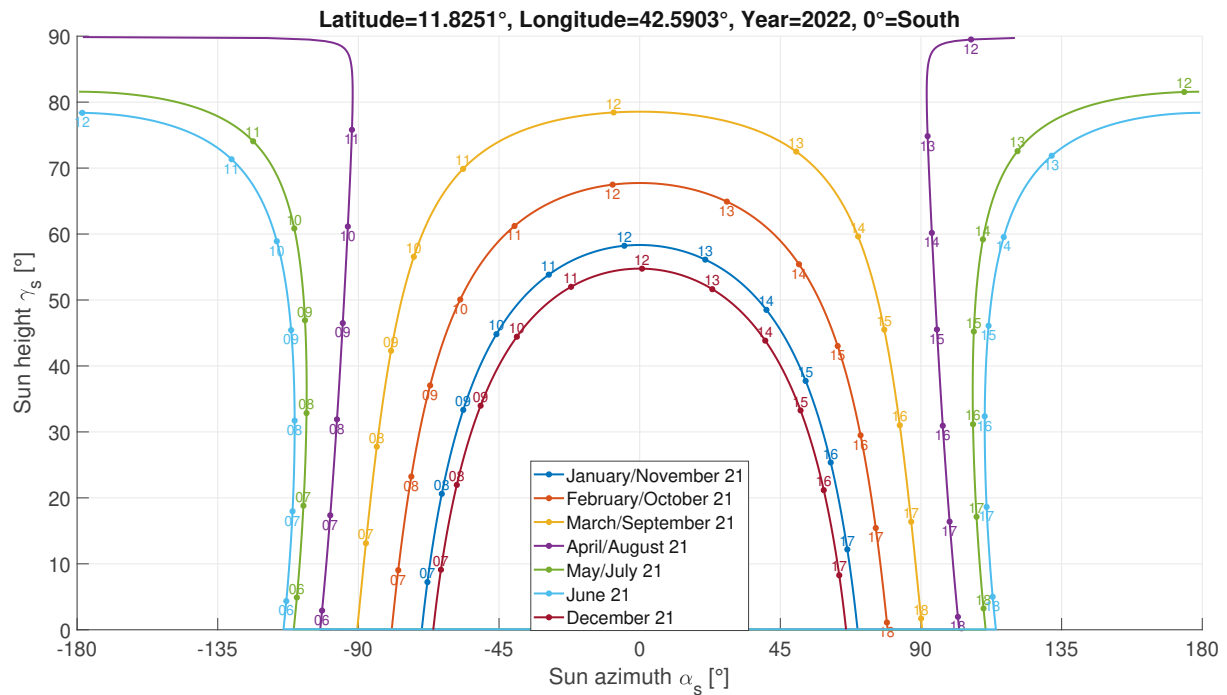


Figure 3.10: Sun path diagramm for Djibuti

Θ_i is needed. It describes the angle of the sun relatively to a plane which is tilted by the tilt angle γ_t and pivoted by the azimuth angle α_t . To keep the input of the azimuth angles of the tilted plane as 0° South, -90° East, $+180^\circ$ North and $+90^\circ$ West, an offset of 180° is needed. $\alpha_{toff} = \alpha_t + 180^\circ$. With this knowledge, the AOI can be calculated as follows:

$$\Theta_i = \arccos(-\cos(\gamma_s) \cdot \sin(\gamma_t) \cdot \cos(\alpha_s - \alpha_{toff}) + \sin(\gamma_s) \cdot \cos(\gamma_t)) \quad (3.10)$$

To avoid any calculation errors especially at sunrise and sunset, if the AOI is greater than 90° , it is set to 90° . Figure 3.12 shows a graphical representation of the aforementioned angles for a better understanding.

3.3.2 Calculation of Irradiance on Inclined Planes

There are four different types of irradiances used in this model:

- Global irradiance G - all components summarized
- Direct beam irradiance G_b - the direct component of the sun
- Diffuse irradiance G_d - the diffuse component of the sun refracted by clouds
- Reflected irradiance G_r - the reflective component of the sun reflected from the ground

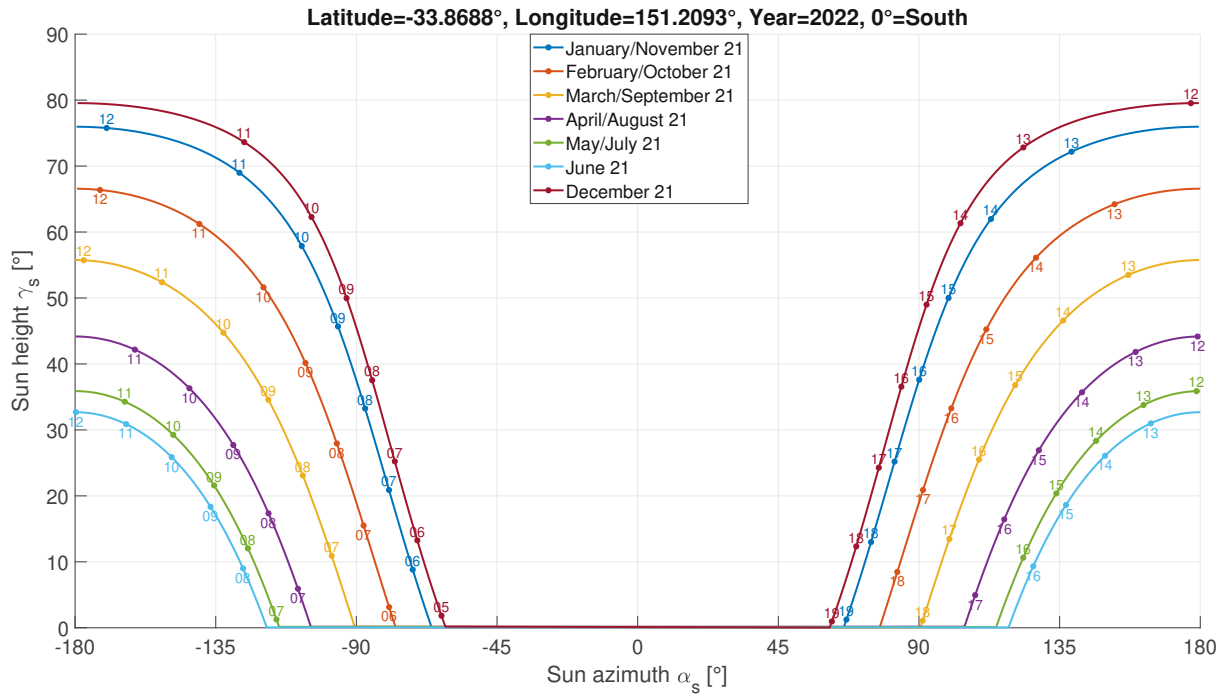


Figure 3.11: Sun path diagramm for Sydney

They are all measured in W/m^2 and stand in relation by:

$$G = G_b + G_d + G_r \quad (3.11)$$

To calculate the global irradiance on a tilted plane G_t , the horizontal direct beam and diffuse irradiance is needed. PVGIS provides two different types of data. One is the TMY which contains:

- Global irradiance on the horizontal plane G_h
- Direct beam irradiance on a plane always normal to the sun rays G_{bn}
- Diffuse irradiance on the horizontal plane G_{dh}

In this format, the direct beam irradiance on the horizontal plane G_{bh} can be calculated with:

$$G_{bh} = G_h - G_{dh} \quad (3.12)$$

On the horizontal plane there is no reflected irradiance so it can be ignored. The hourly data provides the already calculated irradiance data on any inclined plane if requested. To calculate the irradiance for an inclined plane oneself, the irradiance on a horizontal plane (tilt:0°, azimuth:0°) is requested and consists of:

- Global irradiance on the tilted plane G_h

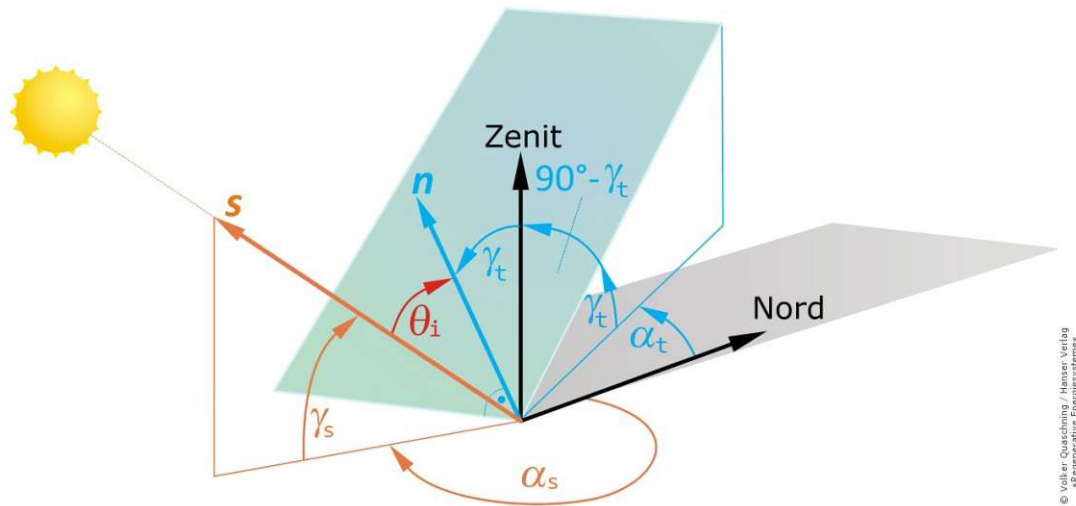


Figure 3.12: Illustration of the AOI (taken from [6] with edited names)

- Direct beam irradiance on the inclined plane G_{bi}
- Diffuse irradiance on the inclined plane G_{di}
- Reflected irradiance on the inclined plane G_{ri}

As already mentioned, since there is no reflective component on a horizontal plane, all the entries for G_{ri} are empty.

Direct Irradiance on an Inclined Plane

With the AOI Θ_i gotten from Equation 3.10 the tilt factor T_f can be derived:

$$T_f = \frac{\cos(\Theta_i)}{\sin(\gamma_s)} \quad \Theta_i > 90^\circ = 90^\circ \quad (3.13)$$

Equation 3.13 is slightly modified compared to other literature [6] [55] by setting all Θ_i larger than 90° to 90° . The reason for this is that at early or late sun hours the AOI is $>90^\circ$ which means that there physically can not be any direct irradiation on the plane. This would normally lead to a negative T_f and furthermore to a negative power generation. When looking at the output data from the PVGIS tool, it seems this step was also taken although not noted anywhere.

After that, the direct beam irradiance on the horizontal plane is multiplied with T_f . This leads to the irradiance on an inclined plane E_{bi} which is tilted by γ_t and rotated by α_t

$$E_{bi} = G_{bh} \cdot T_f \quad (3.14)$$

Table 3.3: Coefficients depending on ε [6] [58]

ε	F_{11}	F_{12}	F_{13}	F_{21}	F_{22}	F_{23}
1.000-1.065	-0.008	0.588	-0.062	-0.060	0.072	-0.022
1.065-1.230	0.130	0.683	-0.151	-0.019	0.066	-0.029
1.230-1.500	0.330	0.487	-0.221	0.055	-0.064	-0.026
1.500-1.950	0.568	0.187	-0.295	0.109	-0.152	-0.014
1.950-2.800	0.873	-0.392	-0.362	0.226	-0.462	0.001
2.800-4.500	1.132	-1.237	-0.412	0.228	-0.823	0.056
4.500-6.200	1.060	-1.600	-0.359	0.264	-1.127	0.131
≥ 6.200	0.678	-0.327	-0.250	0.156	-1.377	0.251

Diffuse Irradiance on an Inclined Plane

For the diffuse irradiance, the Perez model is used [6] [56]. To calculate the irradiance, following variables have to be derived first. To start, the Air Mass (AM) is calculated:

$$AM = \frac{1}{\sin(\gamma_s)} \quad (3.15)$$

With the AM and the solar constant $E_0 = 1361 \text{ W/m}^2$ [57] the brightness index Δ can be derived:

$$\Delta = AM \cdot \frac{G_{dh}}{E_0} \quad (3.16)$$

The previously calculated solar zenith angle Θ_z (Equation 3.9) is used again, this time in radian $\Theta_{z,rad}$. By defining another constant $\kappa = 1.041$, the sky brightness index ε can be determined by:

$$\varepsilon = \frac{\frac{G_{dh} + G_{bh} \cdot \sin(\gamma_s)^{-1}}{G_{dh}} + \kappa \cdot \Theta_{z,rad}^3}{1 + \kappa \cdot \Theta_{z,rad}^3} \quad (3.17)$$

After that, ε can be used to look up the coefficients F_{11} , F_{12} , F_{13} , F_{21} , F_{22} and F_{23} from Table 3.3. There are also updated coefficients from another more recent paper (Table 3.4). These result in an overall lower diffuse irradiance. Because the paper is more recent and seeks to improve the model, the values from Table 3.4 are chosen.

These coefficients allow to calculate the generic circumsolar (F_1) and horizon brightening (F_2) coefficient.

$$F_1 = F_{11}(\varepsilon) + F_{12}(\varepsilon) \cdot \Delta + F_{13}(\varepsilon) \cdot \Theta_{z,rad} \quad (3.18)$$

$$F_2 = F_{21}(\varepsilon) + F_{22}(\varepsilon) \cdot \Delta + F_{23}(\varepsilon) \cdot \Theta_{z,rad} \quad (3.19)$$

Table 3.4: Updated coefficients depending on ε [55]

ε	F_{11}	F_{12}	F_{13}	F_{21}	F_{22}	F_{23}
1.000-1.065	-0.196	1.084	-0.006	-0.114	0.180	-0.019
1.065-1.230	0.236	0.519	-0.180	-0.011	0.020	-0.038
1.230-1.500	0.454	0.321	-0.255	0.072	-0.098	-0.046
1.500-1.950	0.866	-0.381	-0.375	0.203	-0.403	-0.049
1.950-2.800	1.026	-0.711	-0.426	0.273	-0.602	-0.061
2.800-4.500	0.978	-0.986	-0.350	0.280	-0.915	-0.024
4.500-6.200	0.748	-0.913	-0.236	0.173	-1.045	0.065
≥ 6.200	0.318	-0.757	0.103	0.062	-1.698	0.236

Table 3.5: Albedo ρ for different surfaces

Surface	Albedo ρ
Fresh snow [59]	0.80
Ocean ice [59]	0.50-0.70
New concrete [59]	0.55
Desert sand [60]	0.36
Green grass [59]	0.25
Deciduous forest [60]	0.17-0.18
Bare soil [59]	0.17
Tropical forest [60]	0.12-0.15
Evergreen forest [60]	0.12-0.13
Open ocean [60]	0.07

Furthermore, the coefficient limits a and b are derived:

$$a = \max(0, \cos(\Theta_i)) \quad (3.20)$$

$$b = \max(\cos(85^\circ), \cos(\gamma_s)) \quad (3.21)$$

At last, the diffuse irradiance on the inclined plane can be derived with:

$$E_{di} = G_{dh} \cdot \left((1 - F_1) \cdot \frac{1 + \cos(\gamma_t)}{2} + \frac{a}{b} \cdot F_1 + F_2 \cdot \sin(\gamma_t) \right) \quad (3.22)$$

Reflected irradiance on an Inclined Plane

The reflected irradiance is derived rather simple, the only new coefficient is the albedo ρ . It represents the reflectivity of the ground in percent. Table 3.5 shows the albedo values for different surfaces. In general, if the surface is unknown a fixed value of $\rho = 0.2$ is used [55]. The formula for the reflected irradiance is:

$$E_{ri} = \frac{(G_{bh} + G_{dh}) \cdot \rho \cdot (1 - \cos(\gamma_t))}{2} \quad (3.23)$$

Table 3.6: Coefficients to calculate angular losses [61]

Type	a_r	c_1	c_2
m-Si	0.169	$4/(3\pi)$	-0.069
p-Si	0.159	$4/(3\pi)$	-0.074
a-Si	0.163	$4/(3\pi)$	-0.074

3.3.3 Calculation of Angular Losses

When irradiation hits the surface of the solar panel, a part of it will be reflected away without contributing energy to the module. These losses can be calculated with the model from [61] [62]. For this model, again, a few variables are needed: the angular loss coefficient a_r and the fitting parameters c_1 and c_2 . These differ depending on the different manufacturing structure of the solar panel. Table 3.6 expects panels devoid of any dust or dirt. With medium dust quantity a_r increases to 0.2 and with large dust quantity to 0.27, but this is not considered in the present model. This allows the angular loss factors for direct beam AlF_b , diffuse AlF_d and reflected irradiance AlF_r to be derived with:

$$AlF_b = \frac{\exp(-\cos(\Theta_i/a_r)) - \exp(-1/a_r)}{1 - \exp(-1/a_r)} \quad (3.24)$$

$$AlF_d = \exp \left[-\frac{1}{a_r} \left(c_1 \left(\sin(\gamma_t) + \frac{\pi - \gamma_{t,rad} - \sin(\gamma_t)}{1 + \cos(\gamma_t)} \right) + c_2 \left(\sin(\gamma_t) + \frac{\pi - \gamma_{t,rad} - \sin(\gamma_t)}{1 + \cos(\gamma_t)} \right)^2 \right) \right] \quad (3.25)$$

$$AlF_r = \exp \left[-\frac{1}{a_r} \left(c_1 \left(\sin(\gamma_t) + \frac{\gamma_{t,rad} - \sin(\gamma_t)}{1 - \cos(\gamma_t)} \right) + c_2 \left(\sin(\gamma_t) + \frac{\gamma_{t,rad} - \sin(\gamma_t)}{1 - \cos(\gamma_t)} \right)^2 \right) \right] \quad (3.26)$$

Considering that when γ_t is 0° AlF_r can be ignored since there is no reflected irradiance. The final irradiance values on the inclined plane are:

$$E_{bil} = (1 - AlF_b) \cdot E_{bi} \quad (3.27)$$

$$E_{dil} = (1 - AlF_d) \cdot E_{di} \quad (3.28)$$

$$E_{ril} = (1 - AlF_r) \cdot E_{ri} \quad (3.29)$$

And the overall irradiance on an inclined plane considering the angular losses:

$$E_{G_{il}} = E_{bil} + E_{dil} + E_{ril} \quad (3.30)$$

Table 3.7: Roughness length for different terrains [6]

Terrain	Roughness length z_0 [m]
Open sea	0.0002
Wadden sea	0.005
Flat terrain, pastures	0.03
Agricultural terrain, small quantity	0.1
Agricultural terrain, high quantity	0.25
Park terrain, bushes and trees	0.5
Woodland, villages, suburbs	1
City centers	2

Table 3.8: Coefficients to calculate the temperature of rack mounted solar panels [64] [65]

Type	u_0 [W/(°Cm ²)]	u_1 [W/(°Cm ²)]
c-Si	26.90	6.20
a-Si	25.70	6.29
CdTe	23.40	5.44
CIS	23.09	3.11

3.3.4 Temperature of PV Modules

The efficiency of a PV panel is highly dependent on its temperature. Besides the environmental temperature, the amount of irradiance and the wind speed influence it greatly. Since wind is measured most of the time at a height of 10m, it can be scaled to a different height using the log wind profile with the roughness length z_0 . There is also the parameter d which is called "zero displacement" in meters. It can be estimated as around 70% of a given obstacle height. If obstacles are spread wide, it can be set to 0 which is used in this model. With the roughness length from Table 3.7, the wind speed can be transformed from a measured height h_1 to any given height h_2 .

$$v(h_2) = v(h_1) \cdot \frac{\ln\left(\frac{h_2-d}{z_0}\right)}{\ln\left(\frac{h_1-d}{z_0}\right)} \quad (3.31)$$

Free Standing Rack mounted Panels

To calculate the temperature of free standing rack mounted solar panels the following simple model is used [63]. This time, the calculation uses coefficients depending on the material of the solar panel. This allows the module temperature T_{mod} to be calculated with the environmental temperature T_{env} , the wind speed at the height of the installed module v_{wind} , the irradiance with losses (since the reflected light does not contribute to the warming of the module) and the coefficients u_0 and u_1 (Table 3.8):

$$T_{mod} = T_{env} + \frac{E_{Gill}}{u_0 + u_1 \cdot v_{wind}} \quad (3.32)$$

Table 3.9: Coefficients to calculate the temperature of roof mounted mono crystalline solar panels for different gap size [66]

Gap [cm]	w_1	w_2	w_3	c
0	0.034	0.74	-2.02	12.44
2.54	0.033	0.74	-2.31	12.78
5.08	0.033	0.72	-2.53	13.09
7.64	0.032	0.69	-2.85	14.45
10.18	0.029	0.66	-2.99	14.93

Table 3.10: Coefficients to calculate the temperature of roof mounted poly crystalline solar panels for different gap size [66]

Gap [cm]	w_1	w_2	w_3	c
0	0.033	1.08	-1.89	8.09
2.54	0.032	1.10	-1.91	7.16
5.08	0.033	1.05	-2.20	8.80
7.64	0.031	1.02	-2.85	9.90
10.18	0.029	1.02	-3.12	9.95

Panels on Roofs

Most of the PV panels for private use are mounted on roofs to save space. However, this leads to the temperature being higher compared to the free standing variant. A model for mono- and poly crystalline silicon is used [66]. Similarly to other models, coefficients are gotten from measurements (Table 3.9, 3.10). With these parameters, the module temperature can be derived as follows:

$$T_{mod} = w_1 \cdot E_{G\Delta} + w_2 \cdot T_{env} + w_3 \cdot v_{wind} + c \quad (3.33)$$

At the highest gap of 10.18cm from the roof, the temperature values of the modules were not that much higher than the free standing rack.

3.3.5 Power Generation from PV Panels

At last, the power which actually can be generated by the PV modules can be calculated using an equation which is dependent on irradiation and once more coefficients depending on the solar cell material. The following equation factors in the dependence of power generation on low irradiance and temperature [67]. The constants in Table 3.11 can be used to calculate the power produced by the solar panels.

$$P_{gen} = G_s \cdot P_{STC} \cdot (1 + k_1 \cdot \ln(G_s) + k_2 \cdot \ln(G_s)^2 + k_3 \cdot T_{\Delta} + k_4 \cdot T_{\Delta} \cdot \ln(G_s) + k_5 \cdot T_{\Delta} \cdot \ln(G_s)^2 + k_6 \cdot T_{\Delta}^2) \quad (3.34)$$

Table 3.11: Coefficients for calculation of solar power generation [55]

Coefficient	c-Si	CIS	CdTe
k_1	-0.017237	-0.005554	-0.046689
k_2	-0.040465	-0.038724	-0.072844
k_3	-0.004702	-0.003723	-0.002262
k_4	0.000149	-0.000905	0.000276
k_5	0.000170	-0.001256	0.000159
k_6	0.000005	0.000001	-0.000006

E_{std} describes the standard test irradiance which is $1000\text{W}/\text{m}^2$ for most commercial available panels. P_{STC} describes the amount of Watt the sum of the panels are rated for, i.e. 5 panels at 400W equals 2000W P_{STC} . T_{std} is the standard environmental test temperature which is often 25°C . $T_\Delta = T_{mod} - T_{std}$ and $G_s = \frac{E_{G_{il}}}{E_{std}}$. Additionally, to simulate inverter efficiency, an "European efficiency" η_{EE} value from the datasheet [68] of inverters can be used to describe losses from transforming DC to AC

$$P_{gen,real} = P_{gen} \cdot \eta_{EE} \quad (3.35)$$

Alternatively, the efficiency curve depending on load in the datasheet [68] is used to calculate the factor for each derived value.

3.4 Wind Turbine Model

In this section the wind turbine model is discussed. To start, the wind speed at the installed height of the wind turbine is needed. For this, Equation 3.31 can be used again.

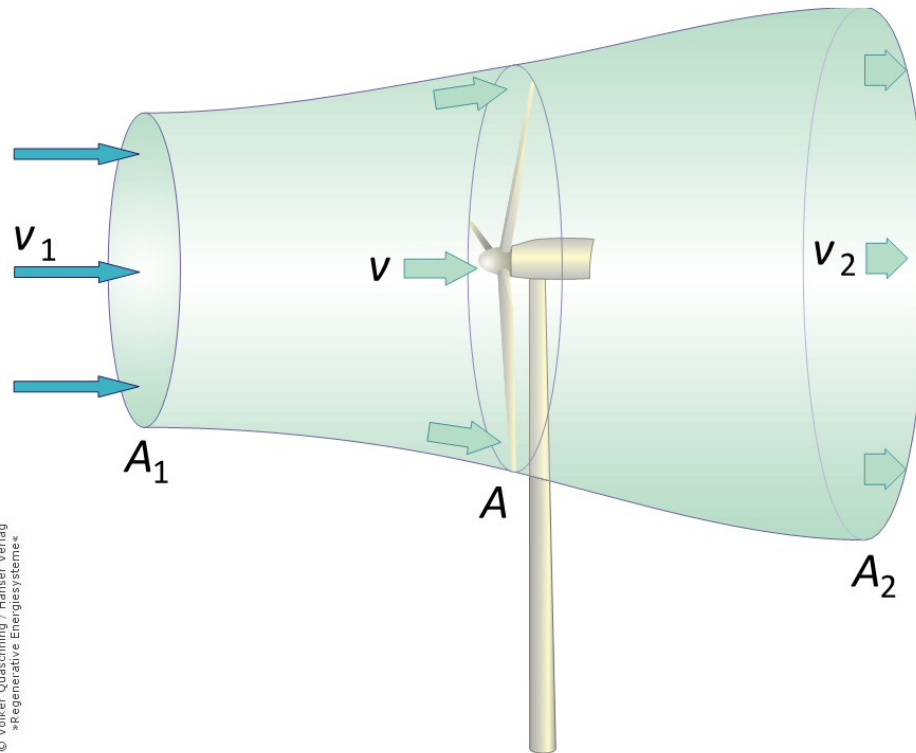


Figure 3.13: Illustration of a wind turbine and its area of attack (taken from [6])

An important factor is the air density which influences how much power the wind has. The power of the wind can be calculated with:

$$P_{wind} = \frac{1}{2} \cdot \rho \cdot A \cdot v^3 \quad (3.36)$$

Where ρ is the air density [kg/m^3], the area of attack A [m^2] and the height scaled wind speed v [m/s].

3.4.1 Calculation of the Air Density

Since depending on the data (TMY, ZAMG, PVGIS hourly), the pressure and humidity is or is not available, there are two different approaches for calculating air density.

Air Density of Dry Air

When only the measured environmental temperature is available, the air density can be approximated using the ideal gas law.

$$\rho_{dry} = \frac{p_0}{R_s \cdot (273.15 + T_{env})} \quad (3.37)$$

p [Pa] is the absolute pressure, $R_s = 287.0528$ [J/(kg·K)] the specific gas constant for dry air and T_{env} [°C] the environmental temperature. Since p is unknown it is set to sea level pressure of $p_0 = 100000$ Pa. At Neusiedl am See in Burgenland, which is at a really low elevation of 133m, the mean difference between using p_0 and measured pressure for air density calculations is about +0.6%. At Spiess in Tyrol (elevation 1804m) this difference increases to +22.58%. For this reason, the approximation of pressure depending on elevation is used [69]:

$$p(h) \approx \exp\left(-\frac{g \cdot h \cdot M}{T_0 \cdot R_0}\right) \quad (3.38)$$

Where h [m] is the elevation, $g = 9.80665$ [m/s²] the earth surface gravitational acceleration, $M = 0.02896968$ [kg/mol] the molar mass of dry air, $R_0 = 8.314462618$ [J/(mol·K)] and $T_0 = 288.16$ [K] the sea level standard temperature. Using this approximation the difference is greatly reduced to -1.02%.

Air Density with Pressure and Humidity

Since humidity influences the specific gas constant of air R_F , it has to be calculated beforehand [70].

$$R_F = \frac{R_s}{1 - \varphi \cdot \frac{p_d}{p} \cdot \left(1 - \frac{R_s}{R_d}\right)} \quad (3.39)$$

φ is the relative humidity (i.e. 45% = 0.45), R_s the gas constant of dry air, $R_d = 461.523$ the gas constant of water vapor, p the pressure and p_d the saturation vapor pressure.

The Magnus formula can be used to derive p_d [71]. First the coefficients depending on temperature need to be defined:

$$C_1 = \begin{cases} 17.08085 & T_{env} \geq 0^\circ\text{C} \\ 17.84362 & T_{env} < 0^\circ\text{C} \end{cases}, C_2 = \begin{cases} 234.175^\circ\text{C} & T_{env} \geq 0^\circ\text{C} \\ 245.425^\circ\text{C} & T_{env} < 0^\circ\text{C} \end{cases} \quad (3.40)$$

$$p_d = 610.78 \cdot \exp\left(\frac{C_1 \cdot T_{env}}{C_2 + T_{env}}\right) \quad (3.41)$$

$$\rho_{humid} = \frac{p}{R_F \cdot (273.15 + T_{env})} \quad (3.42)$$

3.4.2 Calculation of the Power Coefficient

The power coefficient c_p describes how much actual electrical energy the wind turbine can generate at a given wind speed. It can be calculated with:

$$c_p = \frac{P_N}{\frac{1}{2} \cdot \rho_{std} \cdot A \cdot v^3} \quad (3.43)$$

For this the air density $\rho_{std} = 1.225[\text{kg}/\text{m}^3]$ is taken as it is used for standard atmospheric conditions. The information on how much power the turbine produces is extracted from the data graph from different wind turbine producers. Examples of some of them are shown in Figure 3.14.

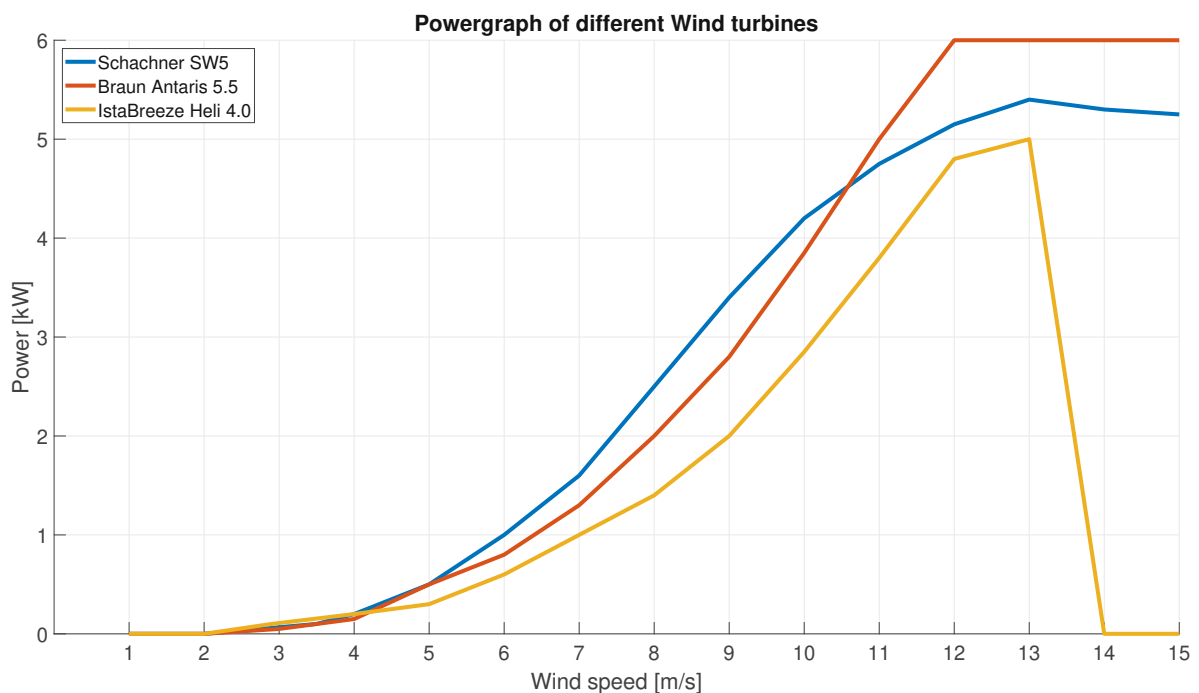


Figure 3.14: Power curve of Schachner SW5 [72], Antaris 5.5kW [73], Istabreeze Heli 4.0 [74]

Rectification losses from DC conversion are not accounted as it is assumed that the given power graphs from the data sheets are already usable DC power. The power coefficient c_p at 1m/s steps is calculated and then interpolated according to the current wind speed $c_{p,act}$. With this, the power generation of the wind turbine at any given wind speed is derived:

$$P_{gen} = \frac{1}{2} \cdot \rho_{env} \cdot A \cdot v^3 \cdot c_{p,act} \quad (3.44)$$

Similar to before, to consider transforming losses, an inverter efficiency factor is implemented as well.

$$P_{gen,real} = P_{gen} \cdot \eta_{inverter} \quad (3.45)$$

3.5 Load Model (Residential Load Simulator)

In this section the source of the load profiles, the RLS [3] is discussed. It allows to create loadprofiles for households of different sizes with data resolution from hours up to seconds. Since it is written in MATLAB and its output consists of matlab files, it is an ideal fit to pair with the AAS. Its was originally written as a diploma thesis but was improved and used in many different projects since then.

3.5.1 Data source

One of the projects which was used to improve the RLS was "Autonome Dezentrale Regenerative EnergieSysteme" (ADRES) [75]. This project included a survey in which participants reported their living and working situation, a detailed list of their owned electronic devices and their overall power usage [75]. Additionally, this survey data was combined and expanded with data from Statistik Austria [76].

3.5.2 Categories of Load Profiles

For the project "Aktives Demand-Side-Management durch Einspeiseprognose" (aDSM) [77], a pre evaluation of the data was taken and the data was categorized depending on different requirements. The result are eight household categories which can be seen in Table 3.12. This work will only focus on

Table 3.12: Load profile categories used in this work [78]

Name	Description	Amount of people	% of people in this category
home_1	single house	1	11%
home_2	couple house	2	14%
home_3	small family house	3	9%
home_4p	family house	4+	15%
flat_1	single flat	1	22%
flat_2	couple flat	2	15%
flat_3	small family flat	3	7%
flat_4p	family flat	4+	7%

the "home" profiles since the combination of solar panels, wind turbines, heating pumps and storage systems are not usable in almost any flat.

3.5.3 Amount of Devices per Household Profile

Using the data from ADRES, the amount of devices for each load profile category is shown in Table 3.13. This information is used to equip the different household types with the respective amount of devices.

Table 3.13: Amount of devices per household profile [77]

Household Profile	Refrigerators	Freezers	Washing machines	Dryers	Dishwashers	Televisions	Computers	Heatpumps	Radiators	Circulation Pumps	Electro Boilers	Water Heaters
home_1	105.8%	59.9%	91.2%	11.8%	49.6%	161.8%	48.2%	0.0%	12.5%	69.2%	29.2%	8.3%
home_2	157.8%	97.4%	93.8%	35.8%	80.7%	200.1%	84.9%	5.1%	2.6%	85.7%	22.2%	2.8%
home_3	183.4%	111.2%	92.3%	42.4%	81.4%	282.1%	161.6%	4.8%	14.3%	72.0%	43.5%	4.3%
home_4p	186.7%	119.8%	91.3%	44.1%	86.8%	262.3%	212.7%	9.3%	4.7%	85.1%	30.0%	3.3%
flat_1	108.6%	26.3%	82.5%	9.0%	50.3%	112.4%	70.0%	0.0%	13.2%	19.6%	45.8%	8.3%
flat_2	124.8%	53.7%	86.2%	12.5%	69.3%	155.4%	116.5%	0.0%	8.1%	39.5%	43.8%	0.0%
flat_3	123.1%	47.8%	90.5%	19.8%	77.7%	188.2.2%	176.5%	0.0%	0.0%	37.5%	43.8%	0.0%
flat_4p	135.3%	56.4%	86.9%	26.5%	76.9%	206.2%	206.0%	0.0%	0.0%	21.4%	66.7%	6.7%

3.5.4 Categories of Device Profiles

The RLS has different device categories which can be enabled/disabled for the load profile generation. An overview of them with their median yearly energy consumption per person can be seen in Table 3.14. By using power consumption data and the amount of devices from Table 3.13, an average power need in kWh per person and year for each of the categories can be derived.

Table 3.14: Load profile categories used in this work [78]

Annual avg. Consumption	Audio Video Devices	Illumination	Office Devices	Misc.	Dishwasher	Kitchen Appliances	Fridge/Freezer	Washing machine	Dryer	Heating	Circulation Pump	Hot Water
kWh/p.	131.09	159.66	65.13	67.65	73.95	228.57	227.73	75.21	29.83	281.51	99.58	317.65

Each device category has an underlying configuration which defines their active- and stand by power consumption and time of use. Furthermore, usage differences depending on season is also accounted for.

3.5.5 Overview of used Data in the RLS

To review, the following data sets are used to create annual load profiles depending on:

- Annual energy consumption of the device groups
- Categorization of different household types

- Amount of devices depending on household type
- Usage of devices depending on time
- Active and standby power consumption of devices

With this, a realistic load profile can be generated. For this work, every category in Table 3.14 will be used except for "Heating" as it will be modeled as a separate model in the upcoming chapter. The data is created for a non leap year. If the simulation calls for a leap year, the load profile of the 28th of February will be taken for the 29th as well. Figure 3.15 shows the distribution of the power demand of different device groups per person for a winter and summer day.

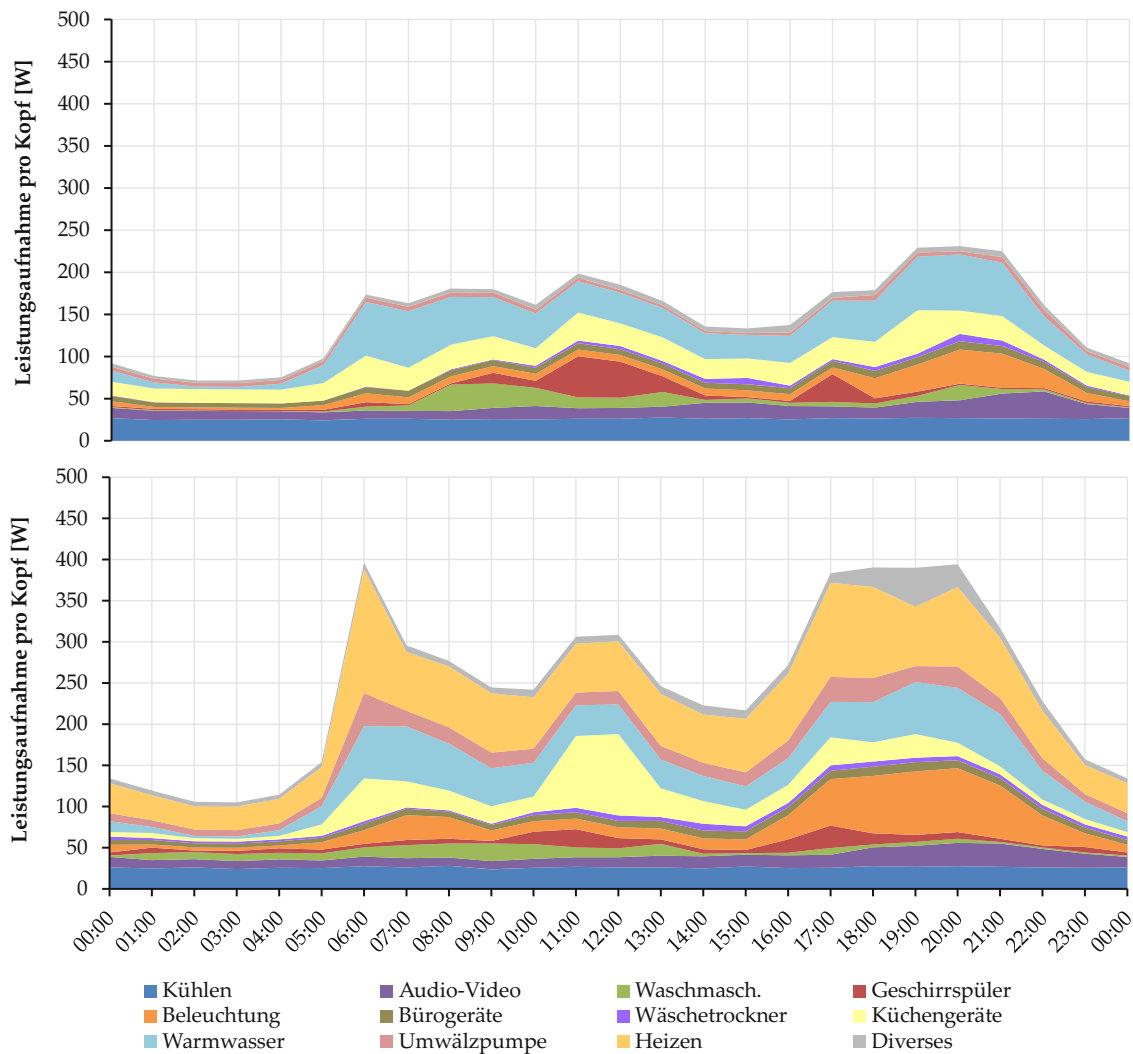


Figure 3.15: Load per person depending on device groups for a working day in summer (top) and winter (bottom) (used with permission from [78])

3.6 Heat Model

The heat model is built on an existing bachelor thesis [79]. Its original purpose was to create a simulation of the heat demand of households depending on different parameters. The source of heat in this model consists of a heating pump. The hot water heating was removed from the model (because it is already modeled in the RLS) and additions such as heat storage losses, proper ventilation, different kinds of heat pumps, improvement of the heat gains through irradiation and calculation of soil temperature were added. This chapter will discuss the overall composition of this model and its parts.

3.6.1 Heat losses of the Outer Surface

The main loss of heat occurs due to the exchange between the inside and outside of the house. To calculate these losses, the surface area of the house needs to be derived. To keep it simple, this model uses a cuboid shape for a house without a cellar. This means that every house has four outside walls ($W_1 - W_4$), a roof (G_R) and ground floor area (G_G) in square meters. Since it is modeled as a box, both the roof and ground floor have the same area. The surface S which comes in contact with the measured environmental temperature is then derived as

$$S_{house} = W_1 + W_2 + W_3 + W_4 + G_R \quad (3.46)$$

The u Value

Next the u value is needed. The u value [$W/(m^2 \cdot K)$] describes how much heat a wall for examples loses to the environment depending on area, time and temperature difference. It is derived by dividing the thermal conductivity λ [$W/(m \cdot K)$] of a material by its thickness. Table 3.15 gives an overview of the thermal conductivity of commonly used building materials. For a better understanding the u value of

Table 3.15: Thermal conductivity of commonly used building materials [6]

Material	Thermal conductivity λ [$W/(m \cdot K)$]
Wood	0.14
Building bricks	0.3-1.4
Concrete	2.1
Autoclaved aerated concrete	0.08-0.25
Insulated building bricks [80]	0.07
Glass	0.76
Glass wool	0.032-0.05
Stone wool	0.035-0.045
PUR insulation	0.024-0.035
Vapor barrier [81]	0.22

an insulated wall is calculated. From outside to inside it consists of 80mm wooden wall, a 0.5mm vapor barrier, 300mm of stone wool and another 20mm wood. Additionally, the u value of the transition between inside to wall $R_{si} \approx 0.13$ and outside to wall $R_{se} \approx 0.04[(m^2 \cdot K)/W]$ [82] [83] has to be considered as well. It has to be noted that these two transition values are dependent on airflow and humidity. With this the u value of the example wall can be calculated:

$$u = \frac{1}{R_{se} + \frac{0.08}{\lambda_{Wood}} + \frac{0.0005}{\lambda_{Barrier}} + \frac{0.3}{\lambda_{SWool}} + \frac{0.02}{\lambda_{Wood}} + R_{si}} = 0.105 \frac{W}{m^2 \cdot K} \quad (3.47)$$

The smaller the u value the less heat losses there are. Considering that walls have windows/doors which have much higher u values the overall mean u value of a house is higher.

Calculation of the Soil Temperature

Since the foundation of the house comes in contact with the soil and not the air, the existing model is expanded and the soil temperature is calculated according to [84]. This model would also consider changes depending on how much snow is lying on the soil. Since this data is not easily available for such a broad range of locations, this part is not considered. The coefficients required for the calculations can be taken from Table 3.16.

Table 3.16: Coefficients for calculating soil temperature [84]

Name	Value
Soil average thermal conductivity K_T	0.4 – 0.8 W/(m·°C)
Specific heat capacity of soil C_S	$1 \cdot 10^6 - 1.3 \cdot 10^6$ J/(m ³ ·°C)
Specific heat capacity frozen water C_{ICE}	$4 \cdot 10^6 - 15 \cdot 10^6$ J/(m ³ ·°C)

The soil temperature can be calculated with:

$$T_{soil}^{t+1} = T_{soil}^t + \frac{\Delta t \cdot K_T}{C_A \cdot (2 \cdot Z_S)^2} + [T_{env}^t - T_{soil}^t] \quad (3.48)$$

When the soil temperature is higher than 0°C, $C_A \approx C_S$, when its lower than 0 then $C_A \approx C_S + C_{ICE}$. For the first step T_{soil}^0 , the starting soil temperature should be used. Since this data is not available, a fixed value or T_{env} is taken. While using the environmental temperature for small depths (0-1m) is viable, it is not when calculating for deeper depths. Z_S is the depth in meters where the temperature is calculated. The original model from [79] uses a fixed soil temperature of 10°C throughout the year. With Equation 3.48, a more realistic approach is introduced.

The overall heating losses through the house surface can be calculated with:

$$\dot{Q}_{hull} = u \cdot S_{house} \cdot (T_{inside} - T_{env}) + u \cdot G_G \cdot (T_{inside} - T_{soil}) \quad (3.49)$$

3.6.2 Heat gains from Solar Irradiation

When the sun shines on a surface, it heats up. To simulate this, the solar gains are also taken into account. Equations 3.1-3.22 are used again to calculate the direct and diffuse irradiation on the walls and roof. This again is an improvement of the original model, since it assumes diffuse irradiation to exist on every plane independent of its angle of incidence and tilt.

The walls have an azimuth of $0^\circ, -90^\circ, -180^\circ$ and 90° (South, East, North, West) and a "tilt angle" of 90° . The flat roof has an azimuth and tilt angle of 0° .

If the sun azimuth is between $\pm 90^\circ$ compared to the wall orientation, the wall is illuminated so the direct irradiation exists. If not it is zero to consider shadowing effects. With this, the direct and diffuse irradiation for each wall and the roof (E_{diff}, E_{dir}) are calculated.

$$P_{S,dir} = E_{w1,dir} \cdot W_1 + E_{w2,dir} \cdot W_2 + E_{w3,dir} \cdot W_3 + E_{w4,dir} \cdot W_4 + E_{roof,dir} \cdot G_R \quad (3.50)$$

$$P_{S,diff} = E_{w1,diff} \cdot W_1 + E_{w2,diff} \cdot W_2 + E_{w3,diff} \cdot W_3 + E_{w4,diff} \cdot W_4 + E_{roof,diff} \cdot G_R \quad (3.51)$$

Depending on the surface of the house, more or less irradiation is absorbed and actually used to heat up the building. For this reason the Solar Irradiation Absorption (SIA) factor is introduced. This coefficient is a mean absorption factor for the building of how much of the irradiated power of the sun can be absorbed. Going by the original model, it is chosen to be 2.75%. The overall heat gain through the sun is derived with:

$$\dot{Q}_{solar} = SIA \cdot (P_{S,dir} + P_{S,diff}) \quad (3.52)$$

Reflected irradiation is not considered in this model as its already low impact gets further diminished by the SIA factor. Figure 3.16 shows the irradiation per square meter for a house in Neusiedl am See. One would expect the south facing wall to receive the most sun since its irradiated the longest and the sun is at its peak. Exactly for that reason the wall with its "tilt" of 90° has the worst tilt factor when the sun is at its peak, resulting in a lower direct irradiance.

3.6.3 Heat losses from Ventilation

To model the losses which occur from ventilation, the following model from [85] is used. The overall amount of air in all the rooms of the building is calculated with:

$$R_{volume} = G_G \cdot F_f \cdot R_{height} \cdot N_{floors} \quad (3.53)$$

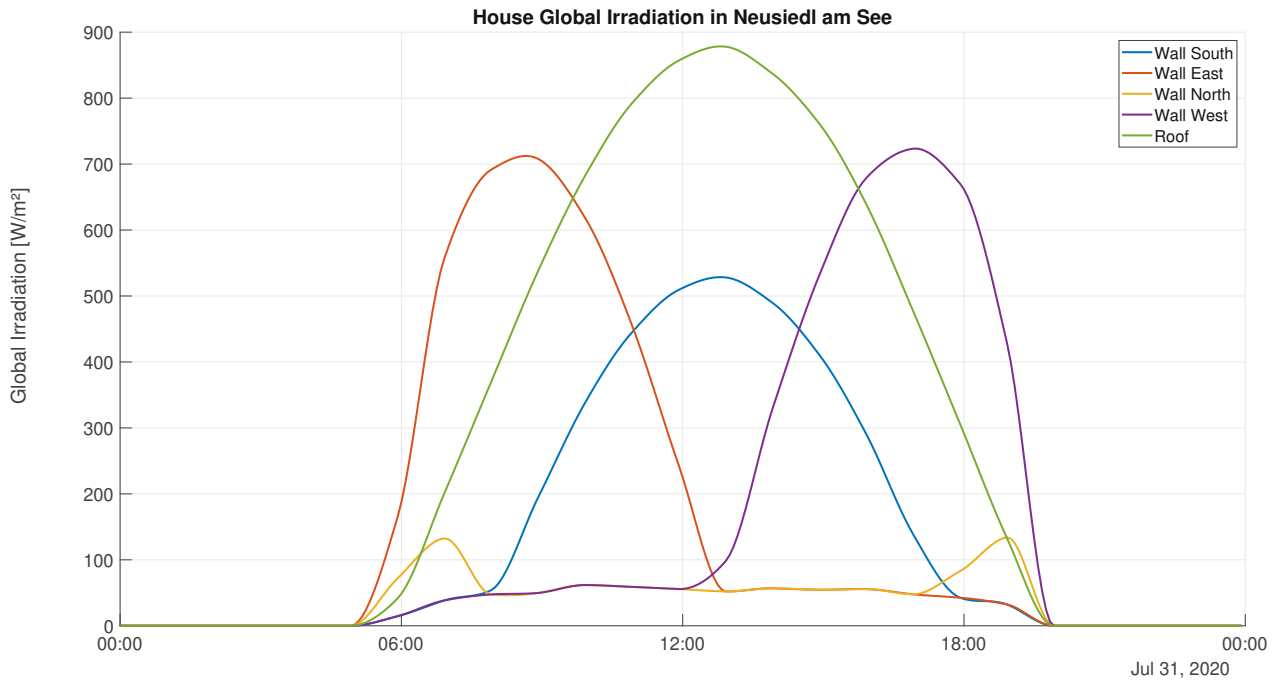


Figure 3.16: Global irradiation on a house throughout the day

where F_f is a floor factor which is around 0.8 (to calculate actual usable floor space - not outside dimensions), R_{height} the height of the rooms in meters and N_{floors} the amount of floors of the building. With this the volume of air inside of the rooms can be calculated. This allows the heat loss $\dot{Q}_{airchange}$ [W] to be derived:

$$\dot{Q}_{airchange} = R_{volume} \cdot c_{air} \cdot \rho_{air} \cdot \frac{airChange}{3600} \cdot (T_{inside} - T_{env}) \quad (3.54)$$

With the specific heat capacity c_{air} [J/(kg·K)] (dry air dependent on outside temperature [86]), the air density ρ_{air} (calculated the same as in Equation 3.42) [kg/m³] and $airChange$ [%/h] which describes how much of the air volume is exchanged with the outside air per hour. Table 3.17 shows reference values for $airChange$, for modern ventilation systems with heat recovery, values may differ. Further-

Table 3.17: $airChange$ in % of the room volume per hour according to [85]

Description	$airChange$ [%/h]
Old building, maximum	200
Tilted windows	100
Hygienic minimum, tilted windows	50
New building	20

more, if the temperature inside the house reaches a certain point (i.e., 25°C) and the outside temperature is lower than the inside temperature, $airChange$ is set to 200%/h to simulate opening the windows to

allow air from the outside to cool down the house.

3.6.4 Calculating the Overall Heat demand

The overall heat demand Q_{need} [Wh] for a given timestep Δt [s] is given by:

$$Q_{need} = (\dot{Q}_{hull} + \dot{Q}_{solar} + \dot{Q}_{airchange}) \cdot \frac{\Delta t}{3600} \quad (3.55)$$

To describe the overall heat capacity of the building the effective heat capacity k_m [J/(m²·K)] is given in Table 3.18. Alternatively, the effective heat capacity can be approximately calculated without con-

Table 3.18: Effective capacity depending on building material [87]

Class	Value [J/(m ² ·K)]	Description
Very light	50000	Light material plastic/wood
Light	75000	5-10cm lightweight brick/concrete
Medium	110000	10-20cm lightweight brick/concrete or <7cm solid brick/concrete
Heavy	175000	7-12cm of solid brick or heavyweight concrete
Very heavy	250000	>12cm of solid brick or heavyweight concrete

sidering the transition resistance [88].

$$k_m = c_{material} \cdot \rho_{material} \cdot d \quad (3.56)$$

Where c is the specific heat capacity, ρ the density of the material and d how thick the object is. With this factor, the overall heat capacity of the house can be calculated by using the following equation:

$$C_{house} = (S_{house} + G_R) \cdot k_m \quad (3.57)$$

3.6.5 Heat storage

The heat storage in this work is modeled as a simple buffer tank. To propose an example: a water buffer tank has 1000l and is heated up to 50°C. We can "use" its energy until the water temperature reaches 30°C. With the following equation, the heat energy stored in kWh can be calculated:

$$Q_{storage} = m_w \cdot \frac{c_w}{3600} \cdot \Delta T \quad (3.58)$$

Where the specific heat capacity of water is $c_w = 4172$ [J/(kg·K)], the mass of the water is m_w [kg] and the temperature difference is ΔT [K]: Considering the isolation losses from the buffer tank, at 1000l it

is in the $p_{storage,loss}=120W$ range [89] [90] and modeled as a parasitic drain throughout the year.

$$Q_{storage,losses} = p_{storage,loss} \cdot \frac{\Delta t}{3600} \quad (3.59)$$

3.6.6 Heat pumps

Using the data sheet of different types of heat pumps, the Coefficient of Performance (COP) is determined depending on the environmental temperature (Table 3.19). Since heat pumps from the company "Bosch" gave detailed COP values for a range of different temperatures, they were chosen to be implemented in the AAS. For temperature values between the given ones, a linear interpolation is used. The

Table 3.19: COP of different heat pumps depending on environmental temperature [91] [92] [93]

Temperature [°C]	Bosch CS3400iAWS 4 OR-S	Bosch CS7800ILW 6	Bosch STE60-1
-17	1.48	2.75	2.65
-7	1.92	2.96	2.84
2	3.28	3.89	3.34
7	4.27	4.59	3.70
12	5.85	4.54	4.11

amount of heat energy a heating pump can provide the following calculation is used:

$$Q_{heatpump} = COP \cdot P_{heatpump} \cdot \frac{\Delta t}{3600} \quad (3.60)$$

Which means that a heat pump with a $P_{heatpump}$ of 1000W and a COP of 3 can generate 3000W of heat energy from only 1000W of electrical power. The amount of heat which can be used to actually heat up the home is limited by the power of the heat system P_{heater} .

$$Q_{heater} = P_{heater} \cdot \frac{\Delta t}{3600} \quad (3.61)$$

The overall heat demand of the model is now dependent of the following equation:

$$Q_{overall} = (T_{house,new} - T_{house,old}) \cdot C_{house} \cdot \frac{1}{3600} + Q_{need} \quad (3.62)$$

Depending if the house needs heating up or not, Equation 3.62 draws energy from the heat storage $Q_{storage}$ but is limited by Q_{heater} . When $Q_{storage}$ reaches a selectable lower threshold, the heat pump turns on and starts "filling" up the heat storage again.

$$Q_{pumped} = P_{heatpump} \cdot COP \cdot \frac{\Delta t}{3600} \quad (3.63)$$

This value is added again to the heat storage. As long as it is turned on, the heat pump uses $P_{heatpump}$ power, creating a reoccurring load depending on how much heating is needed. An example is shown in Figure 3.17.

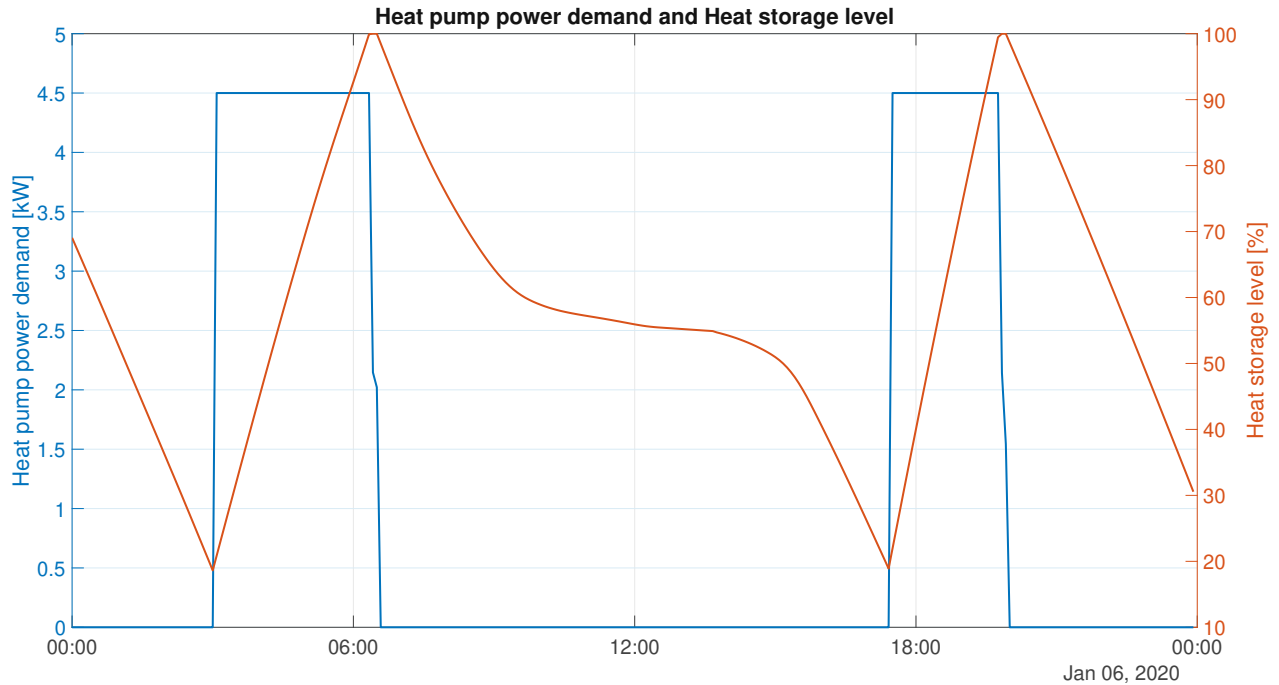


Figure 3.17: Course of heat pump demand and heat storage throughout a day

3.7 Electrical Storage Model

The storage model is kept rather simple. When there is more power generated than used, the excess power is stored in the battery. When the load is greater than the power generated and the battery has sufficient charge, the power is supplied by the storage. Because of this it is very flexible. Except for different efficiency factors, it basically acts similar independent of which storage technology is used.

3.7.1 Parameters of the Storage

To model the storage, the following parameters are used:

- Usable capacity C_{bat} [kWh]
- Maximum current [A]
- Nominal voltage [V]
- Self discharge per month η_{loss} [%]
- Battery charge/discharge efficiency η_{bat} [%]

- Inverter efficiency $\eta_{inv}[\%]$

The battery box HVM 11.0 [22] from the company BYD is used as an example. The usable capacity for this storage system is 11.04kWh. Multiplying the maximum current of 50A with the nominal voltage of 204.8V results in the maximum charge/discharge power of 10.24kW which is considered when charging/discharging the battery. If the load/generation is higher than the maximum discharge/charge limit it is simply cut off and the maximum values are used. The self discharge for lithium based batteries ranges from 5-10% per month [16]. This is modeled with a permanent hourly parasitic drain $E_{parasiticdrain}$ in Wh:

$$E_{parasiticdrain} = C_{bat} \cdot \eta_{loss} \cdot \frac{1000}{30 \cdot 24} \quad (3.64)$$

This model does not factor in a discharge limit and completely empties or charges the battery if possible. To consider different discharge depths, the capacity of the battery is seen as "usable capacity" i.e. 50% of the nominal one for lead-acid batteries.

3.7.2 Battery Charging/Discharging

For each time step Δt all the power generation is summed up and the load is subtracted:

$$P_{difference} = P_{gen} - P_{load} \quad (3.65)$$

If $P_{difference}$ is positive, more power is generated than being used at the moment, this means the battery can be charged (if it is not full) with:

$$C_{storage,new} = C_{storage,old} + P_{difference} \cdot \frac{\Delta t}{3600} \cdot \eta_{bat} - E_{parasiticdrain} \quad (3.66)$$

When $P_{difference}$ is negative, it means that power is required from the battery. The storage level is then derived with:

$$C_{storage,new} = C_{storage,old} + \frac{P_{difference}}{\eta_{bat} \cdot \eta_{inv}} \cdot \frac{\Delta t}{3600} - E_{parasiticdrain} \quad (3.67)$$

Since the power from the storage is DC the inverter losses need to be considered as well when converting it to usable AC power for the usable loads. Edge cases for the full and empty battery will not be described here in detail but are considered in the programming of the model.

3.7.3 Calculation of the Autarky Factors

Since this model is the last of the five (solar, wind, load, heat, storage) and has information of the overall generation and load, it calculates the autarky factor of the experiment.

There are two different autarky factors which are defined as follows: The first one AF_{load} calculates how much percent of the overall load can be sustained by the system:

$$AF_{load} = \left(1 - \frac{wouldNeedPower}{householdLoad} \right) \cdot 100 \quad (3.68)$$

For example, if the overall $householdLoad=5000kWh$ and $wouldNeedPower=500kWh$ which is the power required from the grid to be hundred percent energy self-sufficient, the AF_{load} would calculate to 90%.

The second autarky factor AF_{time} considers how much time of the year the battery is empty (zero charge):

$$AF_{time} = \left(1 - \frac{timestepZeroCharge}{amountTimesteps} \right) \cdot 100 \quad (3.69)$$

To clarify, Equation 3.69 considers times when the battery is empty but an amount of the power need is supplied by the generators but not enough to charge the battery still as not "autark". This is because the edge case when the generation is exactly the same value as the consumption is highly unrealistic. AF_{time} derives how much percent of the year the household can fully power its energy needs.

3.8 Output of the AAS

The output of the AAS is a timeseries of the whole year compromised of energy demand, energy generation, heat demand and State of Charge (SOC) of the energy and heat storage. All this data can be used to create many different key performance indicators ranging from energy generation/consumption, excess/needed energy, heat demand and many more. Figure 3.18 and 3.19 shows just one summer and winter day of the data output from the AAS.

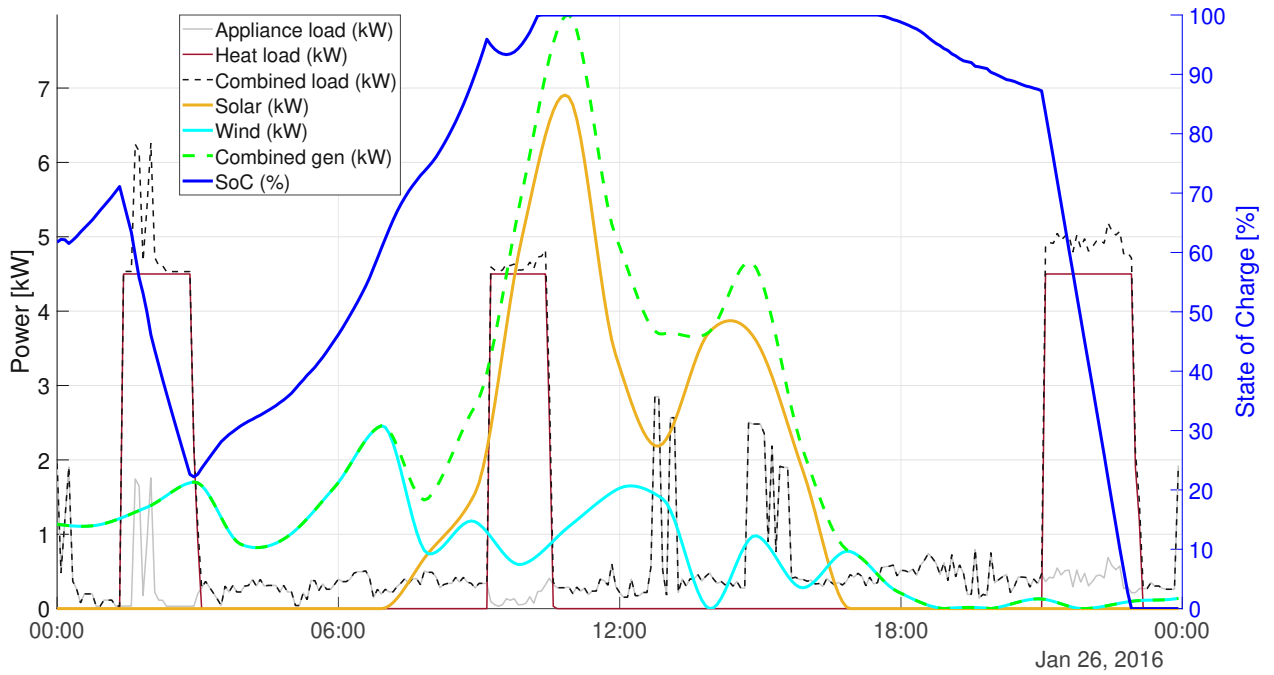


Figure 3.18: Output for one winter day from the AAS

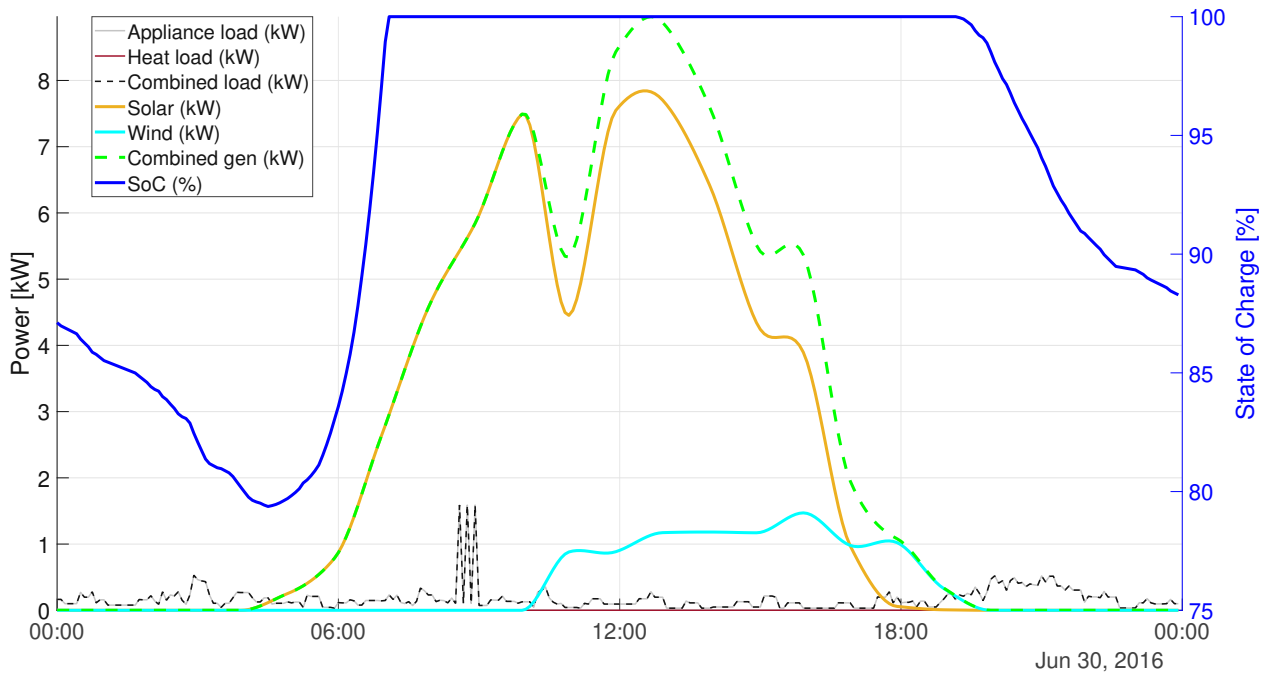


Figure 3.19: Output for one summer day from the AAS

Chapter 4

Results

This chapter discusses the insights which are gained from the AAS in respect to the research questions. The different models, which were described previously, are compared against real world data to validate their accuracy. All of Austria is simulated with a 10x10km grid. Furthermore, an detailed evaluation of different locations is given and discussed. At the end of this chapter, a closer look on autarky depending on PV size and storage size is taken.

4.1 Validation and Accuracy of the Models

For the simulation results to be taken seriously, the accuracy of each model is examined by comparing it to real measured data if available.

4.1.1 Photovoltaic Model

The best way to validate the PV model is to compare it to a real life system. For this, data from a 10kW system installed in May 2022 in Burgenland is taken. The installation is quite peculiar since it is split up into 2 different strings. One string is 6800W oriented 140° from North and is tilted about 4°. The remaining 3200W have the same orientation but are tilted 27°. Both are roof integrated with about 5cm of distance between the roof and the panel. The solar panels are mono-crystalline silicon based. The inverter used for both the simulation and the system is a "Fronius Symo GEN24 10.0 Plus".

Since the system was installed in 2022 and PVGIS data only is available up until the end of 2020, the global irradiation data from the nearest ZAMG weather station in Kleinzicken, Burgenland is used. It has to be noted that the weather station in question is about 10km from the installed system, which can result in deviation in irradiation from the actual location. Additionally, since only the global irradiation is available for the comparison, it will be taken as full beam irradiation without diffuse one. With these limitations in mind Figure 4.1 shows the monthly generated power from the real system compared to the

simulated one. To analyze the data further, daily power generation for June and October can be seen in

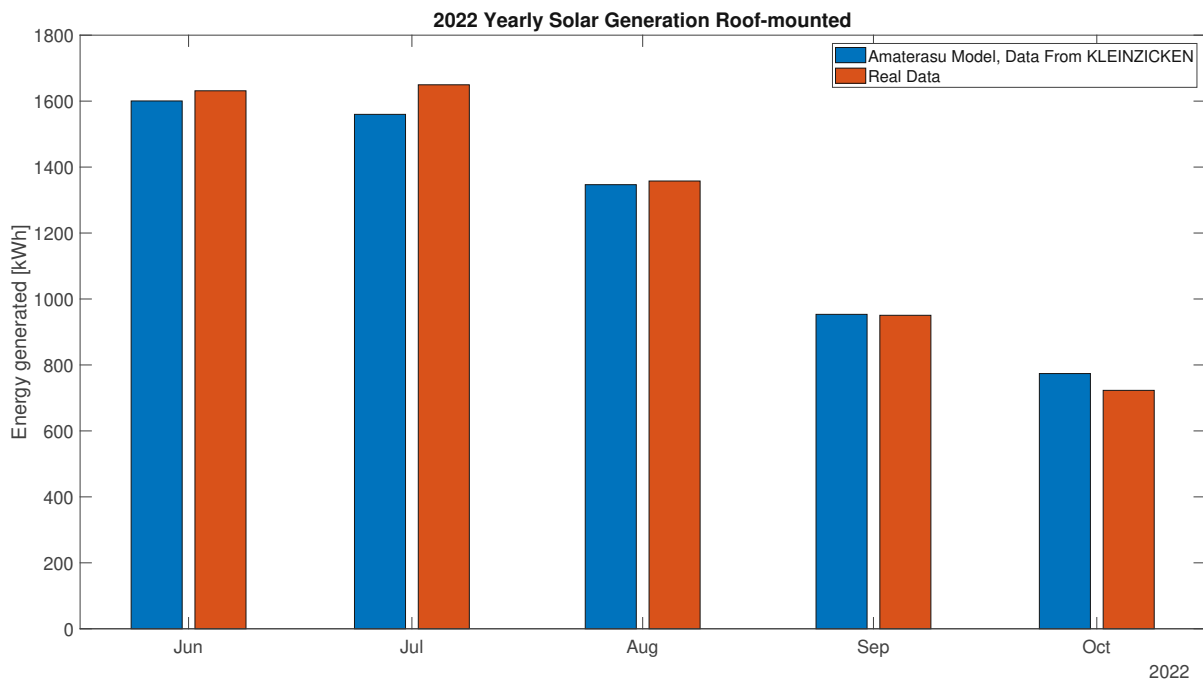


Figure 4.1: Comparison of monthly solar energy generation real vs. simulated

Figure 4.2 and 4.3. In June, the model outputs about 9% more energy than the real data while in October it produces 1% less than reality. When taking into account that cloud cover and in turn irradiation can change significantly over even small distances, the bigger difference especially in June may be caused by divergent cloudiness. On the upside, the trend of the real system is followed adequately and the total deviation is relatively small. Overall, considering the non ideal measuring circumstances of weather data (only global irradiation counted as beam irradiation, distance of the weather station to the system) the model is shown to be quite accurate.

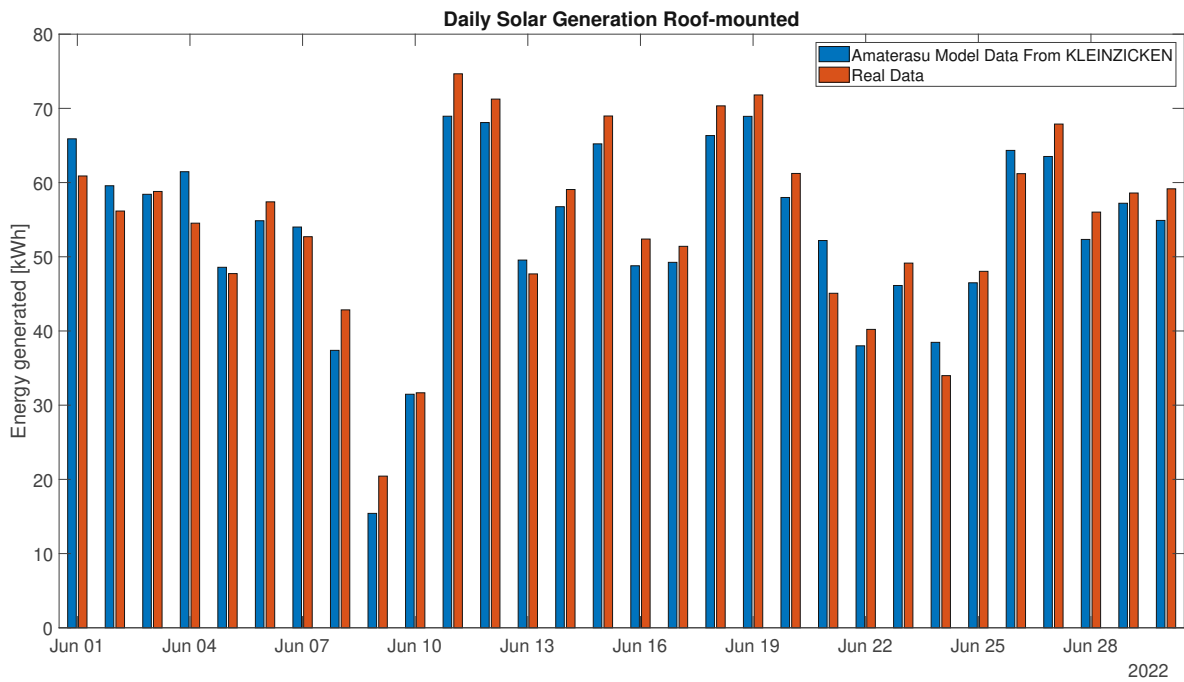


Figure 4.2: Comparison of daily solar energy generation real vs. simulated for June 2022

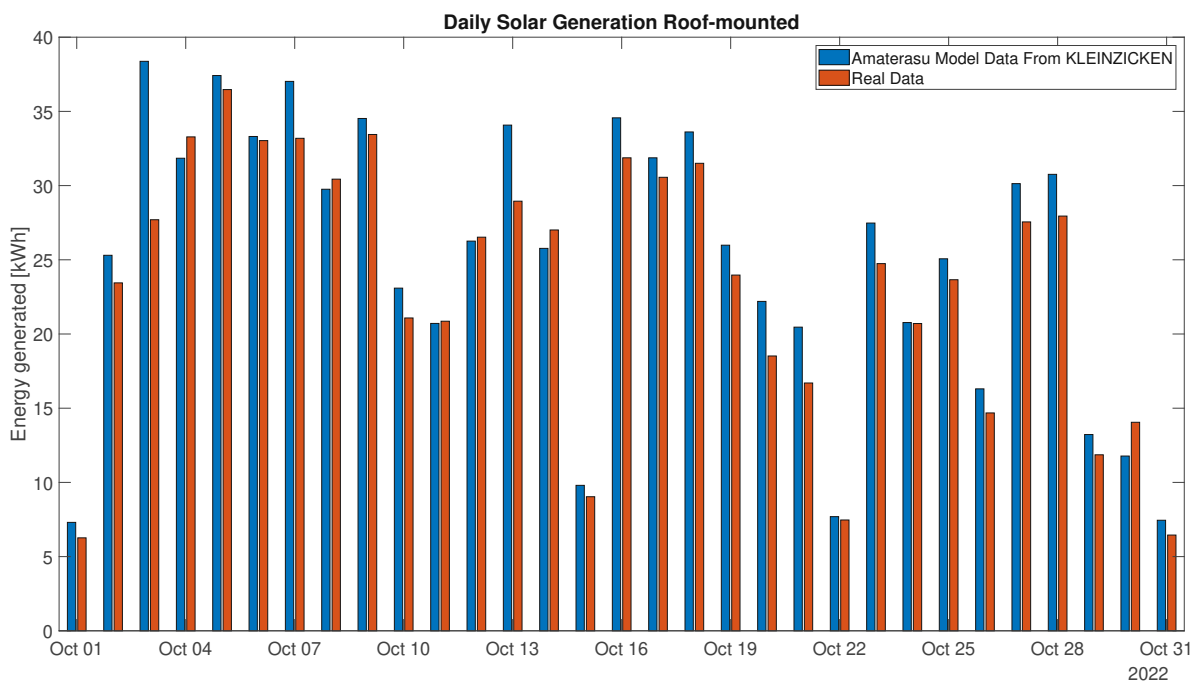


Figure 4.3: Comparison of daily solar energy generation real vs. simulated for October 2022

4.1.2 Wind turbine Model

To validate the wind model, data from the report "Kleinwindkraftreport Österreich" from 2018 [10] is used. Using Figure 4.4, this report claims that (except very small <1kW) wind turbines in Austria

average around 1000 full load hours per year. Using a 10x10km coordinate grid of Austria, data from

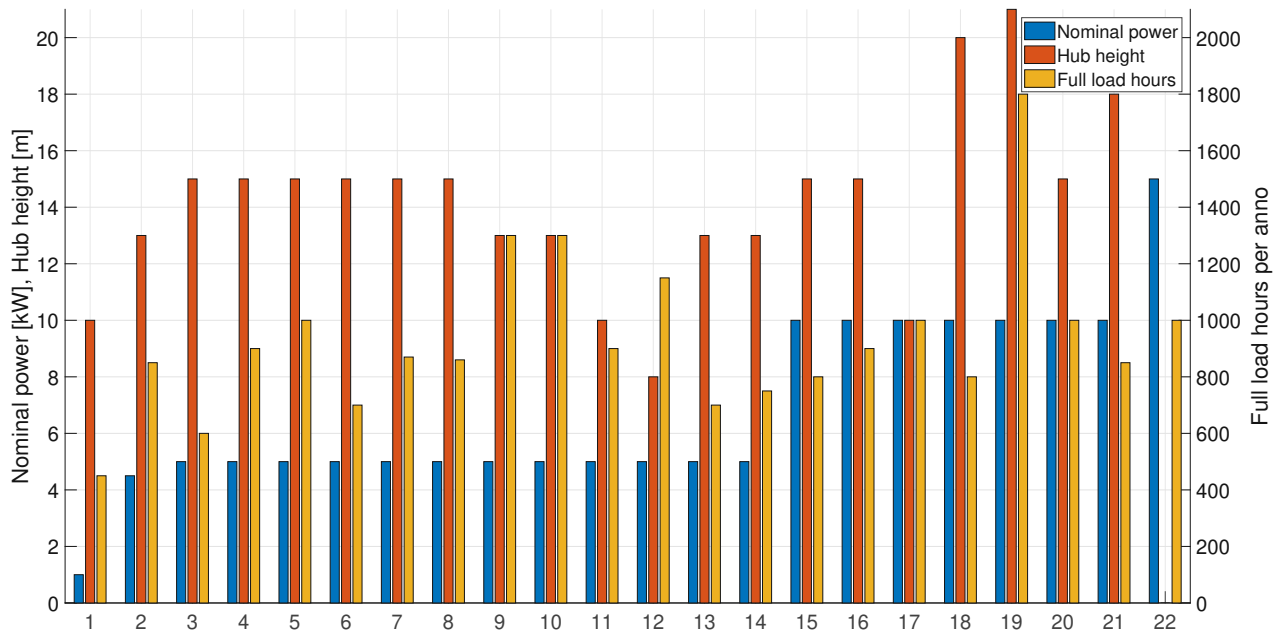


Figure 4.4: Detailed inquired information of small wind turbines in Austria, each value on the x-axis represents a different turbine (recreated from [10])

INCA was parsed and used to simulate a wind turbine with 5kW nominal power [74] of power at 20m hub height. The result can be seen in Figure 4.5. This figure is in line with the statement from the report that "the power yield is primarily dependent on the specific location and the wind situation there". At locations with sufficient wind, the model reaches about 1000 full load hours. At a few specific locations, it even reaches 2000 full load hours or more. Overall, the model does not output unrealistic power generation which conforms with real life data. Since the model assumes a power value dependent on wind speed extracted from the data sheet, the only uncertainty is the wind data. Since INCA only uses averaged hourly values, gusts of wind which would further increase the overall power generation are not included. For a proper comparison, real measured wind speed at the given hub height at different locations would be needed to fully validate the model.

4.1.3 Load Model

To verify the RLS, five households for each "house" category from table 3.12 is run without the device group "Heating" (table 3.14). The device group "Hot Water" is still enabled. Depending on the simulation, the consumption differs from household to household in a single category. This results in a yearly power consumption which is shown in Table 4.1. The average values from the RLS seem to be on the

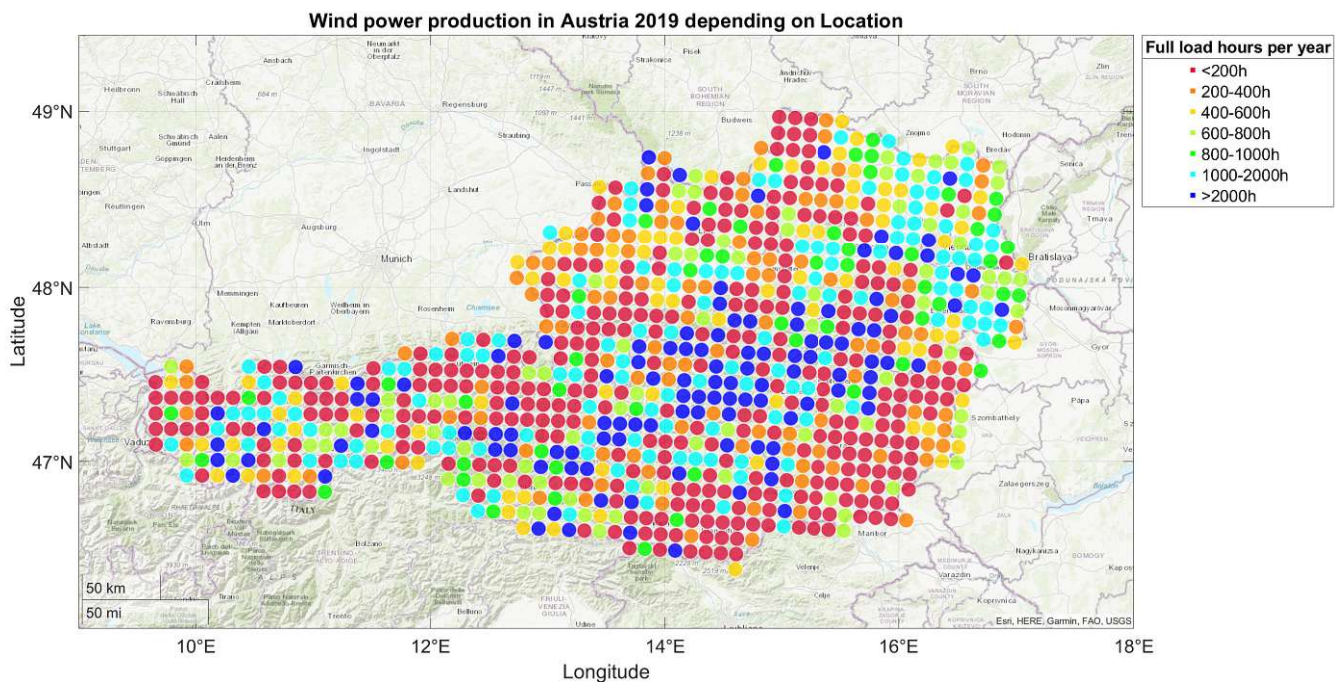


Figure 4.5: Simulated wind power generation with a 5kW turbine at 20m height in Austria with INCA data

Table 4.1: Comparison of the results of the RLS with average power consumption in Austria

Name	Amount of people	Yearly power usage [kWh] RLS	Yearly avg. power usage [kWh] [94]
home_1	1	1266-3430	1800-2000
home_2	2	2284-5437	2800-3100
home_3	3	3151-5904	3600-4000
home_4p	4+	4551-6996	4000-4800

upper side of the values which are taken from statistics [94]. According to the site, power usage for heating and electrical heating of water is included in these values. Comparing personal data, a two person house in Lower Austria without electrical water heating and a wood gasifier for heating and uses about 3500kWh per year. Another example is a multi generation home in Burgenland which houses 6 people, has also no electrical water heating and a wood chip heater for heating uses about 5500kWh per year. To further validate the data, Figure 4.6 shows weekly average load values of a transformer compared to the simulated ones. The location is Köstendorf, Salzburg, which is mainly a residential area. This further affirms that the seasonal load differences and general power consumption is modeled quite accurate. Overall, the RLS produces acceptable results which fall in reality with statistics and personal data. If an exact yearly household consumption is known, the simulation which fits the value the best can be chosen easily.

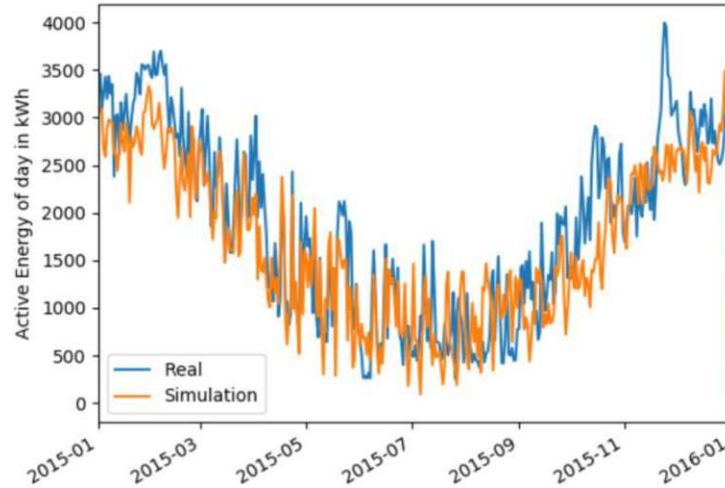


Figure 4.6: Comparison of weekly averages between real and simulated data for the active power of a transformer in Köstendorf, Salzburg (used with permission from [78])

4.1.4 Heat Model

Since the heat model represents a significant amount of the overall electrical energy consumption in a household, proper verification is needed.

Heat Demand

For the heat demand, a so called "Energieausweis" is taken from a relatively new house built in 2021. This is a document which every house in Austria needs if somebody wants to buy it. It documents many heating and isolation parameters of the building are documented. There is a rating system on how little heating a building needs. The maximums of the values are displayed in table 4.2. The Energieausweis

Table 4.2: Classes of energy efficiency of buildings [95]

Class	$HWB_{Ref,SK}$ [kWh/(m ² ·a)]	PEB_{SK} [kWh/(m ² ·a)]	$CO_{2eq,SK}$ [kg/m ² ·a]	$f_{GEE,SK}$
A++	10	60	8	0.55
A+	15	70	10	0.70
A	25	80	15	0.85
B	50	160	30	1.00
C	100	220	40	1.75
D	150	280	50	2.50
E	200	340	60	3.25
F	250	400	70	4.00
G	> 250	>400	>70	>4.00

in question, shows a Heizwärmebedarf Referenz-Lüftungsleitwert Standort Klima ($HWB_{Ref,SK}$) value of 37.0kWh/m²a which states how much kWh per square meter per year the building needs at the built location for a minimum inside temperature of 20°C including ventilation losses. The area used for this

is the gross base area of the building. This puts this house in the class "B". The external dimensions of the house are around 10.65x14m. With two floors this leads to a gross base area of 298.2m² (298.14m² in the document). The overall u value according to the Energieausweis is 0.21W/(m²·K). The class for the effective heat capacity is "medium" so k_m is set to 110000J/(m²·K). The heating system can put out 5kW of power and has a 1000l water buffer storage with about 120W of storage losses. Using the irradiation data from PVGIS and the temperature of INCA this results in a yearly heat demand of around 11100kWh depending on the yearly climate. Dividing this by the gross base area results in a $HWB_{Ref,SK}$ of about 37.2kWh/m²a which comes very close to the values given in the Energieausweis. Since every building is quite different, by changing the SIA and *airChange* variables, the $HWB_{Ref,SK}$ can be fine-tuned very well to accurately represent a quite complex house model in reality with a comparatively simple simulation model.

Soil Temperature Calculation

To validate the soil temperature model, measured data from weather stations is compared to the results of the calculations. Figure 4.7 and 4.8 respectively show one of the overall worst and best results. It has to be noted that for this, the measured starting soil temperature and air temperature was used for this comparison. While using the environmental air temperature for small depths (0.1-0.2m) does not have much of an impact, using it for depths of 0.5 and more leads to quite an offset considering the fluctuations gets less and less at larger depths. At Innsbruck the yearly average difference is 1.6°C while at "Reichenau an der Rax" it is only 0.4°C. Tuning of the soil parameters in equation 3.48 only changes the amount of dampening. Overall, the calculated values seem always less than the measured ones. This is fine since considering autarky, a more conservative model does not overestimate. To conclude, the calculated soil temperature is accurate enough when compared to real life data and an immense improvement over a fixed value throughout the year.

4.1.5 Storage Model

The storage model itself is hard to validate since characteristics depend on the battery, the charge controller used and the power which is available to charge it. Different charge modes depending on the SOC of the battery are not considered. As already mentioned before, to keep it simple but still grounded in reality, battery round-trip efficiency, self-discharge and inverter efficiency are factored in to model the storage as accurately as possible given the limited information retrieved by the data sheets.

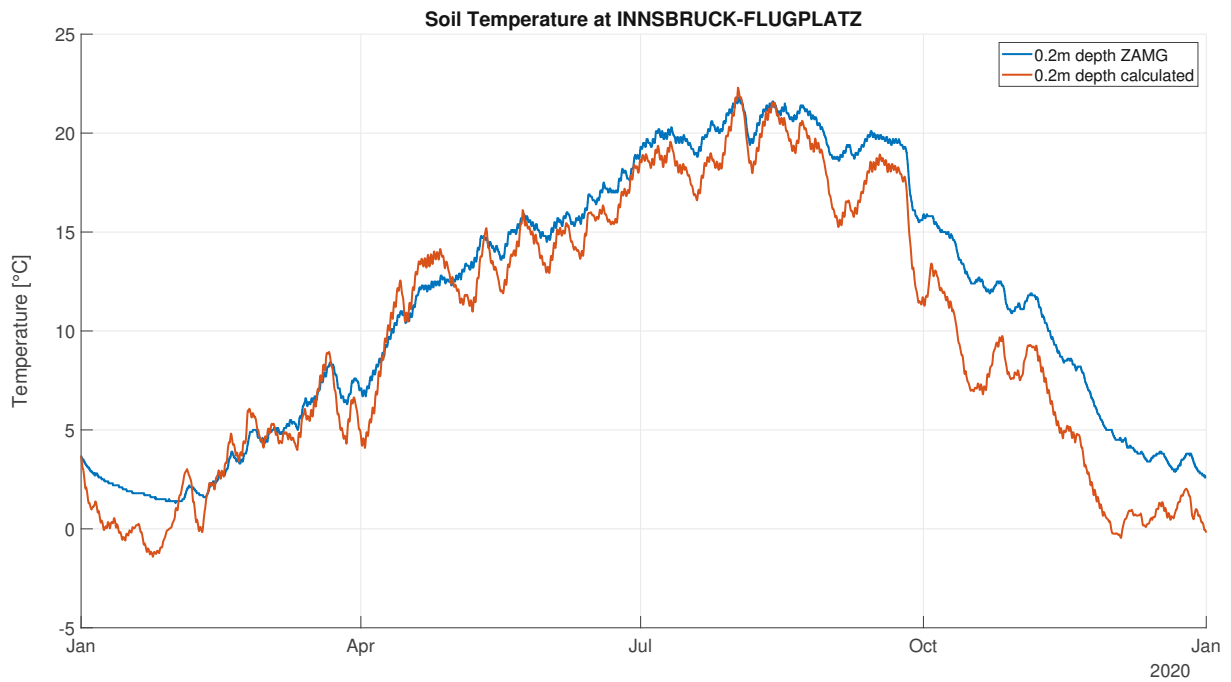


Figure 4.7: Soil temperature in 20cm depth at Innsbruck Airport 2020

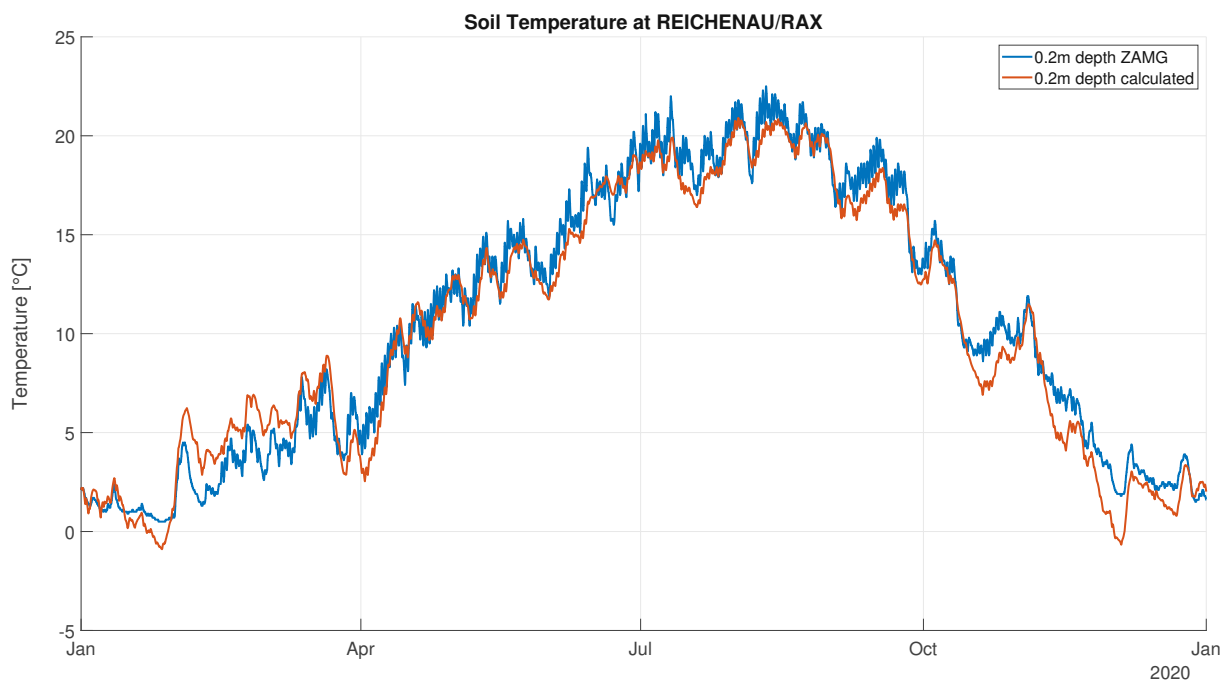


Figure 4.8: Soil temperature in 20cm depth at Reichenau an der Rax 2020

4.2 Location dependent Autarky Analysis of Different Sized Households

In this chapter the results of the Austria wide autarky simulation will be discussed. The fixed setup for the next four subsections will be:

- PV: 10kW mono-crystalline, 35° tilt, orientation 0° (south), 5cm distance from roof integrated at 4m height, albedo=0.2, roughness length=0.4, inverter=Fronius Symo GEN24 10.0 Plus and no aging factor
- Wind turbine: SchachnerSW5 5kW [72], hub height=20m, inverter=Fronius Symo Gen24 6.0 Plus
- Heat model: u value=0.21W/(m²·K), SIA=0.0255, soil parameter: $K_T=0.5\text{W}/(\text{m}\cdot^\circ\text{C})$, $C_S=1\text{e}6\text{J}/(\text{m}^3\cdot^\circ\text{C})$, $C_{ICE}=8\text{e}6\text{J}/(\text{m}^3\cdot^\circ\text{C})$, $Z_S=0.2\text{m}$, $airChange=0.26\%/h$, room height=2.5m, floor factor=80%, wall orientations=[180°, -90°, 0°, 90°] (North, East, South, West), $k_m=110000\text{J}/(\text{m}^2\cdot\text{K})$, heat storage=25kWh, heat losses=120W, heat to temperature=20°C, reheat storage at=20%, heat storage to=100%, starting heat storage=80%
- Storage model: BYD HVM 11.0 [22] usable capacity=11.04kWh, max current=50A, nominal voltage=204.8V, round-trip efficiency=96%, self-discharge=5%/month, inverter=Fronius Symo GEN24 10.0 Plus, storage starting SOC=75%

The fixed heat parameters are chosen to simulate a pretty new or well isolated building which has the u value, ventilation and heat capacity of a house from the energy class "B" (Table 4.2). This is necessary since autarky highly depends on the amount of power a household needs in winter time so a building with an appropriate heat demand is needed. Depending on the size of the simulated house and the amount of people living there, the yearly power consumption, house size and heat pump size are adjusted. To simplify, the bigger the house and the larger the amount of people living there the higher the power consumption. Furthermore, the load profiles are pre-generated and do not take the current storage or weather conditions into account. This means that even though the storage may be low and there is no energy generation in sight, the household will not change its consumption. The experiments aim to investigate the time based autarky without external influences. One of the main highlights of the AAS is that it can simulate any setup. In the following sections some realistic ones will be evaluated.

4.2.1 Small Two Person Home

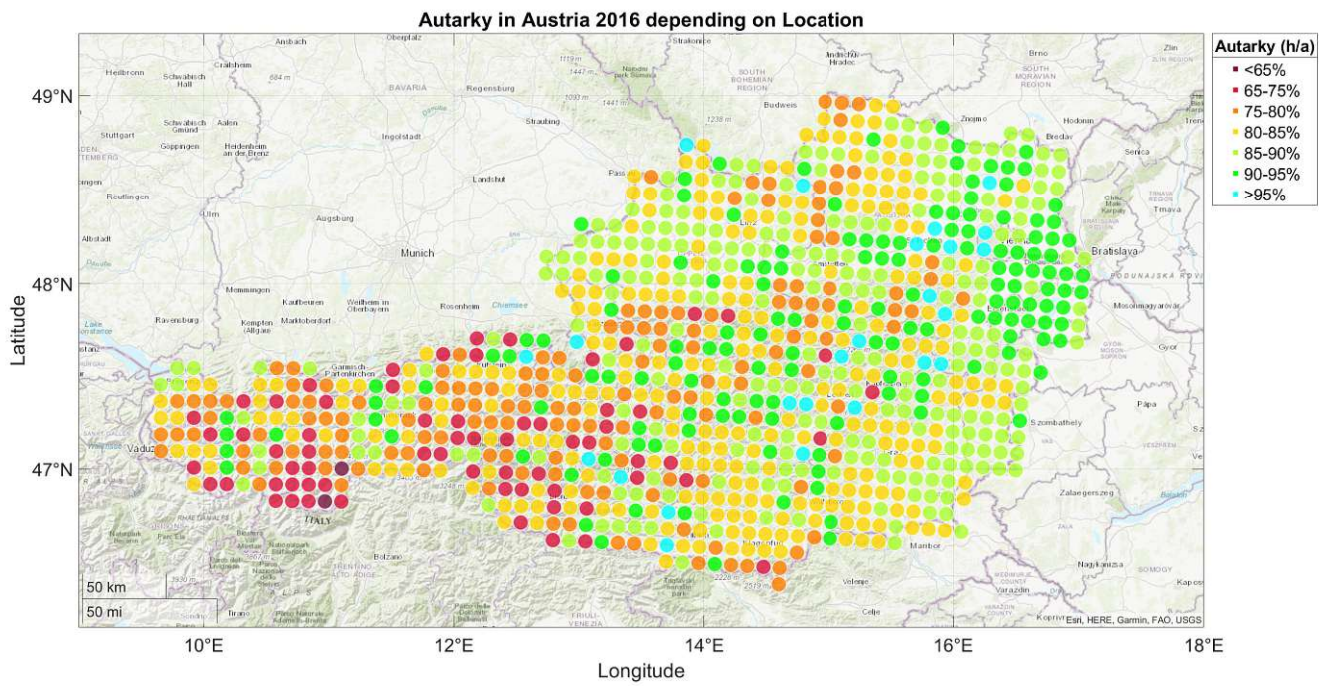
In this section, autarky of a small 10x10m one story house which accommodates two people is simulated. The yearly power consumption of this household is set to 3132kWh which is the upper end

of the country wide average for two people (Table 4.1). Because the house is rather small, the chosen heatpump is an air/water "Bosch CS3400iAWS 4 OR-S" [91]. The power of the actual heating system, which supplies heat to the building, is 5kW.

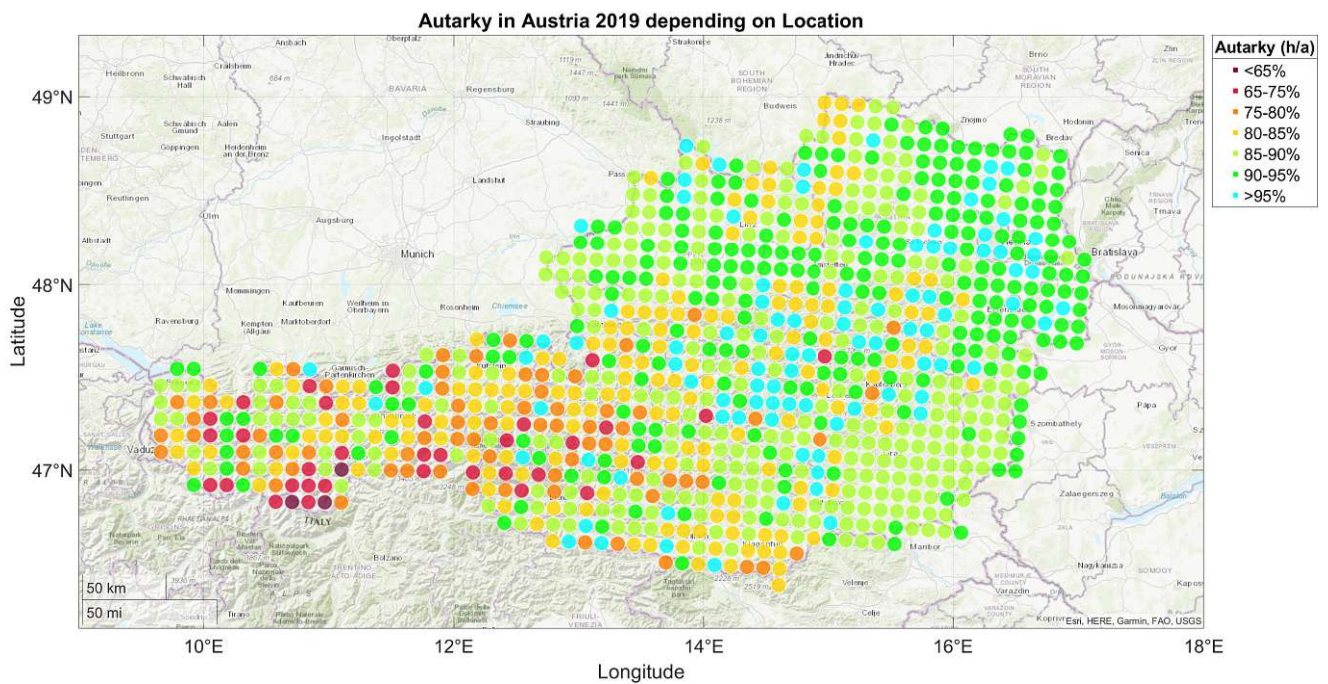
Using a 10x10km grid of Austria, 916 locations are simulated for the years 2015-2020. The result of the best (2019) and worst (2016) year for autarky can be seen in Figure 4.9. The mean power consumption including "normal" load and load from heating from all locations over those five years is 5700kWh per household per year. In both plots, a prominent east-west difference can be seen. Additionally, the mountainous regions in the center of Austria also affect the autarky negatively. The few turquoise/green points in areas of predominantly yellow/orange/red areas stem from the fact that the coordinates are placed in mountainous regions where there is a lot of wind. The wind turbine in these cases is a reliable powerful energy generator throughout the year, which positively affects autarky even though the heat demand is higher there. The year 2016 is a good example for autarky, since the system should always be designed for the worst case. The eastern regions of Austria, especially Vienna and the northern Burgenland, achieve an autarky of around 90-95%. Higher than average yearly temperatures combined with good solar irradiation and a good amount of wind make this area well suited for autarky.

Figure 4.10 is a histogram of the difference in autarky between the year 2019 and 2016. It shows that in 2019, 574 of the households reached 86% autarky or more, while in 2016 only 350 managed this amount of self-sufficiency. This exemplifies the fact that autarky from renewable energy systems is highly depended on the weather. Most of this is affected by the amount of sun in the year. More solar irradiation means more energy production while at the same time increasing temperature and heat gains of the building resulting in a smaller heat demand. This in turn, leads to better autarky. While the time based autarky is pretty good overall (85.7% mean over 5 years and all locations), the mean load based autarky over all households and the five years is only 73% (to reiterate, load based autarky represents how much of the actual required load can be satisfied by the generators and storage). This stems from the fact that because of the heatpump, most of the power gets used during wintertime, where solar energy generation is usually low. In Figure 4.11 this fact is clearly shown.

Die approbierte gedruckte Originalversion dieser Diplomarbeit ist an der TU Wien Bibliothek verfügbar
The approved original version of this thesis is available in print at TU Wien Bibliothek.



(a) Autarky in 2016



(b) Autarky in 2019

Figure 4.9: Autarky in Austria for a small two person home depending on the year

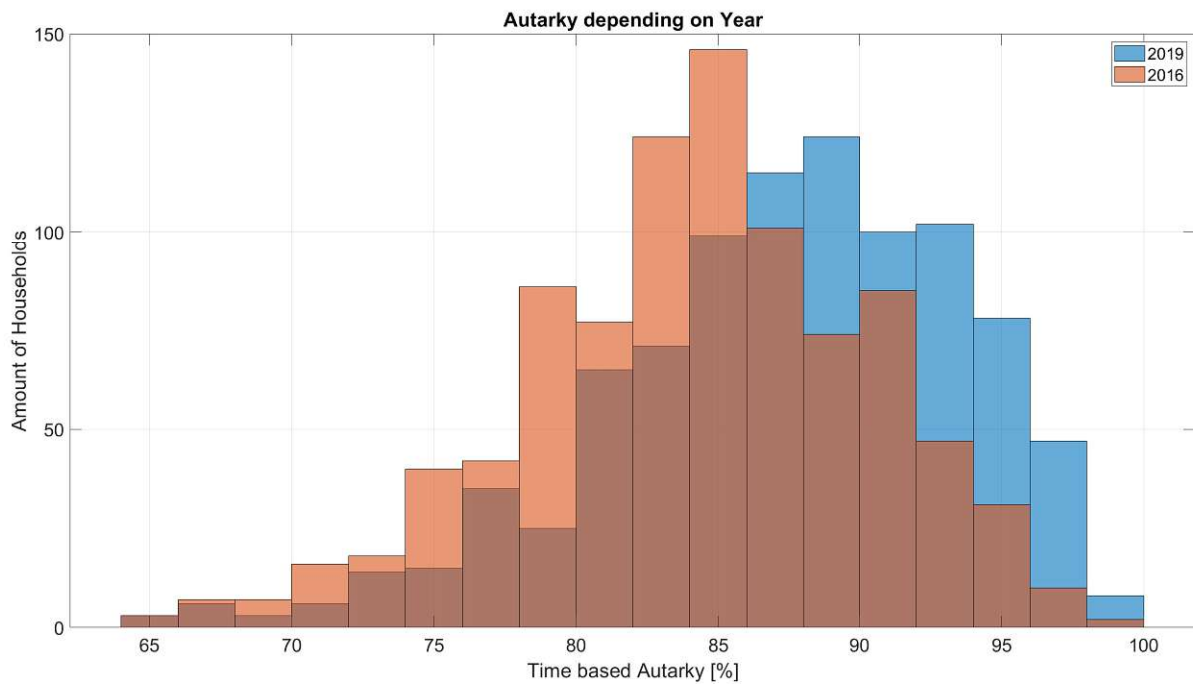


Figure 4.10: Histogram of the time based autarky for a small two person home for the worst and best year

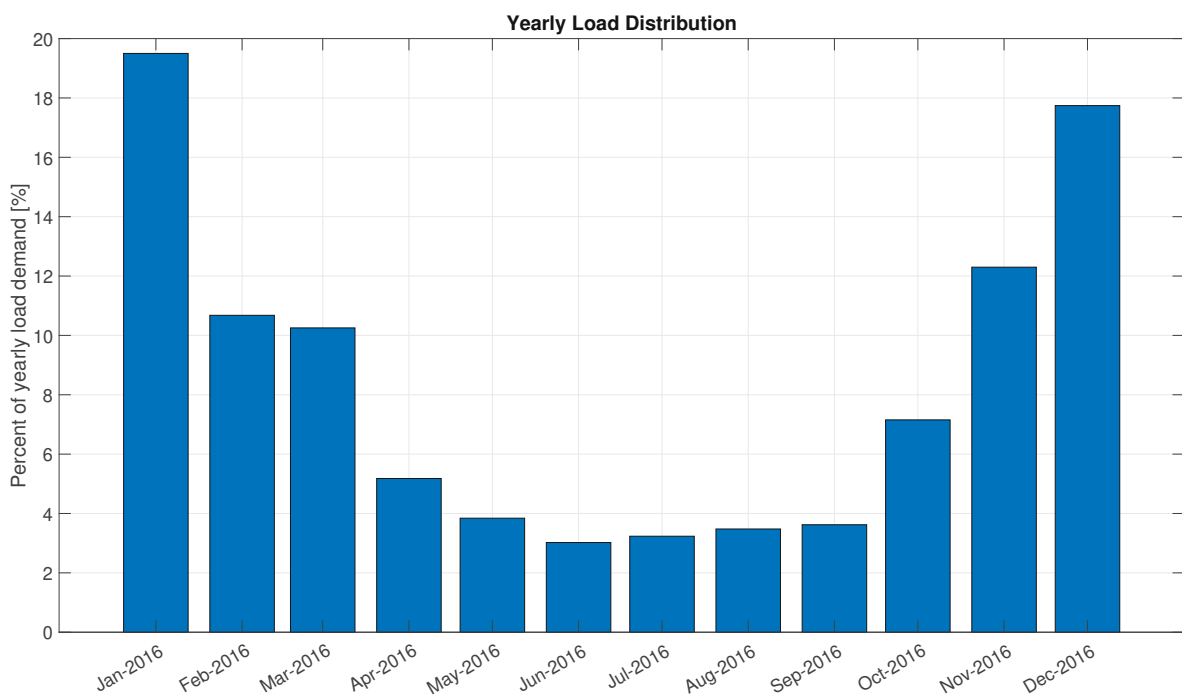


Figure 4.11: Load usage per month for a two person example household

4.2.2 Large Two Person Home

To model a bigger house with two people, the autarky of a 9x10m two story house is simulated. To factor in the bigger building size, the heat pump is upgraded to a "Bosch CS3400iAWS 10 OR-S" [96] and the

heating system now has 7500W of power. The bigger heating system does not affect the simulation that much. It just makes sure that the heat demand can be met. Except for a slightly worse COP of the bigger heat pump, the only difference is the increased amount of space which needs to be heated. The yearly power consumption is still set to 3132kWh. Furthermore, the addition of a second floor results in twice the amount of usable living space while increasing the surface of the house only by a factor of around 1.39. This leads to a better heat demand per square meter compared to a smaller one story home. The average power consumption increases because of the higher heat demand to 6685kWh, about 1000kWh more compared to the small home. While the usable living area is 1.8 times bigger than before, the average power demand for heating increases by a factor of 1.38. This proves the aforementioned claim that the additional floor decreases the required kWh/m² significantly. As before, the results of the same years can be seen in Figure 4.12. Since heating is mostly only necessary in winter, the increased load in the colder months where there is less power from the solar system, worsens the autarky significantly. Now (except some outliers) only a small area around Vienna achieves an autarky of 90-95% in a bad year. Figure 4.13 shows again the histogram of time based autarky between 2016 and 2019. For 2019, the households with an autarky over 86% are now 468, which are 100 less than with the smaller house. In 2016, it was only 242 who managed that, also an decrease of around 100 now larger households.

The mean load based autarky for all households and the five years drops down to 66%. The seasonal load distribution seen in Figure 4.11 only gets worse since there is more heat demand than before.

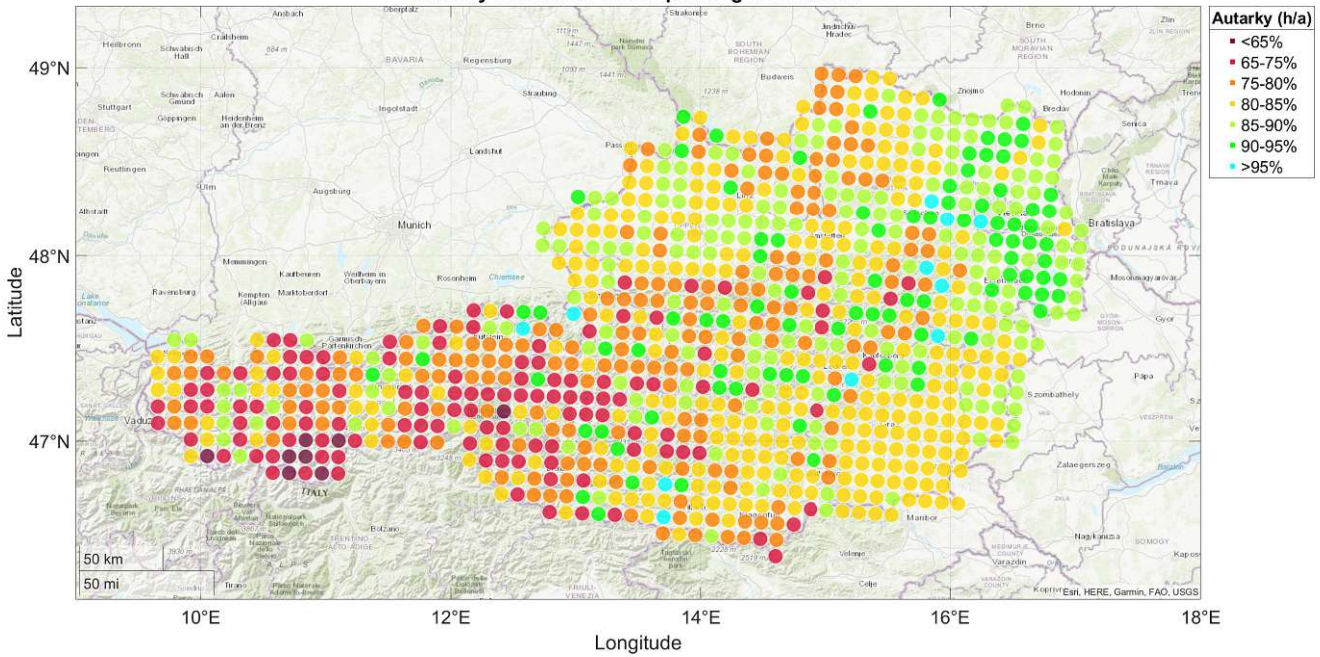
4.2.3 Large Four Person Home

The house and heating stays the same as in the previous chapter, the only difference is that now four people live there. This increases the load demand for appliances and hot water to 5230kWh per year, resulting in an overall mean load demand of 8783kWh. The resulting time based autarky for the best and worst year is seen in Figure 4.14. Once more, Figure 4.15 shows the histogram of the best and worst year. For this setup, in 2019 only 253 households achieve an autarky over 86% while in 2016 only 118 households manage this. It is interesting to note, that even though the overall load demand is more than 2000kWh higher than before, the mean load autarky is 65% - only one percent less than before. This is because the increased power demand can be satisfied by the system when power generation is high. When it is low, it can not be met anyway. This averages out over the year and results only in a small change in load autarky.

4.2.4 Large Four Person Home Without Electrical Heating

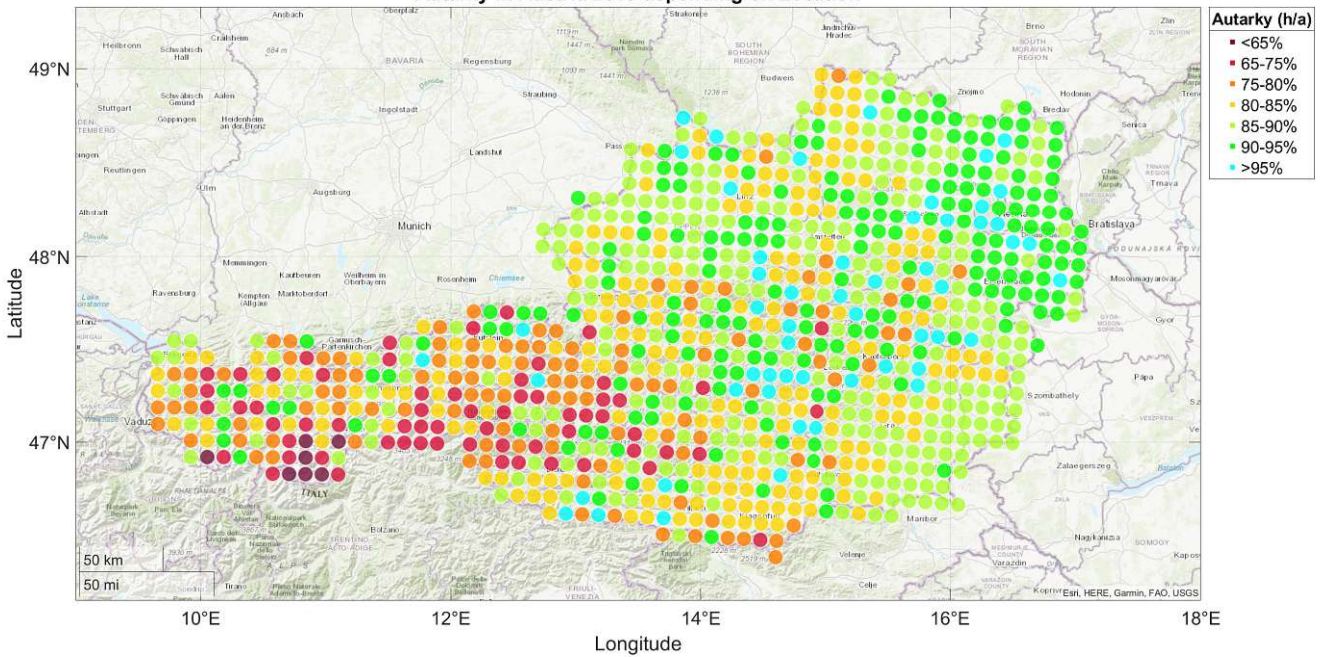
Even though the overall energy system is quite big, the electrical heating in months of little energy generation badly affects autarky. For this reason, this section considers a four person household where

Autarky in Austria 2016 depending on Location



(a) Autarky in 2016

Autarky in Austria 2019 depending on Location



(b) Autarky in 2019

Figure 4.12: Autarky in Austria for a large two person home depending on the year

the heating and hot water demand is satisfied by a conventional heating system which uses wood as fuel. This reduces the overall yearly load demand to 4325kWh which is less than the smaller home with only 2 people. In contrast to before, the autarky even in 2016 is excellent (Figure 4.16a). Figure 4.17

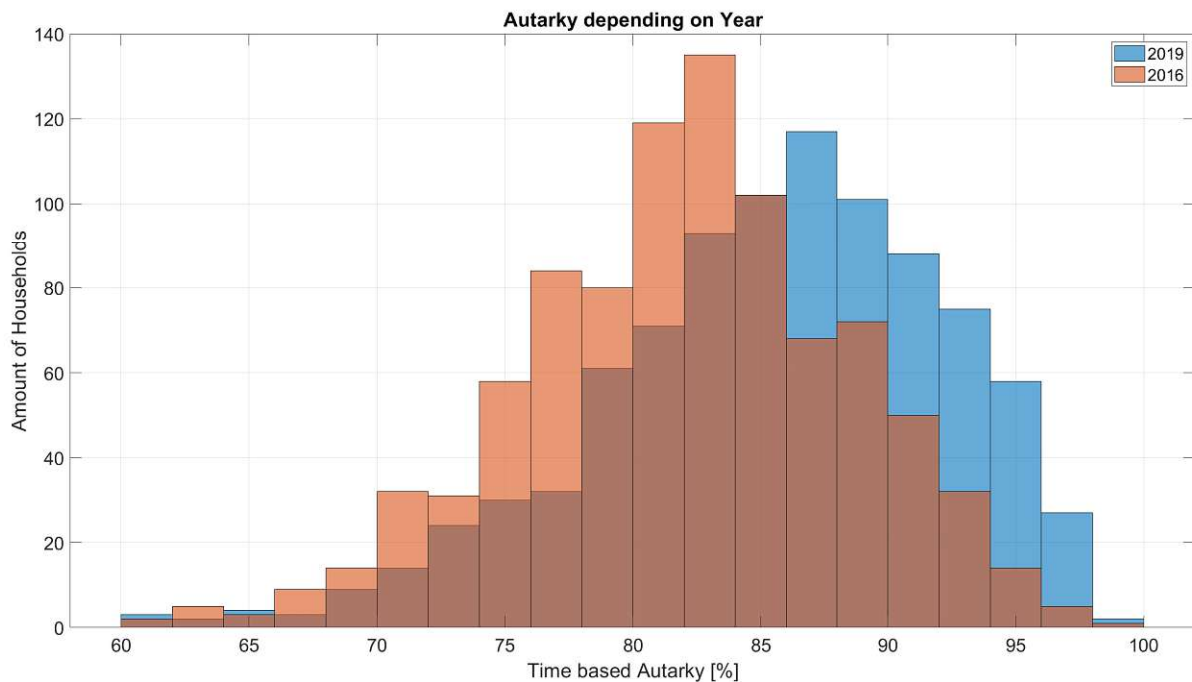


Figure 4.13: Histogram of the time based autarky for a large two person home for the worst and best year

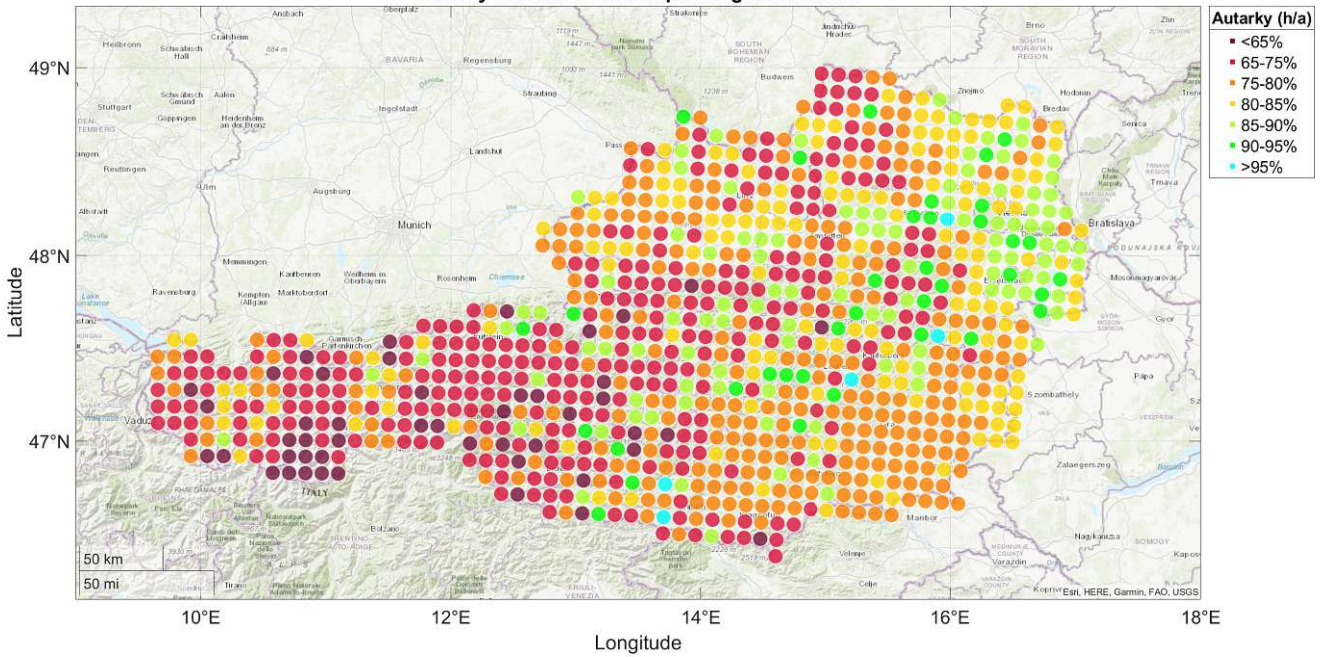
shows that while the seasonal difference in power demand is still there because of more time spend inside and more need for illumination, it is far less pronounced compared to Figure 4.11. Because the household uses 1400kWh less per year compared to the smallest experiment, the values for autarky are a lot better. The mean load autarky over these five years is 91.6%, a definitive improvement. For a higher load demand of 5645kWh, the mean load autarky is still 85.4% - around 12% more than the 5700kWh per year, small two person home with the different load distribution from electrical heating.

While Figure 4.18 still shows some difference between the years, it is not as pronounced as before. Furthermore, for both years, more than 71% of the 916 households manage a time based autarky of over 90%.

4.2.5 Small Two Person Home With Only PV

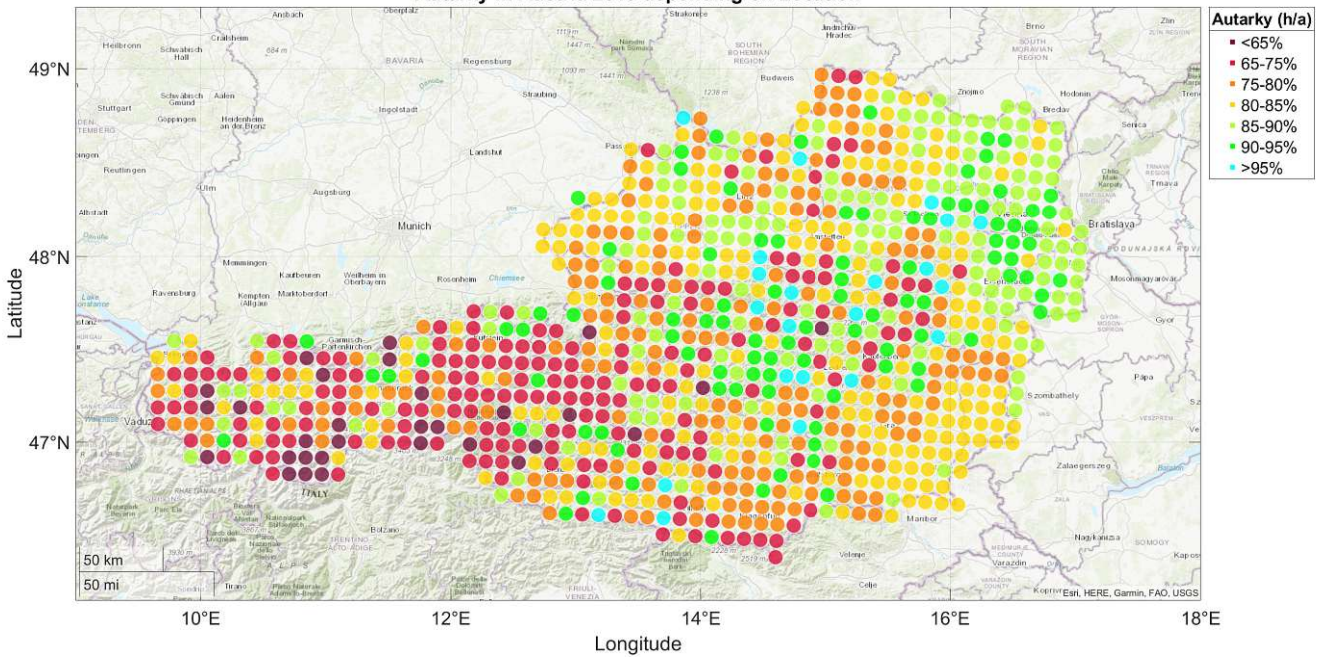
Wind turbines are an excellent energy generator which are completely decoupled from the time of day. Sadly, only selected locations in Austria have sufficient wind to efficiently use them. More so, local legal regulations or space constraints further restrict their usability. For this reason, the same experiment as in section 4.2.1 is simulated but now without a wind turbine. The experiment with only PV generation now has 2015 as the best year and 2017 as the worst year autarky wise (Figure 4.19). The drop by 6.3% in time based autarky (mean 79.4%) in contrast to the experiment with the wind turbine is relatively

Autarky in Austria 2016 depending on Location



(a) Autarky in 2016

Autarky in Austria 2019 depending on Location



(b) Autarky in 2019

Figure 4.14: Autarky in Austria for a large four person home depending on the year

small. The mean load autarky over the years on the other hand is now 63.5% - 10% less compared to before. Figure 4.20 shows that even the best year only has 115 homes which achieve a time based autarky above 86%. All in all, the lack of an additional power generator besides solar impacts autarky

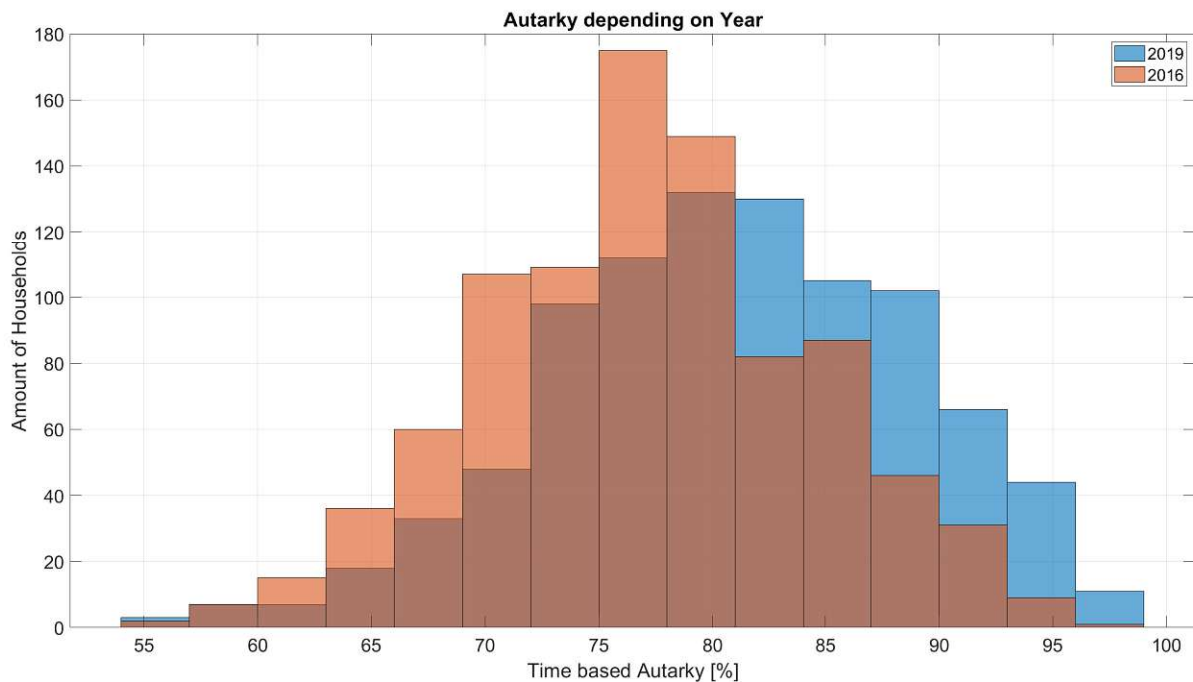
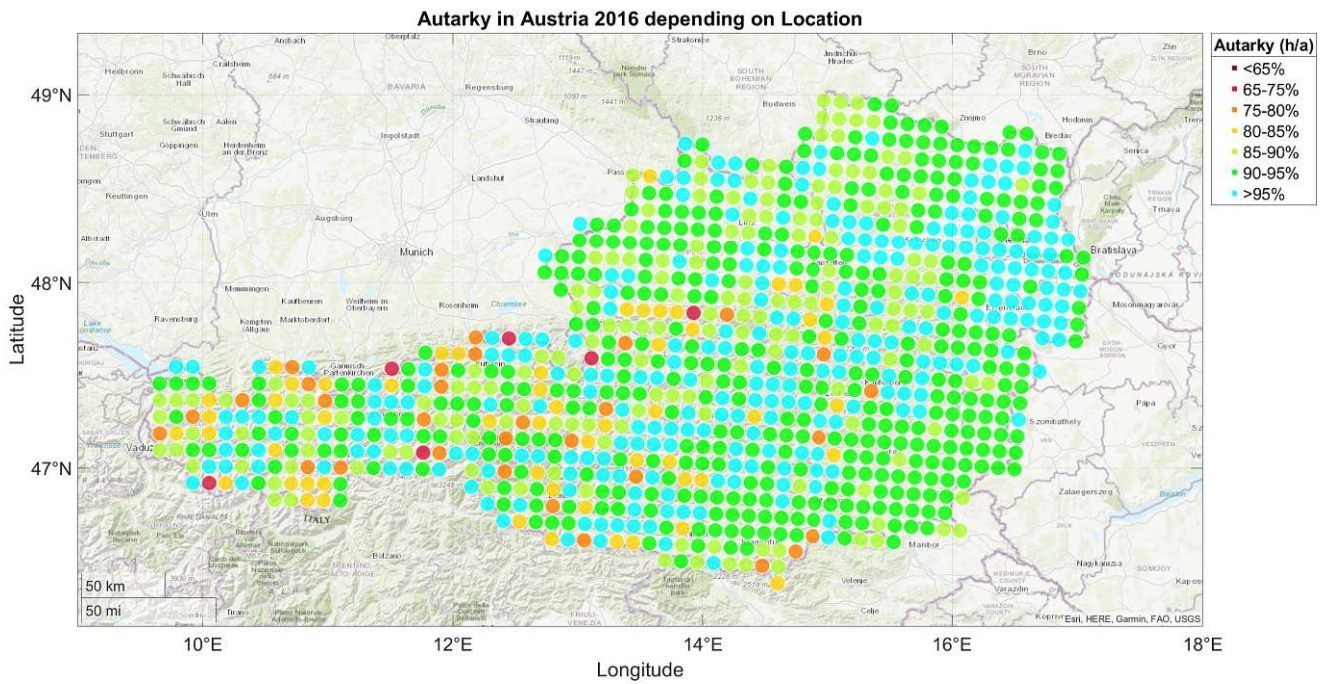


Figure 4.15: Histogram of the time based autarky for a large four person home for the worst and best year

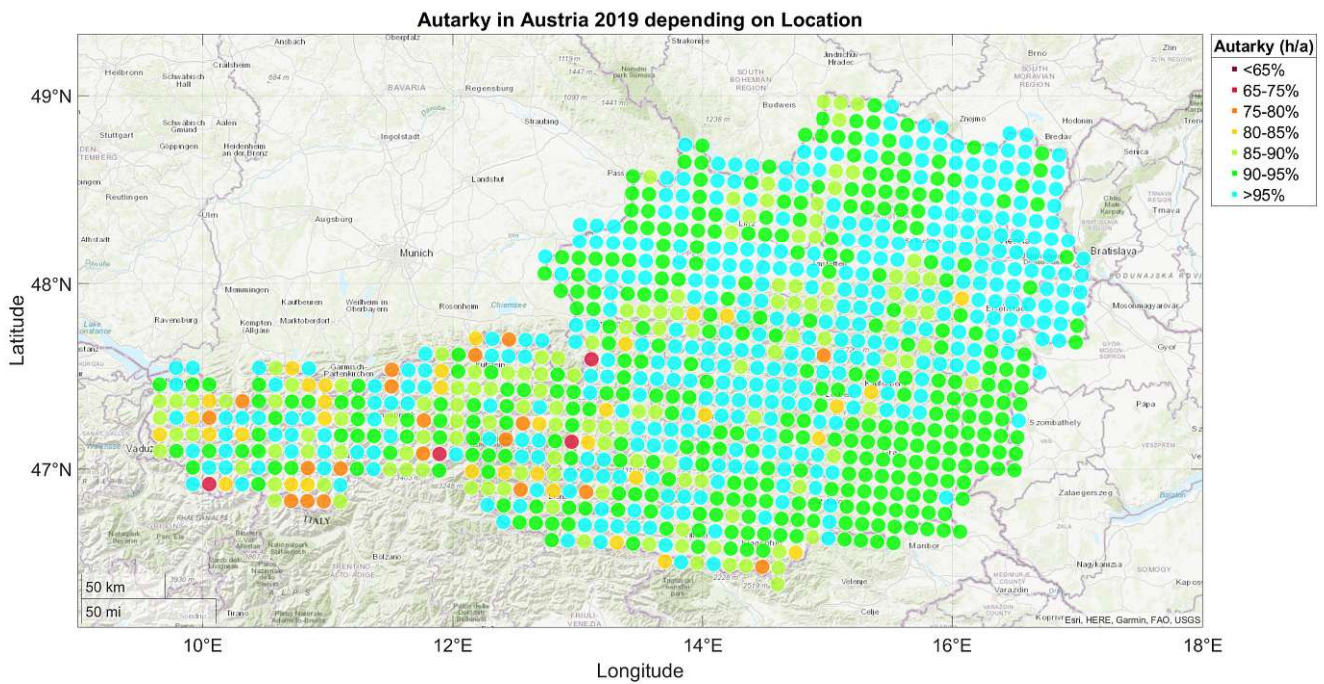
severely. Especially the high load which occurs in winter for heating combined with no power from wind generation impacts the energy self sufficiency badly. Upper Austria, Vienna and the northern Burgenland are impacted the most autarky wise. The reason for this is that while these locations have higher than average wind speeds, the solar irradiation in the east of Austria is especially low in winter times because of fog and almost constant cloud cover.

4.2.6 Small Two Person Home With Only Wind Power

As an interesting counterpoint compared to before, a small two person home with a big wind turbine is simulated. The model of the wind turbine in question is an "ANTARIS 12.0kW" [97] from the company "Braun". The website claims it is "specially made for inland locations with weak to moderate wind conditions". To further increase its efficiency, it is mounted at 30m hub height, with the biggest mast the company sells. Instead of a 6kW inverter from Fronius, the 10kW version is used. The two plots in Figure 4.21 show that besides Northeastern Austria and a few outliers, energy self sufficiency in Austria with a wind turbine alone is (predominantly) not possible. The mean time autarky in Austria is 52.3% while the load autarky is 43.4%. The histogram in Figure 4.22 is now different compared to the other experiments as the autarky now does not follow a bell curve in any way. While solar power is available everywhere with adequate performance, there are just some locations where the wind speeds do not



(a) Autarky in 2016



(b) Autarky in 2019

Figure 4.16: Autarky in Austria for a large four person home depending on the year without electrical heating

reach significant levels. For this reason the histogram is distributed more evenly. Considering that the used wind turbine is one of the largest one which is available for private customers and that the 30m

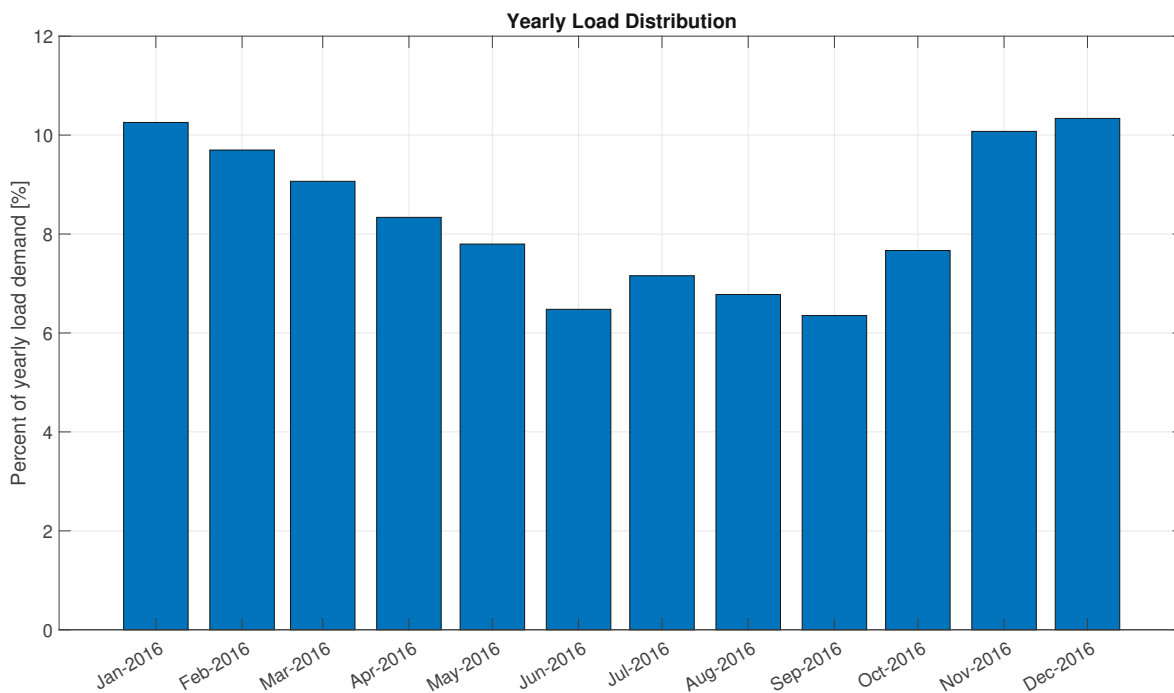


Figure 4.17: Load Usage per month for a four person example household without electrical heating

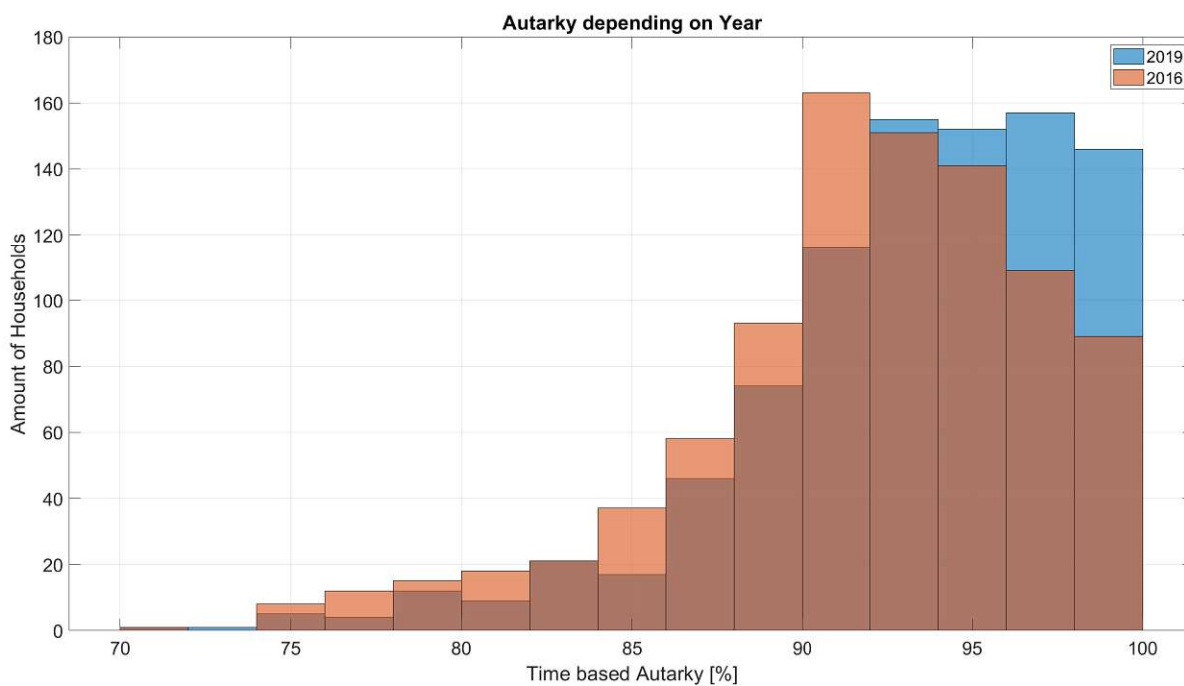
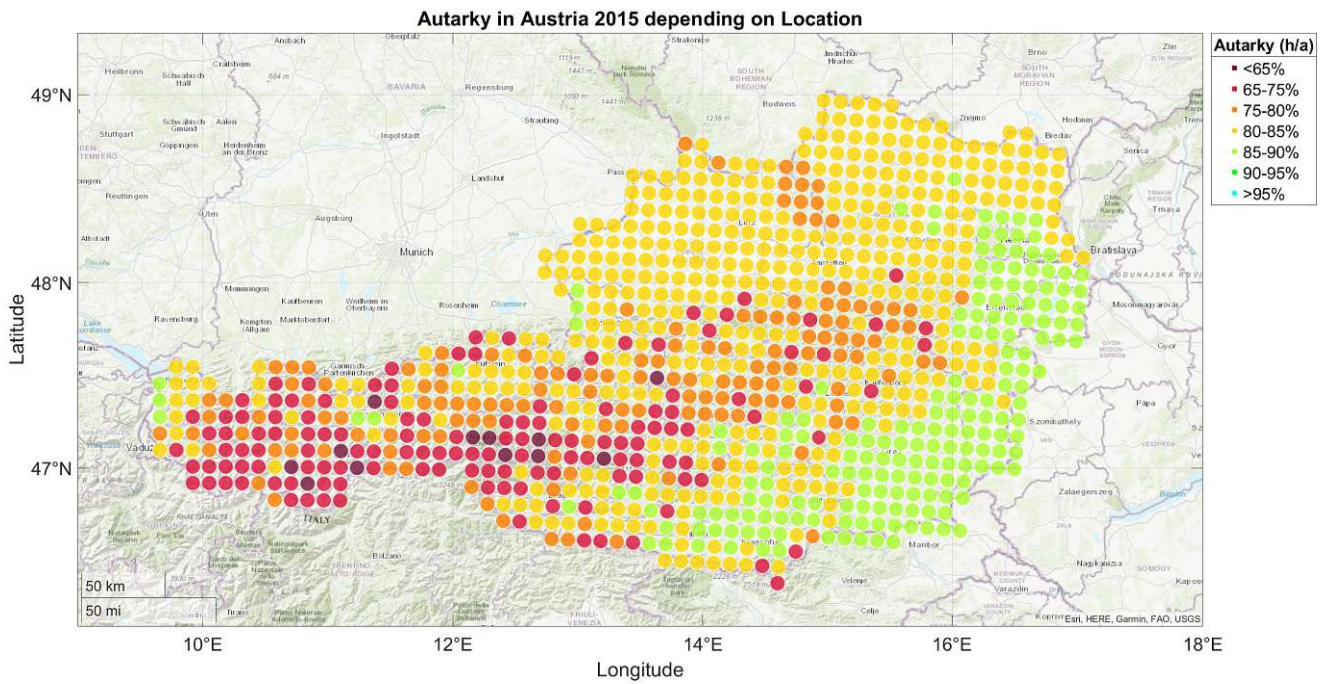
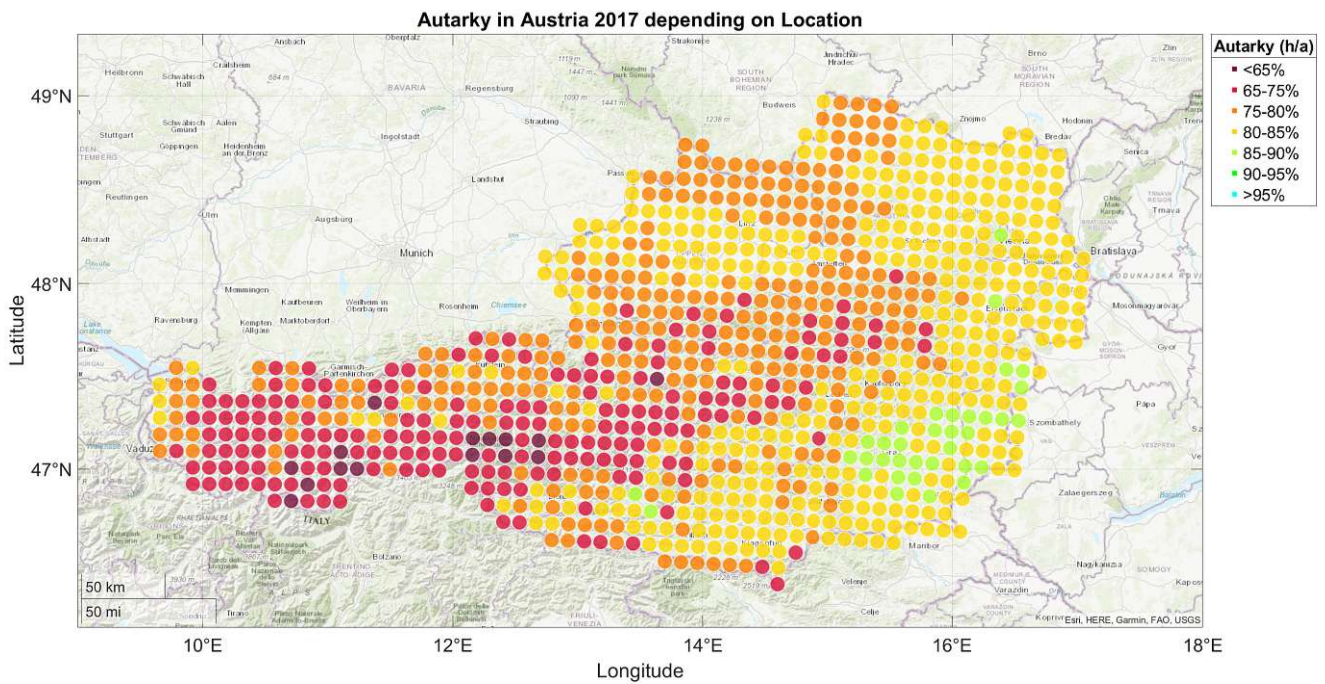


Figure 4.18: Histogram of the time based autarky for a large four person home for the worst and best year without electrical heating

tower comes with a lot of preparation, supplying the home solely with wind power is not reasonable.



(a) Autarky in 2015



(b) Autarky in 2017

Figure 4.19: Autarky in Austria for a small two person home depending on the year with only solar generation

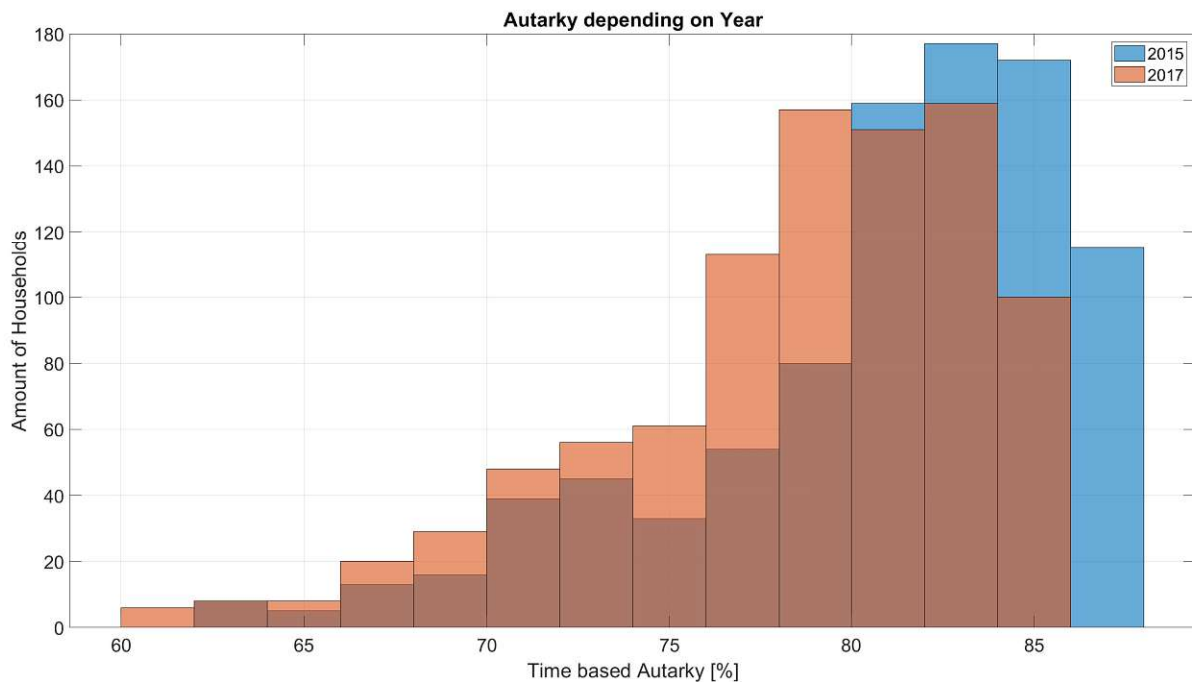


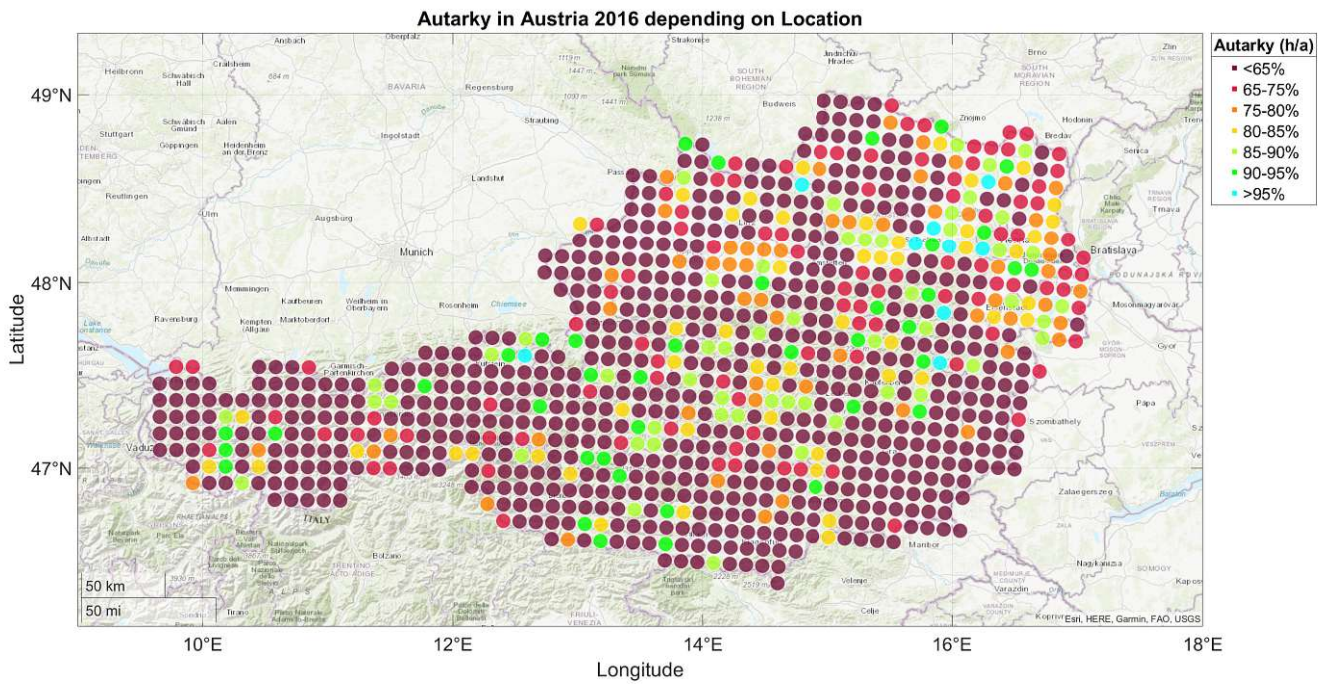
Figure 4.20: Histogram of the time based autarky for a small two person home for the worst and best year with only solar generation

4.2.7 Conclusion

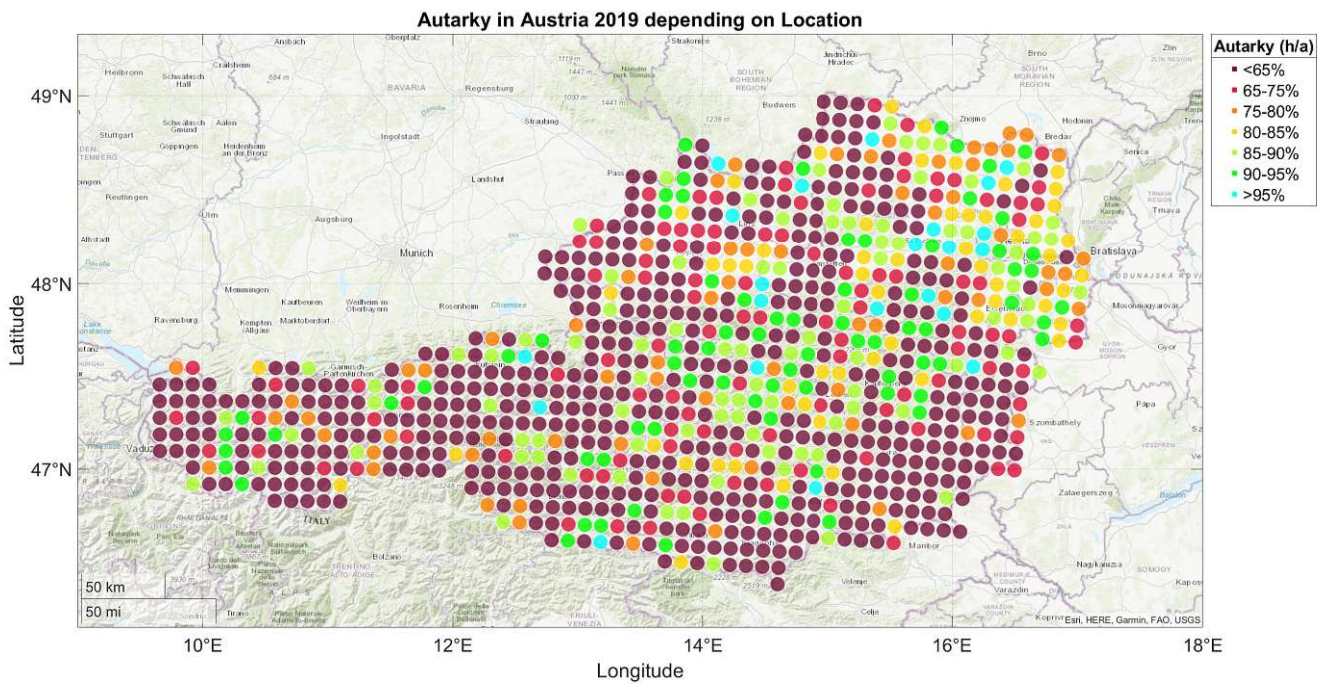
Passing review on the simulated experiments, autarky is heavily dependent on location and (while not as significant) also on the weather conditions of the current year. Autarky with electrical heating in general, is only feasible if the location has enough wind to have a sufficient energy supply throughout winter.

Difference in Solar Power Generation per Region

To break down the different parts of the autarky calculation, first, only the solar power generation depending on location is shown in Figure 4.23. The map is similar to 4.19a, showing that again Vienna, Burgenland, parts of Styria and Carinthia have the most irradiation over the year. The mountainous regions in central and western Austria can also be clearly seen as they influence energy yield by shadowing effects. The mean PV energy production in Austria over those five years for a 10kW system is 11700kWh, significantly more than the "1000kWh per installed kW PV" rule of thumb. The highest yield from the PV was 14441kWh in 2017 at the best location and the lowest 6800kWh in 2016 at the worst location. This assumes almost ideal orientation (south) and tilt (35°) of the panels which is not possible all the time. The average difference in energy production between the worst year 2016 and the best year 2020 is around 880kWh.



(a) Autarky in 2016



(b) Autarky in 2019

Figure 4.21: Autarky in Austria for a small two person home depending on the year with only solar generation

Difference in Wind Power Generation per Region

As already mentioned, the yield from wind is largely dependent on location. With a 5kW wind turbine from the company "Schachner" the mean power generation in Austria over five years is only 3328kWh

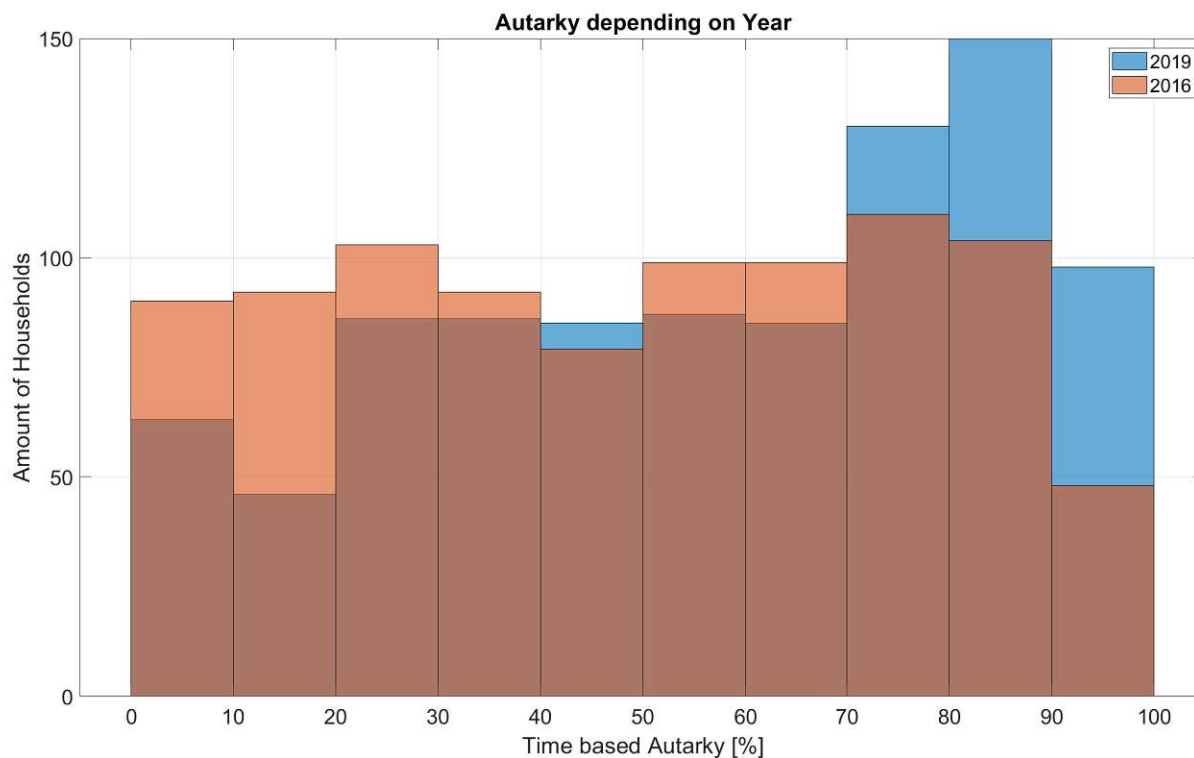


Figure 4.22: Histogram of the time based autarky for a small two person home for the worst and best year with only wind generation

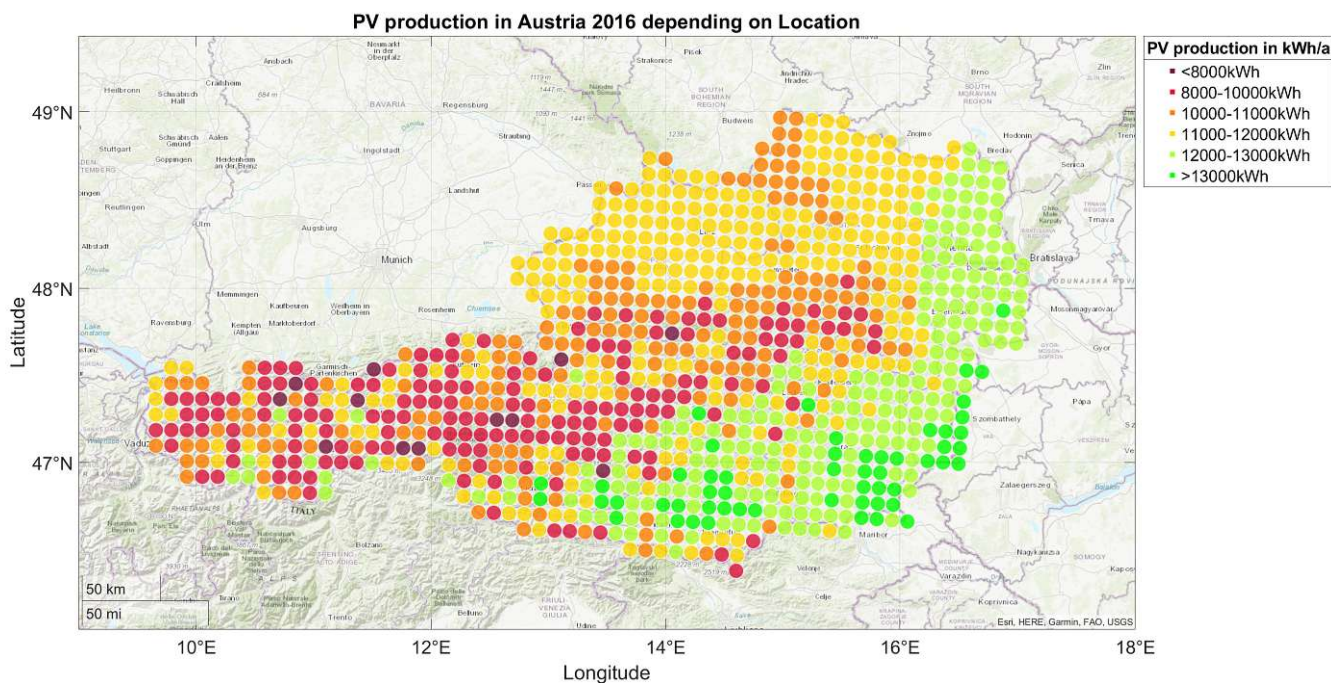


Figure 4.23: Solar power generation in Austria depending on the location in 2016

which translates to around 665 load hours per year. Wind is a lot more volatile per year compared to solar. The difference between the worst year 2016 and the best year 2019 is on average around 1274kWh. This is also the reason why the autarky for the year 2019 was generally better in the experiments even though the best "solar" year was 2020. Figure 4.24 shows that there is no clear location bias except the area around Vienna and upper Burgenland. Based exclusively on the amount of energy generation, wind turbines for private use are mostly not worth it. The big advantage, however, is their energy generation independent of the sun.

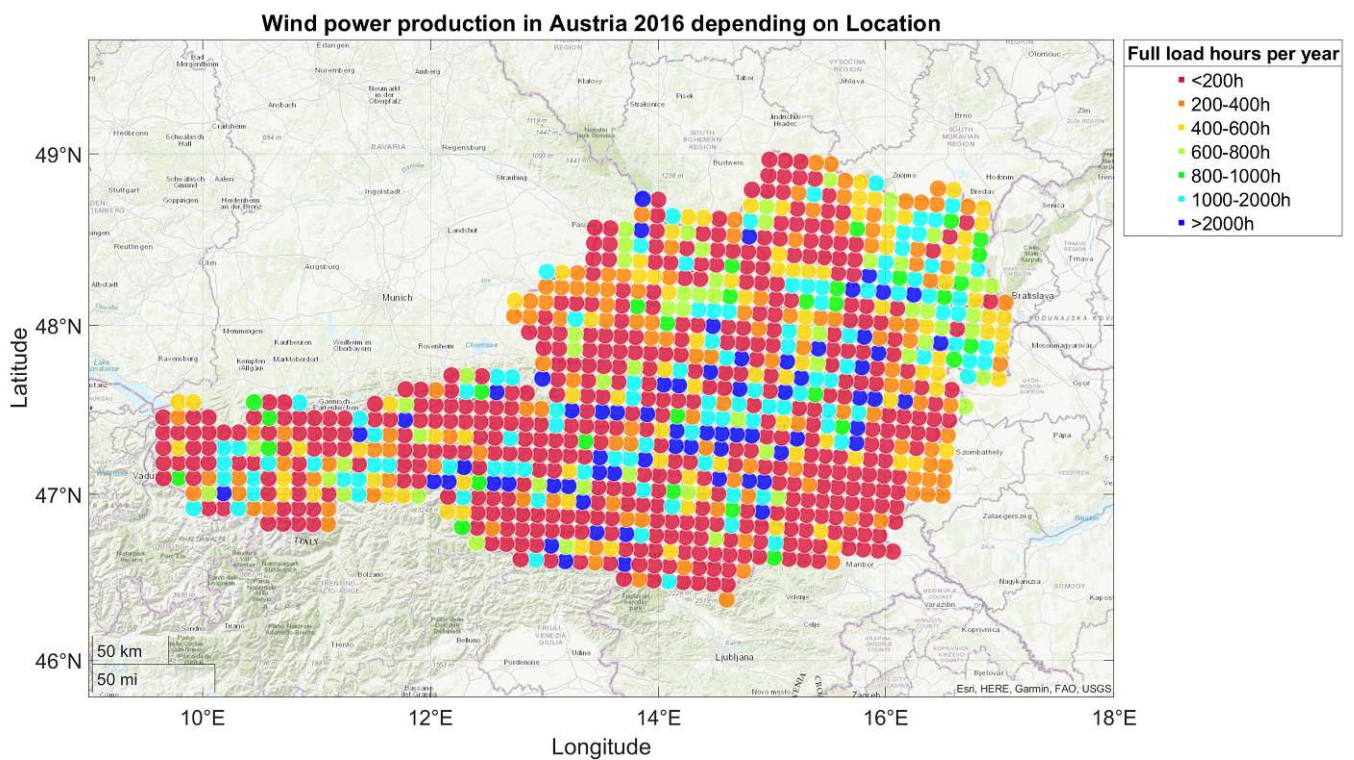


Figure 4.24: Wind power generation in Austria depending on the location in 2016

Difference in Heat Demand per Region

The heat demand depending on locations basically gives information about the temperature of the environment. As Figure 4.25 shows, similarly to the solar generation map, the worst locations considering heat demand are in central and western Austria. The higher elevation and rough terrain result in a colder climate compared to the eastern part of Austria, which is quite warm in comparison. While years with more energy generation from PV have higher irradiation and in turn reduce the heat demand slightly, the bigger factor is the environmental temperature. Figure 4.26 shows a correlation between mean yearly energy production from PV and the mean yearly temperature. Even though it diverges slightly, the thought that sunnier years are warmer in general seems not far fetched. As mentioned be-

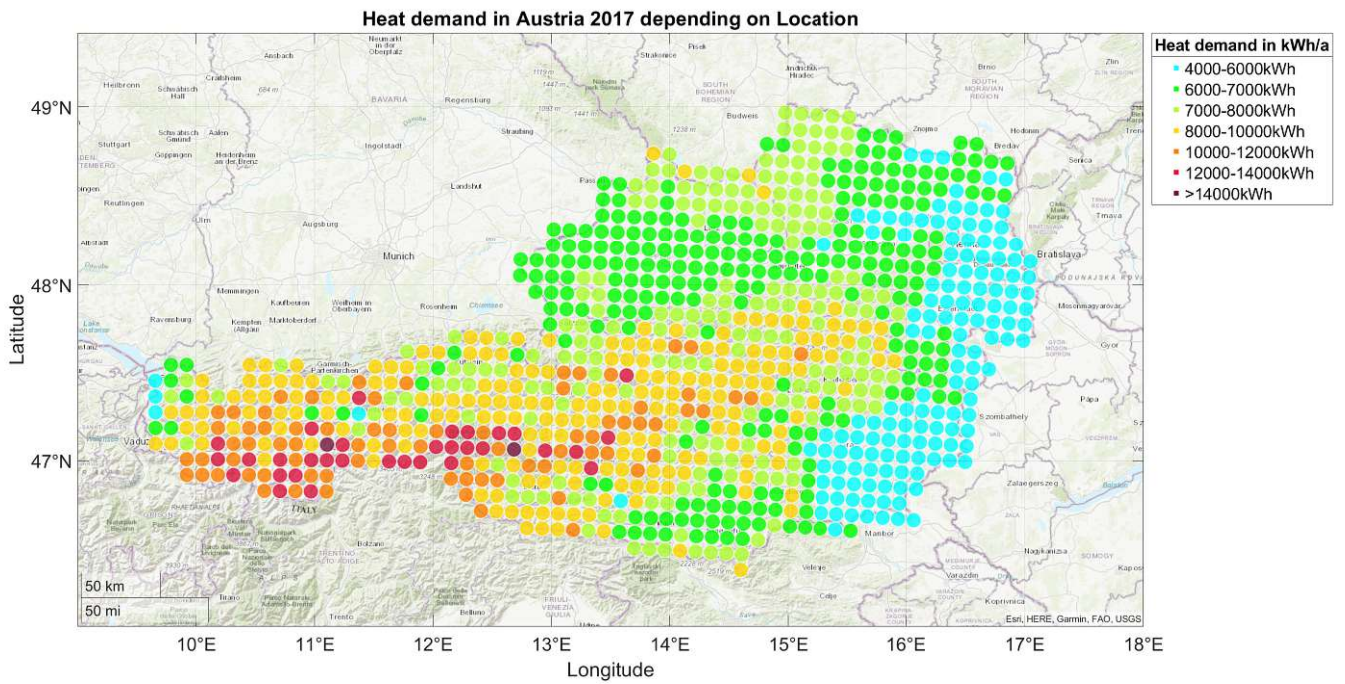


Figure 4.25: Heat demand for a small home in Austria depending on the location in 2017

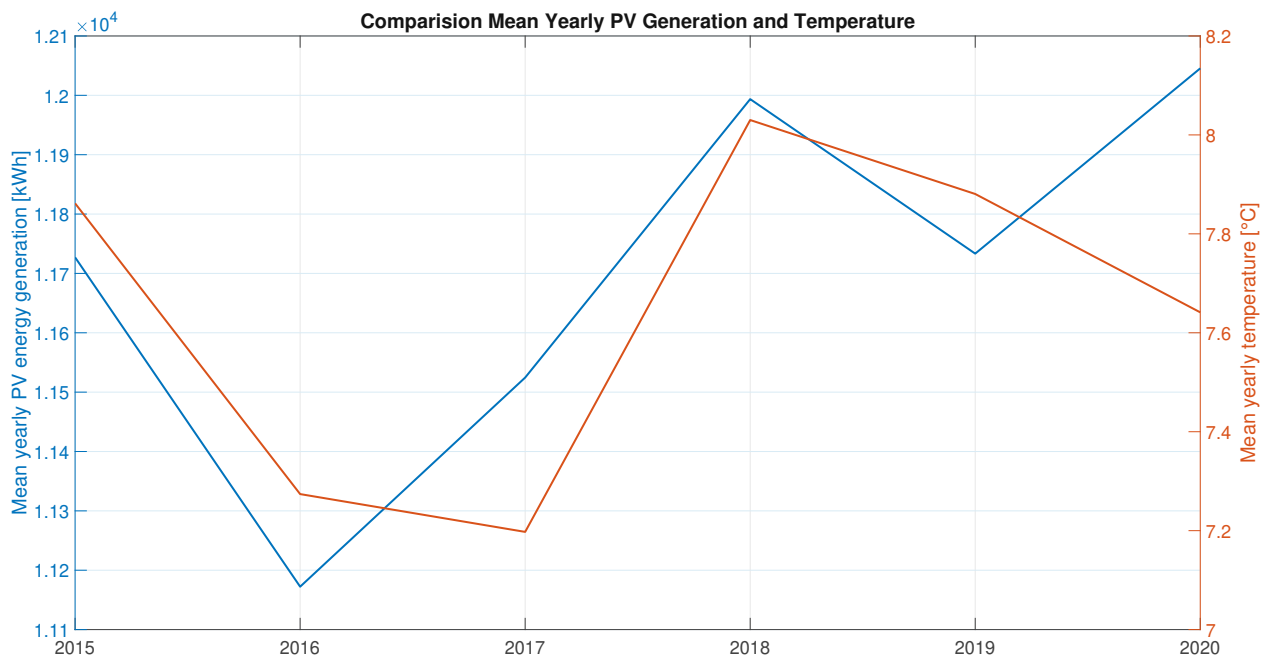


Figure 4.26: Comparison of yearly mean PV generation and temperature

fore, a warmer year with more solar power does not automatically translate into more self-sufficiency. The year 2020 had the most sun overall, but 2019 was warmer and had about 24% more wind than average, giving it an edge concerning autarky.

4.3 Autarky Depending on Photovoltaic and Battery Size

Since PV systems are quite easy to install on roofs and storage system's only requirement is a bit of space, they can be installed almost everywhere. This chapter takes a look at a few distinct locations and varies PV and usable storage size to find out how big the system needs to be to achieve different grades of autarky. This time, the main focus is on the load autarky as the goal is to be fully energy self-sufficient. The large two person home from Section 4.2.2 is used with an annual base load of 3132kWh. Furthermore, only the year 2016 is considered as it was shown that it performed the worst autarky wise. The maximum inverter power in the following experiments is set to the size of the simulated PV system. So a 15kW PV has an inverter which also can manage 15kW. To simplify, the efficiency of the inverter is always set to 97.1%. The maximum charging/discharging rate of the battery is dependent on size, appropriate values were taken from the "BYD HVM" batteries [22].

4.3.1 Neusiedl am See, Burgenland

The first experiment is set in Neusiedl am See (latitude=47.958256, longitude=16.873508), a region which is one of the better places for autarky in all of Austria. The resulting overall power need including the heat pump for this location is 5136kWh. Figure 4.27 shows that even with an absurdly large system, the

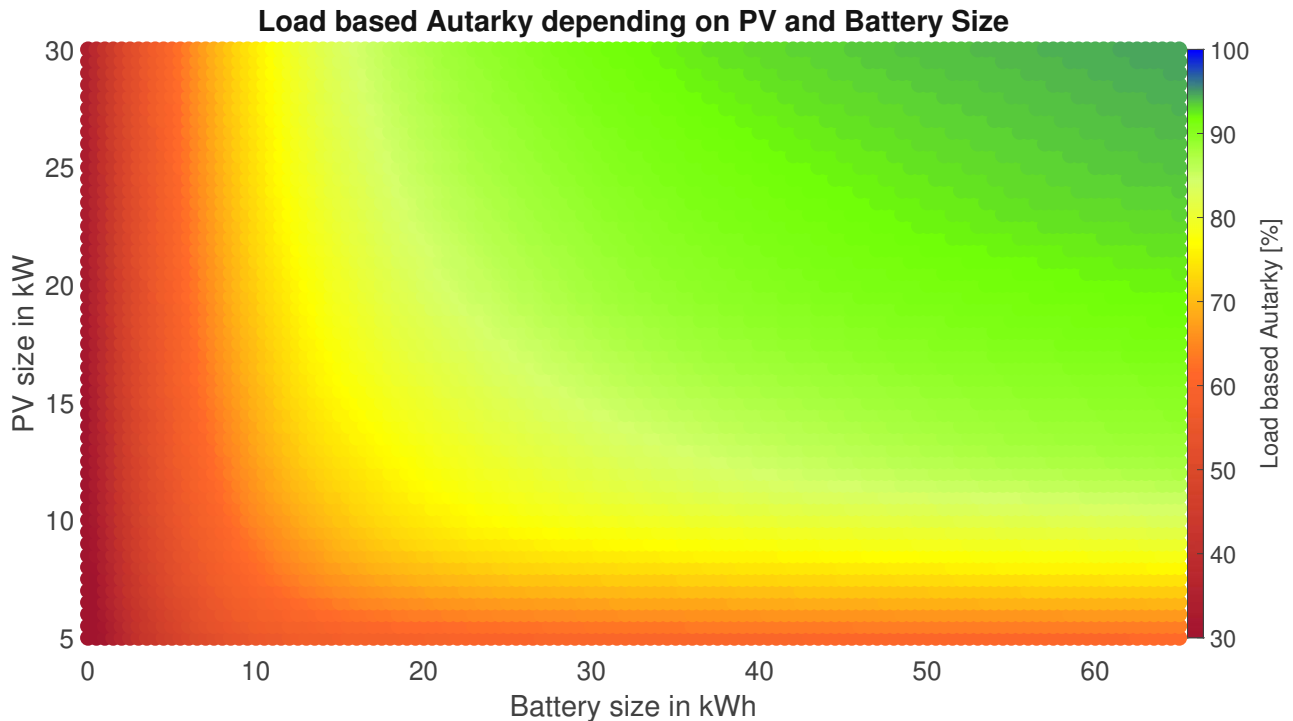


Figure 4.27: Load autarky depending on PV and usable storage size in Neusiedl am See in 2016

maximum amount of load autarky this setup reaches is 94.76%. It also shows the diminishing returns which the scaling up of the components brings. As an example, with a 30kW PV system and a 30kWh

storage system, the load autarky is 91.33%. Doubling the storage size results in a load autarky of 94.76% - an insignificant increase considering the action taken. When using the system size of the previous chapter (10kW PV and 11kWh storage, further referenced as "base system") a load autarky of 66.04% is achieved. To compare, the same graph of a household which has an overall load of 5459kWh but no heat pump is shown in Figure 4.28. Just as in the experiments before, the different load distribution throughout the year (Figure 4.11, 4.17) has a significant impact on autarky. The highest load autarky from before with the heat pump (94.76%), which took 30kW of solar panels and a 65kWh storage is now achieved with a system of 16kW solar panels and a 20kWh storage. Using the smaller household load of 3132kWh from before without heating shows a similar result. Those 94.76% can then be achieved by a 12.5kW solar system with 11kWh of storage.

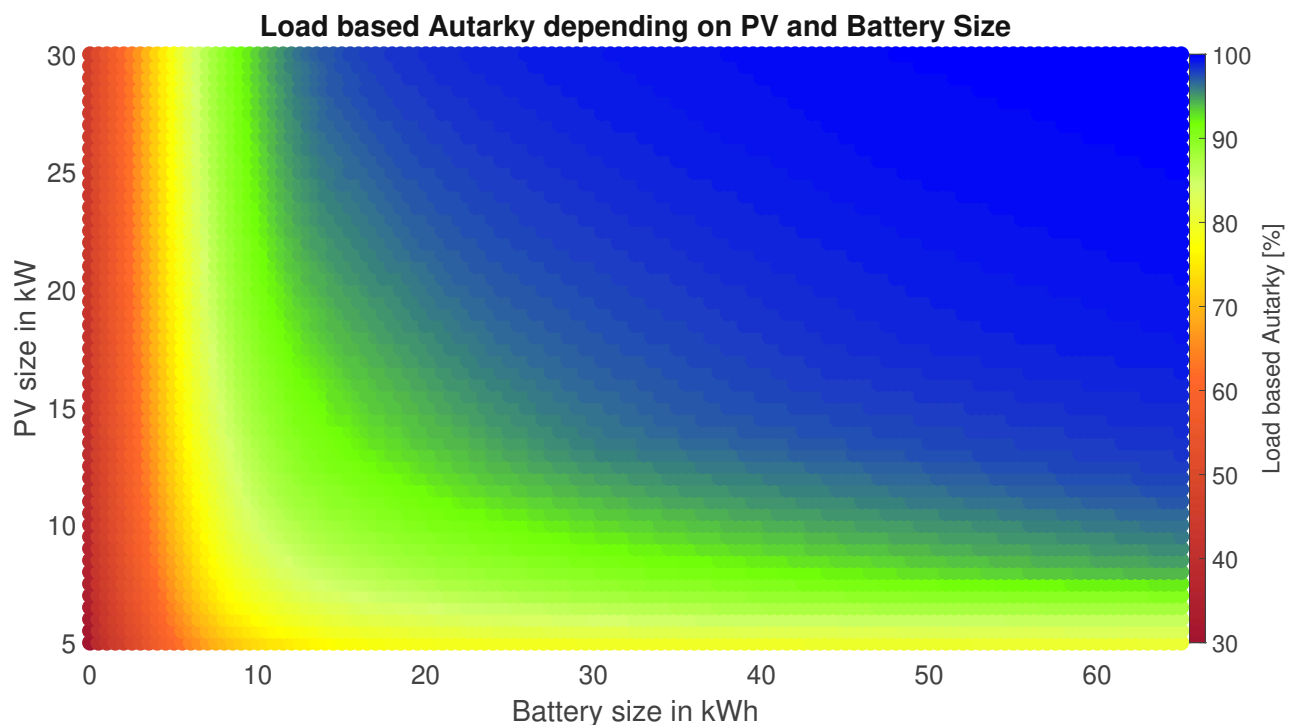


Figure 4.28: Load autarky depending on PV and usable storage size in Neusiedl am See in 2016 without electrical heating and 5459kWh power demand

4.3.2 Rudmanns at Zwettel, Lower Austria

Now the experiment takes place in Rudmanns, a municipality of Zwettel (latitude=48.598731, longitude=15.202934). At this location the energy yield from the PV is lower than before and the heat demand is higher. The overall yearly household load is now 6382kWh, 1200kWh more than compared to Neusiedl. The result is shown in Figure 4.29. As the energy yield is lower and demand higher because there is more heating required, the overall autarky suffers from it. The maximum amount of autarky

reached within the given limits is 93.38%. In contrast to before, a 30kW PV, 30kWh storage system results in a load autarky of 87.92%. Again, using the base system the load autarky only reaches 56.12% - a decrease of almost 10%.

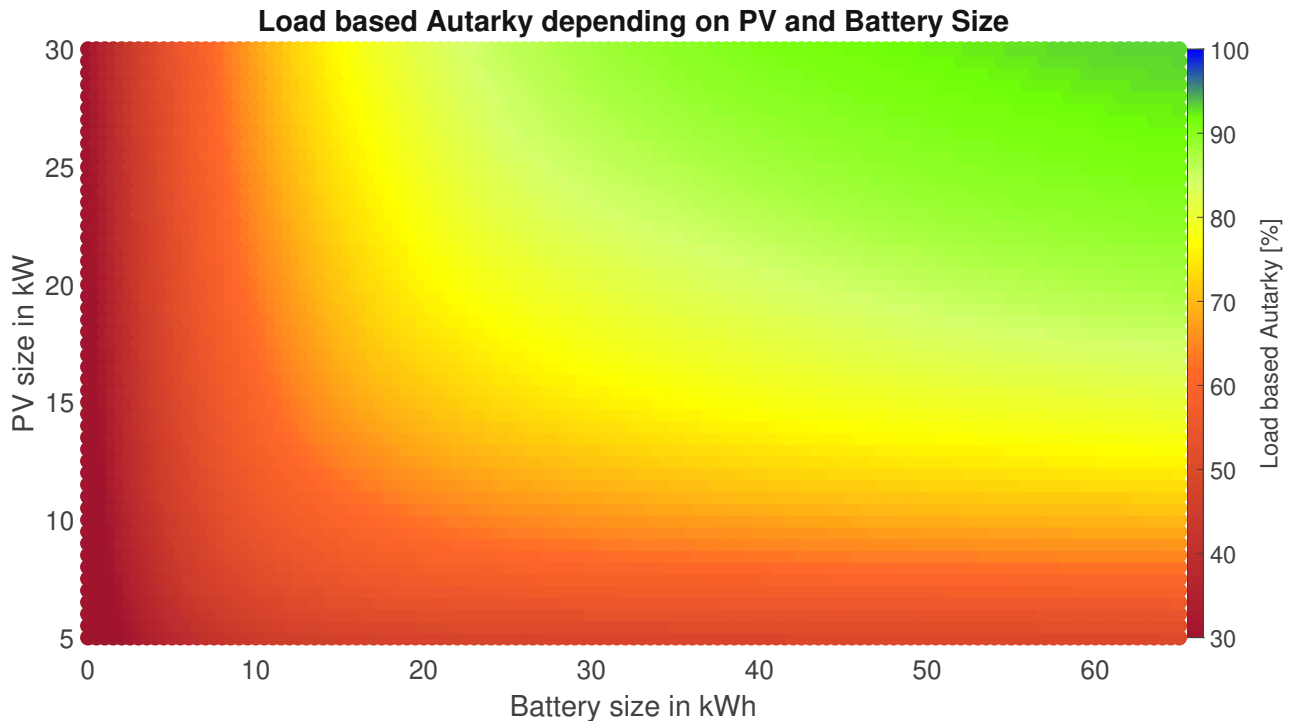


Figure 4.29: Load autarky depending on PV and usable storage size in Rudmanns in 2016

4.3.3 Tultschnig at Klagenfurt am Wörthersee, Carinthia

Tultschnig is a small town outside of Klagenfurt am Wörthersee in Carinthia (latitude=46.655389, longitude=14.245961). The heat demand at this location is smaller than at Rudmanns but a bit larger than Neusiedl, namely 5850kWh. Figure 4.30 shows immediately, that the load autarky for larger systems is far better in comparison to the previous locations. This stems from the fact that in the critical months of December and January, irradiation was higher in Tultschnig compared to Neusiedl. The maximum system size results in a load autarky of 98.25% and the 30/30 system produces a self-sufficiency of 94.31%. The base system achieves an autarky of 63.39%. This shows that while the smaller system performs better in Neusiedl because of higher irradiation in the warmer months, the larger systems perform better in Tultschnig because of the higher energy generation in winter.

4.3.4 Liezen, Styria

Liezen is a town in north-western Styria (latitude=47.565530,longitude=14.232494). The yearly overall load demand is 6103kWh which is on the higher end. Even though it has a larger load demand from heat,

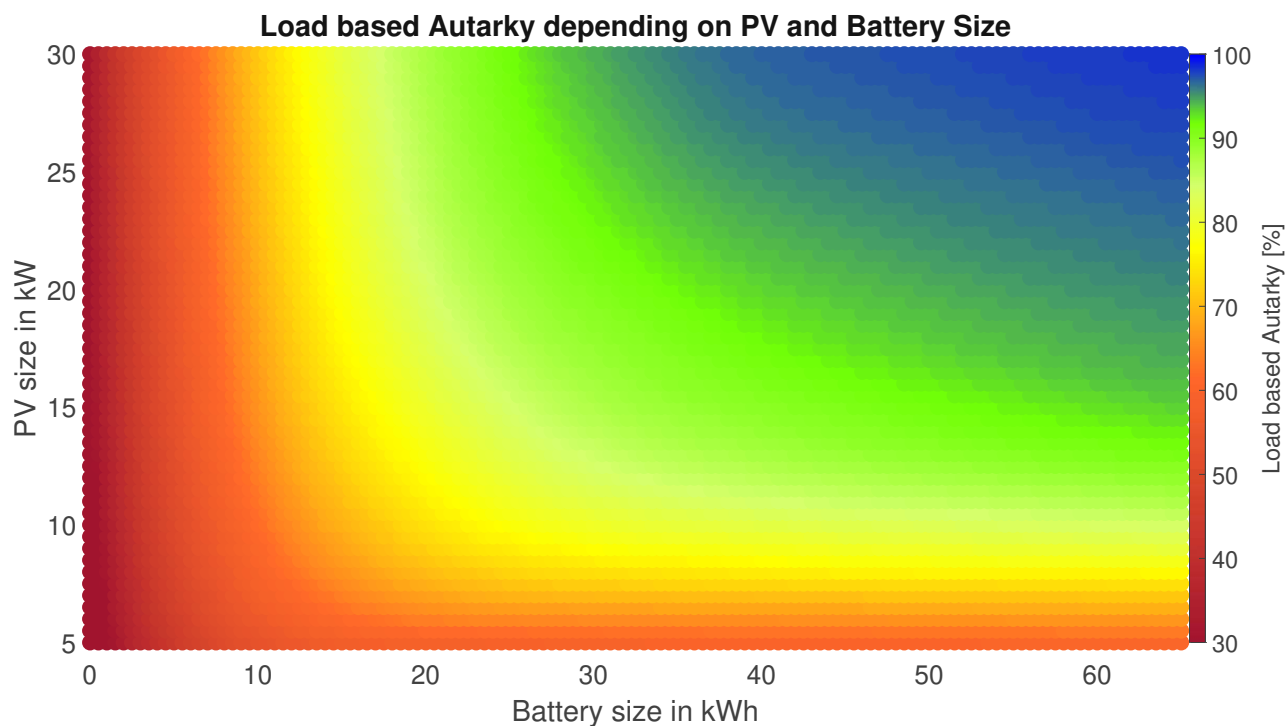


Figure 4.30: Load autarky depending on PV and usable storage size in Tultschnig in 2016

Figure 4.31 shows that the larger systems again perform quite well. The maximum system size now produces the best results overall, reaching a load autarky of 99.46%. This again indicates that although the solar system generally outputs less energy compared to for example Tultschnig, the critical winter months seem to be the best until now. The 30/30 system results in a autarky of 93.99% and the base system allows for a self-sufficiency of 62.42%.

4.3.5 Imst, Tyrol

For the last location, Imst a town in western Tyrol (latitude=47.249364,longitude=10.748335) was chosen. With a yearly overall load demand of 6118kWh, it is the second highest of all the locations. Figure 4.32 shows the calculated sweep of the load autarky. The maximum value reached is 98.47%, the 30/30 system achieves 96.12% and the base system 63.43%. Imst performs similarly to Tultschnig but has the best results for the 30/30 system of all the experiments. Overall, better load autarkies are reached with a smaller storage, which translates to more consistent solar irradiation throughout the year. The Plots in 4.33 exemplify the claim from before. Given a large enough system, the solar energy generation in winter is better in Tultschnig, Liezen and Imst compared to Neusiedl or Rudmanns. Except for Rudmanns, the better performing locations are at a few hundred meters higher sea level in contrast to Neusiedl. Reduced cloud cover and less fog at those locations in winter could be the reason for the better performance in the critical months.

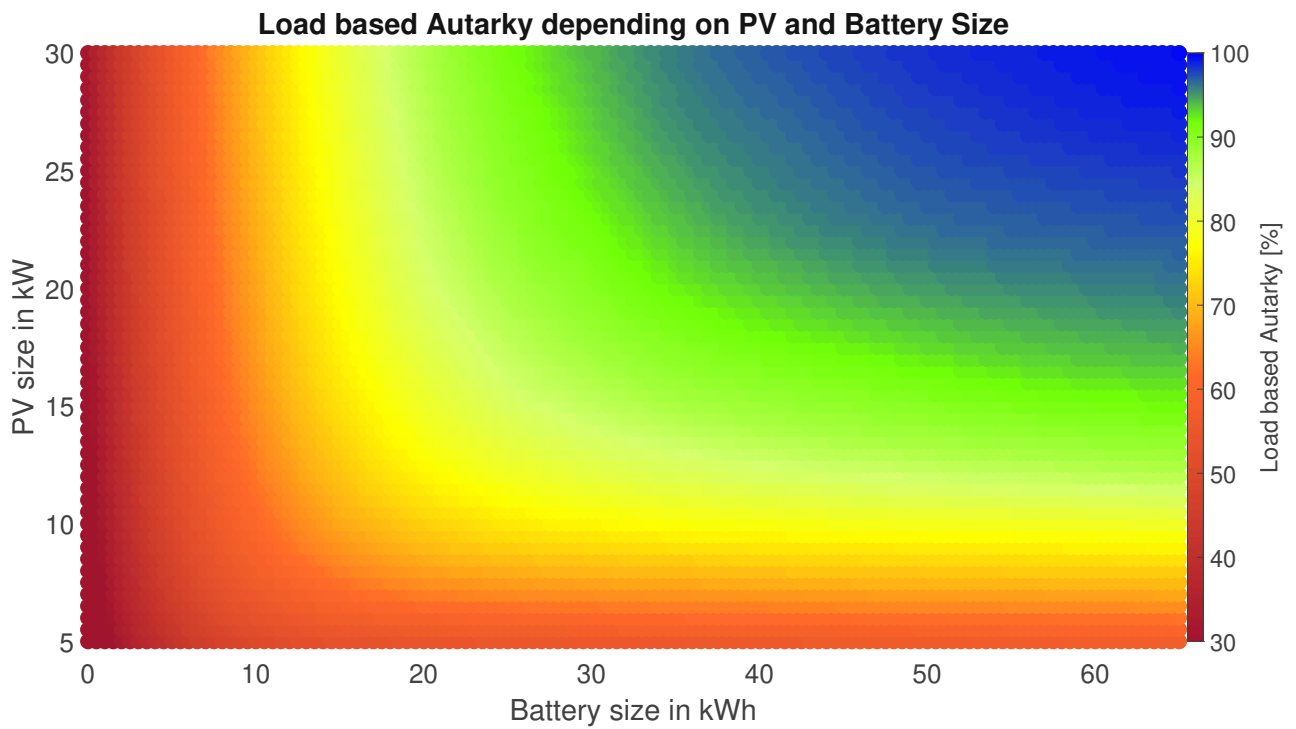


Figure 4.31: Load autarky depending on PV and usable storage size in Liezen in 2016

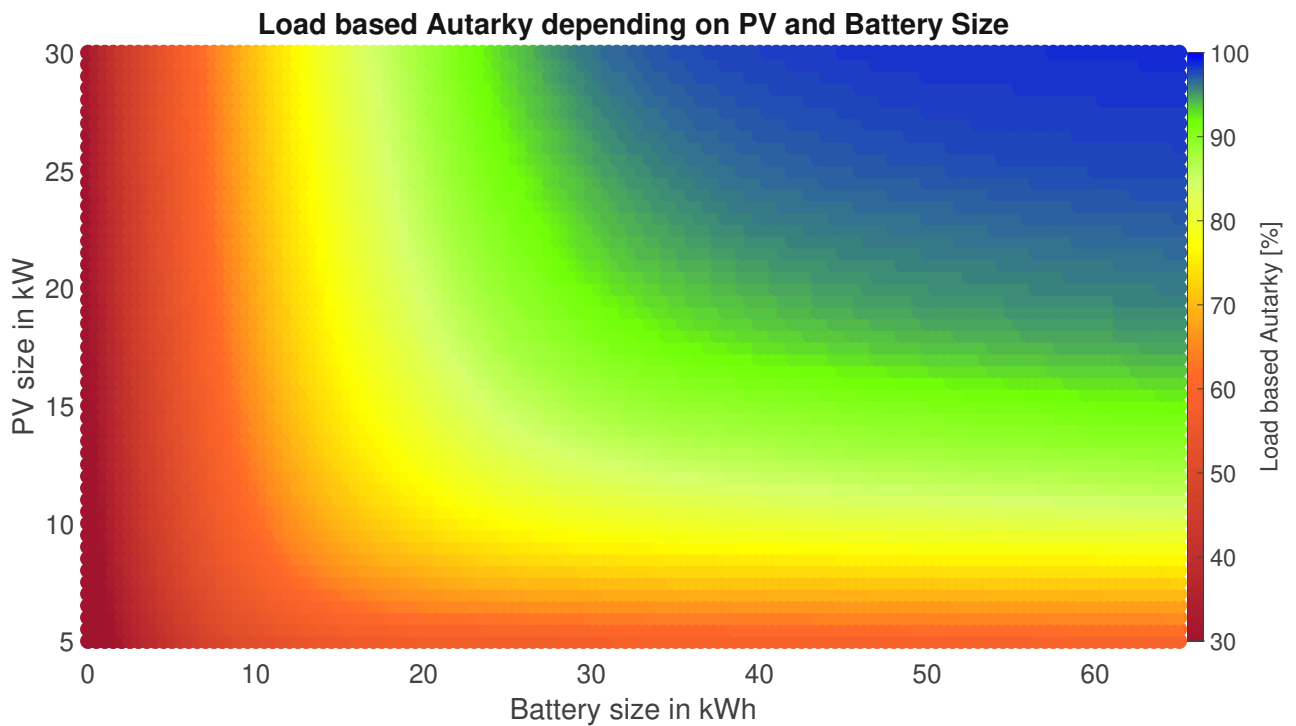
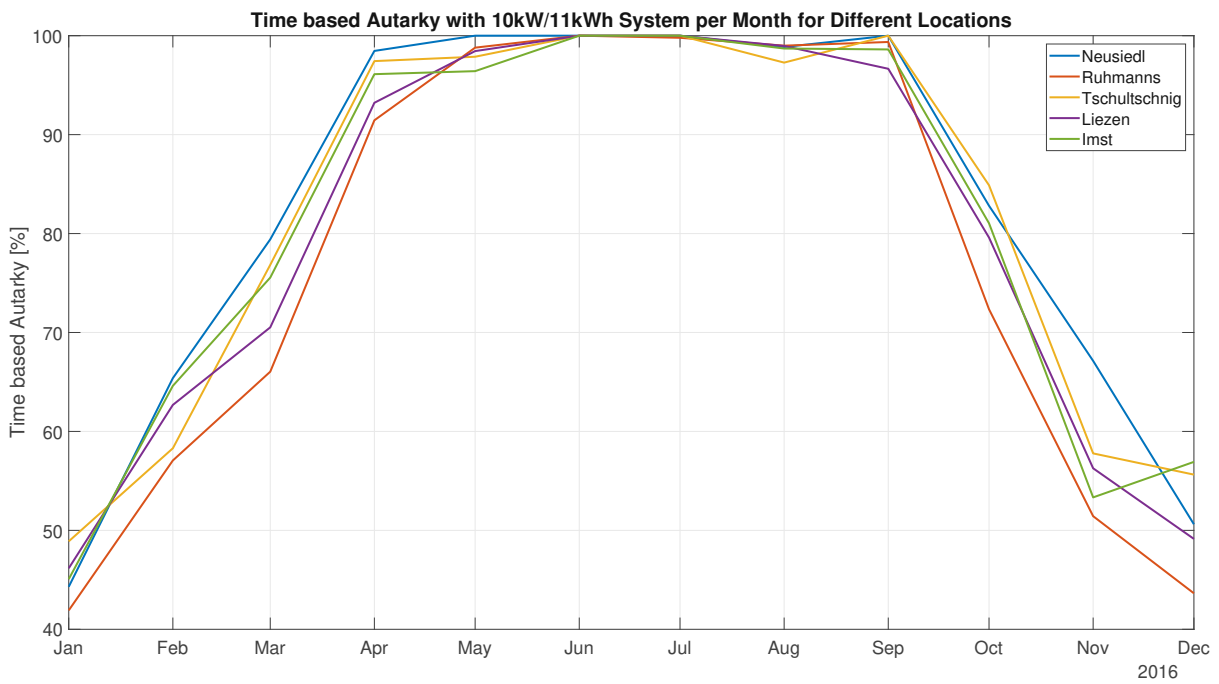
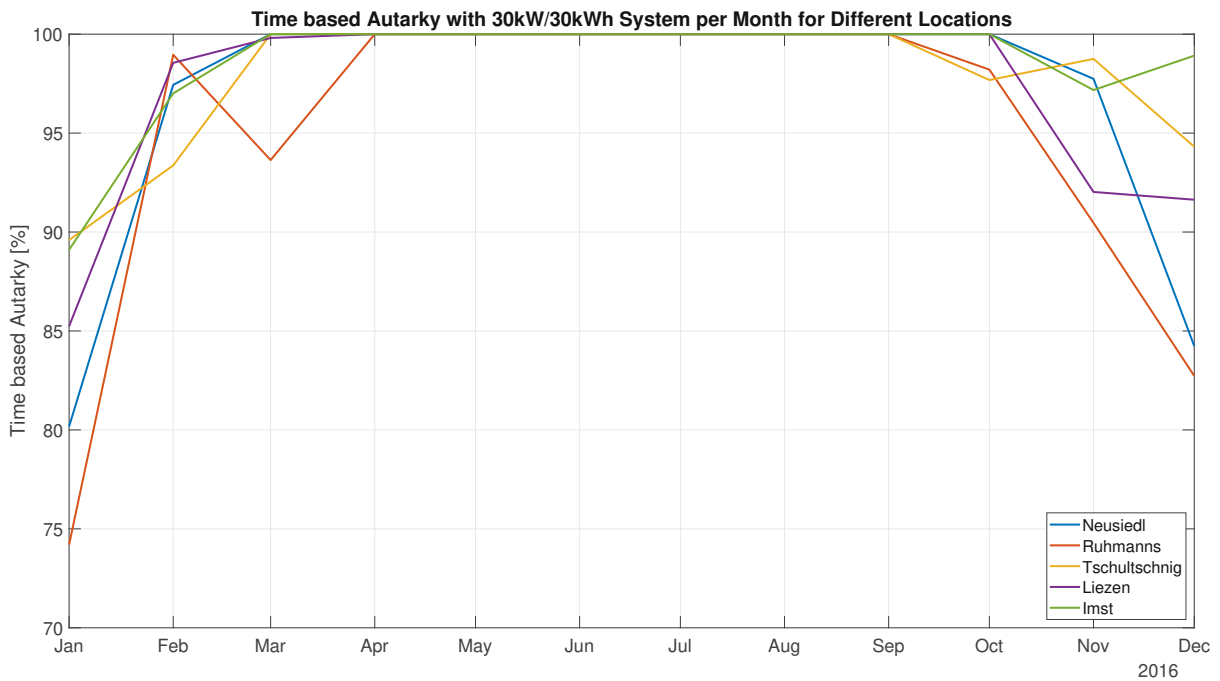


Figure 4.32: Load autarky depending on PV and usable storage size in Imst in 2016



(a) Time based autarky in 2016 for different Locations with a 11kW Solar and 11kWh Storage System



(b) Time based autarky in 2016 for different Locations with a 30kW Solar and 30kWh Storage System

Figure 4.33: Time based autarky in 2016 for different Locations with the base- and 30/30 System

Chapter 5

Conclusion and Outlook

In this work, the AAS, a location independent single household simulation model was created. It consists of a solar energy generation model, a wind turbine generation model, an (already existing) load simulation model, a heat supply and demand model and a storage model. Together, they create a yearly autarky analysis tool which outputs a variety of data describing the experiment in detail.

To compare, a few available autarky simulators which are available online were analyzed and given a review. All of them except for one did not consider the effects of different geographical location on autarky. Furthermore, the validity of different available weather data in Austria was determined by comparing modeled data to measured data.

Autarky throughout Austria was simulated with different household sizes and energy generation setups. The regional environmental differences in Austria were highlighted (Section 4.2.1-4.2.6). It was shown that energy self-sufficiency with a heat pump is possible but only if the environmental circumstances allow for it. The location needs to have sufficient wind to make up for the months where the power yield from the solar panels is not enough or the PV and storage needs do be scaled up excessively while having enough irradiation in winter. Using a conventional wood based heating system allows for far more widespread autarky (Figure 5.1). More so, the effects which yearly weather differences have on autarky were discussed. This answers the first three research questions mentioned in Section 1.2. To answer the question on how scaling of the components influences autarky, the effect of PVs and storage systems of different sizes were analyzed at five different key locations in Austria (Section 4.3). To further improve the AAS, there are a few points which could be built upon. Firstly, the battery model is currently very simple. An improvement would be the implementation of multiple storage systems just like the hydrogen storage described in the second chapter. For example, a smaller "short term" storage with high efficiency and if it is full and there is still an excess of energy created, a less efficient "long term" storage. Furthermore, the exemption of the inverter losses if the battery can

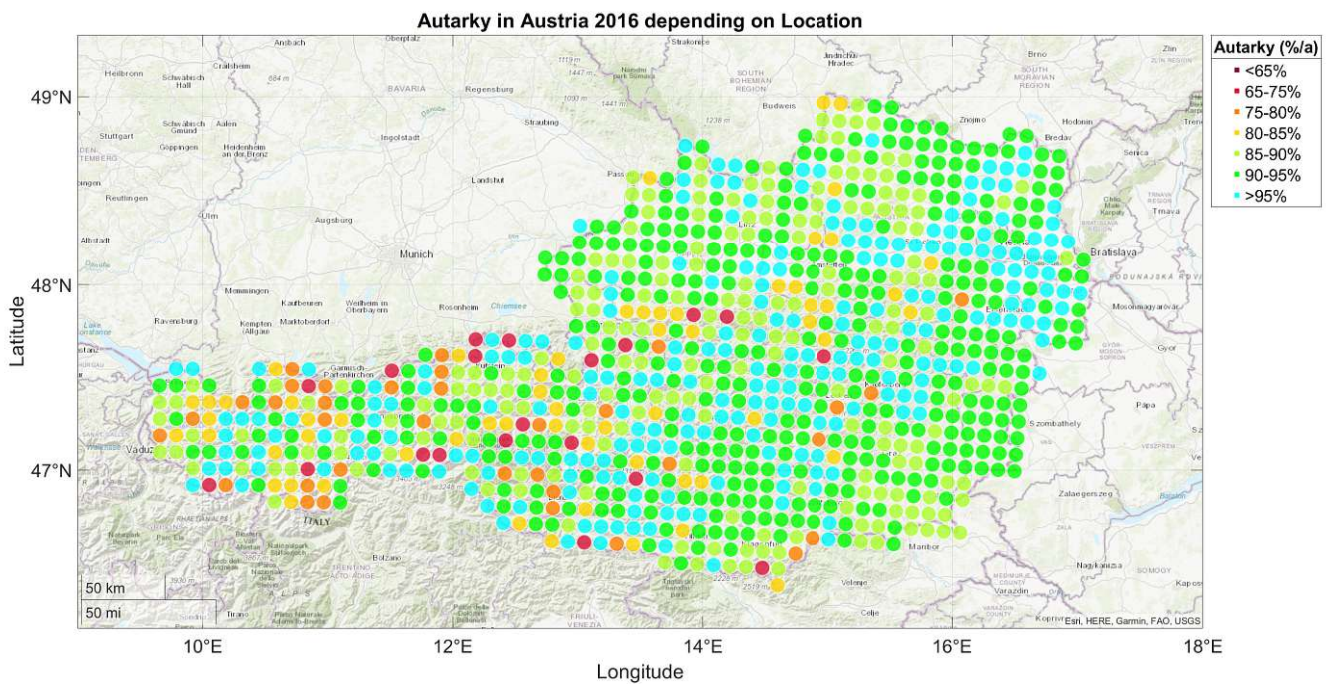


Figure 5.1: Load autarky for a four person household without electrical heating in 2016

be directly charged by the solar panels could also be implemented. An additional small enhancement would be the usage of self measured load profiles. More so, the heat model could be enhanced by using information of the real life load demand and efficiencies of heat pumps and not just data sheets. Also, instead of just a cube, the house geometry may be upgraded to allow for conventional sloping roofs.

Considering other reviewed autarky simulators, calculation of the economical effects and ecological impacts of the given system could be added. This would allow for computation on how long it takes for the system to be profitable or how much CO₂ can be saved with it. The AAS could also be implemented as a web based tool to allow everyone to simulate their setup. Another aspect would be the implementation of other weather data so that other countries could also be analyzed. To conclude, the AAS also could be scaled up to not only simulate single households but whole residential buildings with a large amount of tenants.

Bibliography

- [1] "Climate in Austria," last Accessed: September 21, 2022. [Online]. Available: <https://climate-adapt.eea.europa.eu/en/countries-regions/countries/austria>
- [2] "PVGIS Tool," last Accessed: September 21, 2022. [Online]. Available: https://re.jrc.ec.europa.eu/pvg_tools/en/
- [3] "Residential Load Simulator Github," last Accessed: September 21, 2022. [Online]. Available: <https://github.com/FXaverZ/ResidentialLoadSimulator>
- [4] "PV-systems development in Austria," last Accessed: October 17, 2022. [Online]. Available: <https://positionen.wienenergie.at/grafiken/photovoltaik-ausbau-in-oesterreich/>
- [5] "Compera Price per PV kWp ," last Accessed: October 17, 2022. [Online]. Available: <https://www.compera.at/strom/photovoltaik/>
- [6] V. Quaschnig, *Regenerative Energiesysteme*. Carl Hanser Verlag, 2021.
- [7] "Panasonic Evervolt Datasheet," last Accessed: October 17, 2022. [Online]. Available: https://ftp.panasonic.com/solar/datasheet/ds_evpv410h_400h.pdf
- [8] "Enercon 101," last Accessed: October 17, 2022. [Online]. Available: <https://www.wind-turbine-models.com/turbines/130-enercon-e-101#datasheet>
- [9] "Windpower,legal requirements in Austria," last Accessed: October 17, 2022. [Online]. Available: ["https://www.kleinwindkraft.at/?xmlval_ID_KEY%5b0%5d=1284"](https://www.kleinwindkraft.at/?xmlval_ID_KEY%5b0%5d=1284)
- [10] K. Leonhartsberger, M. Mauro, and P. A. Hirschl, "Kleinwindkraftreport Österreich 2018." [Online]. Available: www.technikum-wien.at
- [11] "Generator,Turbine and Box for Micro-Hydro," last Accessed: October 17, 2022. [Online]. Available: <https://www.kit-elec-shop.com/gb/129-synchronous-generators>

- [12] "Water-rights Austria," last Accessed: October 17, 2022. [Online]. Available: "<https://info.bml.gv.at/dam/jcr:c1c3bc31-4854-4c16-9acf-707f0e665ab9/WRG%201959%20idF%20BGBI%20I%20Nr%2073/2018.pdf>"
- [13] "Datasheet of Q-Batteries," last Accessed: October 17, 2022. [Online]. Available: "<https://online-batterien.at/media/pdf/db/83/e5/68da3036-48a7-454a-bbfd-8b9cba941a19.pdf>"
- [14] "Datasheet of Hoppecke-Batteries," last Accessed: October 17, 2022. [Online]. Available: "https://www.europe-solarstore.com/download/hoppecke/opzv/OPzV_solar.power_en.pdf"
- [15] "Anern Lead-acid Battery Datasheet," last Accessed: October 17, 2022. [Online]. Available: "<https://www.anerngroup.com/uploads/file/solar-lead-acid-battery.pdf>"
- [16] K. Khan, M. Hossain, A. K. M. Obaydullah, and M. Wadud, "Pkl electrochemical cell and the peukert's law," *International Journal Of Advance Research And Innovative Ideas In Education*, vol. 4, pp. 4219–4227, 04 2018.
- [17] D. A. J. Rand and P. T. Moseley, "Ah efficiency this reduces the ah efficiency and results in an increasing self-discharge of the cells. from: Encyclopedia of electrochemical power sources energy storage with lead-acid batteries," 2009.
- [18] "AGM Battery 12V 193Ah," last Accessed: October 17, 2022. [Online]. Available: "<https://online-batterien.at/1323/q-batteries-12lc-180/12v-193ah-blei-akku-zyklentyp-agm-deep-cycle-vrla>"
- [19] "Forklift Battery," last Accessed: October 17, 2022. [Online]. Available: "<https://www.foreverpureplace.com/12-75-5-wc-p/12-75-5.wc.htm>"
- [20] "Recyclability of Lead-based Batteries," last Accessed: October 17, 2022. [Online]. Available: "https://batteryCouncil.org/Portals/0/Docs/About_Batteries/BCI_482347-20_2019-Study.pdf"
- [21] "Lifetime LiFePo4," last Accessed: October 17, 2022. [Online]. Available: "<https://www.powertechsystems.eu/home/tech-corner/lithium-iron-phosphate-lifepo4/>"
- [22] "BYD Battery Box Data-sheet," last Accessed: October 10, 2022. [Online]. Available: "https://bydbatterybox.com/uploads/downloads/220426%20BYD%20Battery-Box%20Premium%20HVS_HVM%20Datasheet%20V1.6%20EN-626901613c1a0.pdf"
- [23] "Victron LiFePo4 Battery 1.28kWh," last Accessed: October 17, 2022. [Online]. Available: "<https://www.europe-solarstore.com/batteries/battery-type/lithium-ion/victron-lithium-superpack-12-8v-100ah-m8.html>"

- [24] "BYD LiFePo4 Battery 24kWh," last Accessed: October 17, 2022. [Online]. Available: "<https://www.europe-solarstore.com/batteries/battery-type/lithium-ion/byd-battery-box-premium-lvs-24-0-24-kwh.html>"
- [25] M. Mahesh, D. V. Bhaskar, R. K. Jisha, R. Krishan, and R. Gnanadass, "Lifetime estimation of grid connected lifepo4 battery energy storage systems," *Electrical Engineering*, vol. 104, pp. 67–81, 2022.
- [26] "Home Power Solutions," last Accessed: October 17, 2022. [Online]. Available: "<https://www.homepowersolutions.de/>"
- [27] "Home Power Solutions Datasheet," last Accessed: October 17, 2022. [Online]. Available: "https://www.homepowersolutions.de/wp-content/uploads/2022/09/20220614_picea_Broschuere_Doppelseiten_V08_digital.pdf"
- [28] "Home Power Solutions FAQ, Technik," last Accessed: October 17, 2022. [Online]. Available: "<https://www.homepowersolutions.de/faq/#collapse-1-2285>"
- [29] "PVGIS Offgrid Calculator," last Accessed: October 11, 2022. [Online]. Available: https://joint-research-centre.ec.europa.eu/pvgis-photovoltaic-geographical-information-system/getting-started-pvgis/pvgis-user-manual_en#ref-6-calculation-of-off-grid-pv-system-performance
- [30] "Quaschnig Website," last Accessed: November 09, 2022. [Online]. Available: <https://www.volker-quaschnig.de/index.php>
- [31] "Quaschnig Independence Calculator," last Accessed: October 11, 2022. [Online]. Available: https://www.volker-quaschnig.de/software/unabhaengig/index_e.php#seitenstart
- [32] J. Weniger, T. Tjaden, and V. Quaschnig, "Sizing and grid integration of residential pv battery systems," 2013.
- [33] "PV Austria," last Accessed: October 11, 2022. [Online]. Available: <https://pvaustria.at/>
- [34] "Sonnenklar Rechner," last Accessed: October 11, 2022. [Online]. Available: https://pvaustria.at/sonnenklar_rechner/
- [35] "STORE4HUC Project," last Accessed: October 12, 2022. [Online]. Available: <https://www.interreg-central.eu/Content.Node/Store4HUC.html>

- [36] "Autarky Rate Tool," last Accessed: October 12, 2022. [Online]. Available: <https://store4huc-autarky.4wardenergy.at/>
- [37] "Autarky Rate Tool Calculation," last Accessed: October 12, 2022. [Online]. Available: <https://www.interreg-central.eu/Content.Node/Store4HUC/CE1344-Store4HUC-Background-information-of-the-Autarky-Rate.pdf>
- [38] "Load Profile Generator Website," last Accessed: October 12, 2022. [Online]. Available: <https://www.loadprofilegenerator.de/>
- [39] N. Pflugradt, "Modellierung von Wasser und Energieverbräuchen in Haushalten," Ph.D. dissertation, 08 2016.
- [40] "Benefit Tool - Erneuerbare Energiegemeinschaft," last Accessed: October 12, 2022. [Online]. Available: <https://www.energieinstitut.at/tools/benefit/>
- [41] "SUSI - Strom Unabhängigkeits-Simulation," last Accessed: October 12, 2022. [Online]. Available: <https://www.energieinstitut.at/tools/susi/>
- [42] "Energieinstitut Website," last Accessed: October 12, 2022. [Online]. Available: <https://www.energieinstitut.at/>
- [43] "Python Website," last Accessed: September 26, 2022. [Online]. Available: <https://www.python.org/>
- [44] "Numpy Website," last Accessed: September 26, 2022. [Online]. Available: <https://numpy.org/>
- [45] "Mathlab Website," last Accessed: September 26, 2022. [Online]. Available: <https://www.mathworks.com/products/matlab.html>
- [46] "ZAMG Website," last Accessed: September 26, 2022. [Online]. Available: <https://www.zamg.ac.at/cms/de/aktuell>
- [47] "Creative Commons License," last Accessed: September 26, 2022. [Online]. Available: <http://opendefinition.org/licenses/cc-by/>
- [48] "ZAMG Datahub," last Accessed: September 26, 2022. [Online]. Available: <https://data.hub.zamg.ac.at/>
- [49] "ZAMG Messdaten," last Accessed: September 21, 2022. [Online]. Available: <https://data.hub.zamg.ac.at/dataset/klima-v1-10min>

- [50] “ZAMG Messdaten,” last Accessed: September 29, 2022. [Online]. Available: <https://data.hub.zamg.ac.at/dataset/klima-v1-1h>
- [51] “ZAMG INCA_L,” last Accessed: September 21, 2022. [Online]. Available: <https://data.hub.zamg.ac.at/dataset/inca-v1-1h-1km>
- [52] “PVGIS Calculation Methods,” last Accessed: September 21, 2022. [Online]. Available: https://joint-research-centre.ec.europa.eu/pvgis-photovoltaic-geographical-information-system/getting-started-pvgis/pvgis-data-sources-calculation-methods_en
- [53] “DIN 5034 Tageslicht in Innenräumen,” last Accessed: September 27, 2022. [Online]. Available: <https://www.beuth.de/de/norm/din-5034-2/1178518>
- [54] T. Mahachi and A. Rix, “Energy yield analysis and evaluation of solar irradiance models for a utility scale solar pv plant in south africa,” Ph.D. dissertation, 12 2016.
- [55] A. M. Gracia, T. Huld, E. C. J. R. C. I. for Energy, and Transport., *Performance comparison of different models for the estimation of global irradiance on inclined surfaces : validation of the model implemented in PVGIS*. Publications Office, 2013.
- [56] R. Perez, R. Seals, P. Ineichen, R. Stewart, and D. Menicucci, “A new simplified version of the perez diffuse irradiance model for tilted surfaces,” *Solar Energy*, vol. 39, pp. 221–231, 1987.
- [57] C. A. Gueymard, “A reevaluation of the solar constant based on a 42-year total solar irradiance time series and a reconciliation of spaceborne observations,” *Solar Energy*, vol. 168, pp. 2–9, 7 2018.
- [58] R. Perez, P. Ineichen, R. Seals, J. Michalsky, and R. Stewart, “Modeling daylight availability and irradiance components from direct and global irradiance,” *Solar Energy*, vol. 44, no. 5, pp. 271–289, 1990. [Online]. Available: <https://www.sciencedirect.com/science/article/pii/0038092X9090055H>
- [59] *Practical Handbook of Photovoltaics*. Academic Press, 2011.
- [60] J. Coakley, “Reflectance and albedo, surface,” *Encyclopedia of Atmospheric Sciences*, 12 2003.
- [61] N. Martin and J. M. Ruiz, “Calculation of the pv modules angular losses under field conditions by means of an analytical model,” *Solar Energy Materials and Solar Cells*, vol. 70, pp. 25–38, 12 2001.
- [62] —, “Corrigendum to “calculation of the pv modules angular losses under field conditions by means of an analytical model” [sol. energy mater. sol. cells 70 (1) (2001) 25–38] (s0927024800004086) (10.1016/s0927-0248(00)00408-6),” p. 154, 3 2013.

- [63] D. Faiman, "Assessing the outdoor operating temperature of photovoltaic modules," *Progress in Photovoltaics: Research and Applications*, vol. 16, pp. 307–315, 6 2008.
- [64] A. M. G. Amillo, T. Huld, P. Vourlioti, R. Müller, and M. Norton, "Application of satellite-based spectrally-resolved solar radiation data to pv performance studies," *Energies*, vol. 8, pp. 3455–3488, 2015.
- [65] M. Koehl, M. Heck, S. Wiesmeier, and J. Wirth, "Modeling of the nominal operating cell temperature based on outdoor weathering," *Solar Energy Materials and Solar Cells*, vol. 95, pp. 1638–1646, 7 2011.
- [66] J. Oh, G. Tamizhmani, and E. Palomino, "Temperatures of building applied photovoltaic (bapv) modules air gap effects temperatures of building applied photovoltaic (bapv) modules: Air gap effects."
- [67] T. Huld, G. Friesen, A. Skoczek, R. P. Kenny, T. Sample, M. Field, and E. D. Dunlop, "A power-rating model for crystalline silicon pv modules," *Solar Energy Materials and Solar Cells*, vol. 95, pp. 3359–3369, 12 2011.
- [68] "Fronius Symo GEN24Plus Inverter," last Accessed: October 4, 2022. [Online]. Available: "https://www.fronius.com/~/downloads/Solar%20Energy/Datasheets/SE_DS_Fronius_Symo_GEN24_Plus_DE.pdf"
- [69] "Atmospheric Pressure," last Accessed: November 25, 2022. [Online]. Available: <https://ntrs.nasa.gov/api/citations/19770009539/downloads/19770009539.pdf>
- [70] "Air Density," last Accessed: November 25, 2022. [Online]. Available: https://atmos.nmsu.edu/education_and_outreach/encyclopedia/humidity.htm
- [71] "DIN EN ISO 13788[1013-05]," last Accessed: November 25, 2022. [Online]. Available: <https://www.beuth.de/de/norm/din-en-iso-13788/165528681>
- [72] "Schachner SW5," last Accessed: October 26, 2022. [Online]. Available: "<http://www.kleinwind.at/Windrad-SW5>"
- [73] "Antaris 5.5kW Power Curve," last Accessed: October 1, 2022. [Online]. Available: <https://i2.wp.com/www.braun-windturbinen.com/wp-content/uploads/ANTARIS-5kW-Power-Curve.jpg>
- [74] "Istabreeze Heli 4.0," last Accessed: October 21, 2022. [Online]. Available: "<https://en.istabreeze.store/products/windgenerator-istabreeze%C2%AE-heli-4-0>"

- [75] A. Einfalt, A. Schuster, C. Leitinger, D. Tiefgraber, M. Litzlbauer, S. Ghaemi, D. Wertz, A. Frohner, and C. Karner, "Adres-concept: Konzeptentwicklung für adres - autonome dezentrale regenerative energiesysteme," *TU Wien Institut für Elektrische Anlagen und Energiewirtschaft*, 3 2011.
- [76] D. S. Ghaemi, "Efficiency potential in private sector in ADRES: (Autonomous Decentralized Renewable Energy Systems)," *Institut für Energiesysteme und Elektrische Antriebe - Technische Universität Wien*, 2011, last Accessed: October 5, 2022. [Online]. Available: <http://www.ub.tuwien.ac.at/diss/AC07810532.pdf>
- [77] W. Gawlik, C. Groß, M. Litzlbauer, C. Maier, A. Schuster, F. Zeilinger, A. Kann, I. Meirold-Mautner, G. Günther, C. Eugster, R. Nennung, J. Scalet, P. Österle, H. Jussel, C. Karner, G. Wolfram, and H. Petschauer, "aDSM - Aktives Demand-Side-Management durch Einspeiseprognose: Publizierbarer Endbericht zum Projekt," 3 2014, last Accessed: October 5, 2022. [Online]. Available: <https://energieforschung.at/wp-content/uploads/sites/11/2020/12/aDSM-834612-vorlaeufiger-Endbericht.pdf>
- [78] F. Zeilinger, "Methodik zur automatischen Bewertung und Vergleich von Verteilnetz-Management-Konzepten," Ph.D. dissertation, 9 2022.
- [79] M. Kern, "die Entwicklung eines Wärmebedarf-Modells für eine Simulationsumgebung und dessen methodische Parametrierung," 6 2022.
- [80] "Insulated Brick - Mein Ziegelhaus," last Accessed: October 8, 2022. [Online]. Available: <https://meinziegelhaus.de/ziegel/thermoplan-mz70/>
- [81] "u-Value Calculator," last Accessed: October 8, 2022. [Online]. Available: <https://www.ubakus.de/u-wert-rechner/>
- [82] "Rs Values," last Accessed: October 8, 2022. [Online]. Available: https://www.uni-due.de/ibpm/Aufgabensammlung/NeuNorm_A4.pdf
- [83] "ISO-6946," last Accessed: October 8, 2022. [Online]. Available: <https://www.beuth.de/de/norm/din-en-iso-6946/255315365>
- [84] K. Rankinen, T. Karvonen, and D. Butterfield, "A simple model for predicting soil temperature in snow-covered and seasonally frozen soil: Model description and testing," *Hydrology and Earth System Sciences*, vol. 8, pp. 706–716, 2004.
- [85] "Ubaku Ventilation Calculator," last Accessed: October 18, 2022. [Online]. Available: <https://www.ubakus.de/berechnung/luftungs-rechner/>

- [86] "Specific Heat Capacity of Air at Different Temperatures," last Accessed: October 19, 2022. [Online]. Available: "https://www.ohio.edu/mechanical/thermo/property_tables/air/air_Cp_Cv.html#:~:text=The%20nominal%20values%20used%20for,v%20%3D%200.718%20kJ%2Fkg."
- [87] N. A. Efkarpidis, G. C. Christoforidis, and G. K. Papagiannis, "Modeling of heating and cooling energy needs in different types of smart buildings," *IEEE Access*, vol. 8, pp. 29 711–29 728, 2020.
- [88] "DIN V 4108-6," last Accessed: October 8, 2022. [Online]. Available: <https://www.beuth.de/de/vornorm/din-v-4108-6/63939447>
- [89] "Solar Bayer Buffer-tanks," last Accessed: October 10, 2022. [Online]. Available: <https://www.solarbayer.com/Stratification-buffer-tank-SLS.html>
- [90] "EN-15332," last Accessed: October 10, 2022. [Online]. Available: <https://www.beuth.de/de/norm/din-en-15332/310225133>
- [91] "Bosch CS3400iAWS 4 OR-S," last Accessed: October 10, 2022. [Online]. Available: <https://b5-web-product-data-service.azurewebsites.net/pdf/de-DE/8750722680.pdf>
- [92] "Bosch CS7800ILW 6," last Accessed: October 10, 2022. [Online]. Available: <https://b5-web-product-data-service.azurewebsites.net/pdf/de-DE/8738212050.pdf>
- [93] "Bosch STE60-1," last Accessed: October 10, 2022. [Online]. Available: <https://b5-web-product-data-service.azurewebsites.net/pdf/de-DE/7738600326.pdf>
- [94] "Average Power usage per Person in Austria," last Accessed: October 18, 2022. [Online]. Available: "https://www.klimaaktiv.at/energiesparen/effiziente_geraete/Stromcheck.html"
- [95] "Österreichisches Institut für Bautechnik, Richtlinie 6," last Accessed: October 19, 2022. [Online]. Available: "https://www.oib.or.at/sites/default/files/richtlinie_6_12.04.19_1.pdf"
- [96] "Bosch CS3400iAWS 10 OR-S," last Accessed: October 28, 2022. [Online]. Available: <https://b5-web-product-data-service.azurewebsites.net/pdf/de-DE/8750722683.pdf>
- [97] "Anataris 12.0kW," last Accessed: November 1, 2022. [Online]. Available: "<https://www.braun-windturbinen.com/produkte/antaris-kleinwindanlagen/antaris-12-kw/>"